

canadian acoustics

acoustique canadienne

Journal of the Canadian Acoustical Association - Revue de l'Association canadienne d'acoustique

SEPTEMBER 2021

Volume 49 - - Number 3

SEPTEMBRE 2021

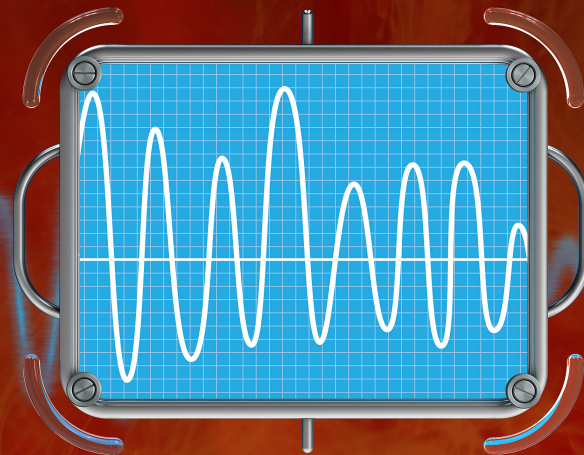
Volume 49 - - Numéro 3

ACOUSTICS WEEK IN CANADA 2021 - SEMAINE CANADIENNE DE L'ACOUSTIQUE 2021	1
GENERAL PLANNING - PLENARIES - VIRTUAL ROOMS - PLANIFICATION GÉNÉRALE - CONFÉRENCES PLÉNIÈRES - CARTE VIRTUELLE	3
THEME 1 - ACOUSTICS AND STRUCTURES - THÈME 1 - ACOUSTIQUE ET STRUCTURES	7
THEME 2 - ACOUSTICS AND LIVING BEINGS - THÈME 2 - ACOUSTIQUE ET ÊTRES VIVANTS	27
THEME 3 - ACOUSTICS AND COMPUTERS - THÈME 3 - ACOUSTIQUE ET ORDINATEURS	61
ACOUSTIC WEEK IN CANADA 2022 NEWFOUNDLAND CONFERENCE ANNOUNCEMENT - APPEL À COMMUNICATION - SEMAINE CANADIENNE DE L'ACOUSTIQUE 2022 À TERRE-NEUVE	74
CAA ANNOUNCEMENTS - ANNONCES DE L'ACA	79

2021

**Acoustics Week
in Canada**

**Semaine
canadienne
de l'acoustique**



**Actes de la conférence
Conference Proceedings**

canadian acoustics

acoustique canadienne

Canadian Acoustical Association/Association
Canadienne d'Acoustique P.B. 74068 Ottawa,
Ontario, K1M 2H9

Association canadienne d'acoustique B.P. 74068
Ottawa, Ontario, K1M 2H9

Canadian Acoustics publishes refereed articles and news items on all aspects of acoustics and vibration. Articles reporting new research or applications, as well as review or tutorial papers and shorter technical notes are welcomed, in English or in French. Submissions should be sent only through the journal online submission system. Complete instructions to authors concerning the required "camera-ready" manuscript are provided within the journal online submission system.

L'Acoustique Canadienne publie des articles arbitrés et des informations sur tous les aspects de l'acoustique et des vibrations. Les informations portent sur la recherche, les ouvrages sous forme de revues, les nouvelles, l'emploi, les nouveaux produits, les activités, etc. Des articles concernant des résultats inédits ou des applications ainsi que les articles de synthèse ou d'initiation, en français ou en anglais, sont les bienvenus.

Canadian Acoustics is published four times a year - in March, June, September and December. This quarterly journal is free to individual members of the Canadian Acoustical Association (CAA) and institutional subscribers. **Canadian Acoustics** publishes refereed articles and news items on all aspects of acoustics and vibration. It also includes information on research, reviews, news, employment, new products, activities, discussions, etc. Papers reporting new results and applications, as well as review or tutorial papers and shorter research notes are welcomed, in English or in French. The *Canadian Acoustical Association* selected **Paypal** as its **preferred system** for the online payment of your subscription fees. Paypal supports a wide range of payment methods (Visa, Mastercard, Amex, Bank account, etc.) and does not require you to have already an account with them. If you still want to proceed with a manual payment of your subscription fee, please [Membership form](#) and send it to the Executive Secretary of the Association (see address above). - - Dr. Roberto Racca - Canadian Acoustical Association/Association Canadienne d'Acoustique c/o JASCO Applied Sciences 2305-4464 Markham Street Victoria, BC V8Z 7X8 - - secretary@caa-aca.ca

Acoustique canadienne est publié quatre fois par an, en mars, juin, septembre et décembre. Cette revue trimestrielle est envoyée gratuitement aux membres individuels de l'Association canadienne d'acoustique (ACA) et aux abonnés institutionnels. **L'Acoustique canadienne** publie des articles arbitrés et des rubriques sur tous les aspects de l'acoustique et des vibrations. Ceci comprend la recherche, les recensions des travaux, les nouvelles, les offres d'emploi, les nouveaux produits, les activités, etc. Les articles concernant les résultats inédits ou les applications de l'acoustique ainsi que les articles de synthèse, les tutoriels et les exposés techniques, en français ou en anglais, sont les bienvenus. L'Association canadienne d'acoustique a sélectionné **Paypal** comme solution pratique pour le paiement en ligne de vos frais d'abonnement. Paypal prend en charge un large éventail de méthodes de paiement (Visa, Mastercard, Amex, compte bancaire, etc) et ne nécessite pas que vous ayez déjà un compte avec eux. Si vous désirez procéder à un paiement par chèque de votre abonnement, merci de remplir le [formulaire d'inscription](#) et de l'envoyer au secrétaire exécutif de l'association (voir adresse ci-dessus). - - Dr. Roberto Racca - Canadian Acoustical Association/Association Canadienne d'Acoustique c/o JASCO Applied Sciences 2305-4464 Markham Street Victoria, BC V8Z 7X8 - - secretary@caa-aca.ca

EDITOR-IN-CHIEF - RÉDACTEUR EN CHEF

Dr. Umberto Berardi
Ryerson University
editor@caa-aca.ca

DEPUTY EDITOR RÉDACTEUR EN CHEF ADJOINT

Romain Dumoulin
Soft dB
deputy-editor@caa-aca.ca

JOURNAL MANAGER DIRECTRICE DE PUBLICATION

Cécile Le Cocq
ÉTS, Université du Québec
journal@caa-aca.ca

EDITORIAL BOARD RELECTEUR-RÉVISEUR

Pierre Grandjean
Université de Sherbrooke
copyeditor@caa-aca.ca

ADVERTISING EDITOR RÉDACTEUR PUBLICITÉS

Mr Bernard Feder
HGC Engineering
advertisement@caa-aca.ca

ADVISORY BOARD COMITÉ AVISEUR

Prof. Frank A. Russo
Ryerson University
Prof. Ramani Ramakrishnan
Ryerson University
Prof. Jérémie Voix
ÉTS, Université du Québec
Prof. Bryan Gick
University of British Columbia

Acoustics Week in Canada 2021 Semaine canadienne de l'acoustique 2021



Online meeting

We are pleased to present you in this unusual September issue of Canadian Acoustics journal, the list of accepted abstracts and 2-page papers for the upcoming 3-day AWC2021 conference. As most of you know, because of the COVID-19 situation, the Acoustics Week in Canada (AWC) originally planned for October 2020 in Sherbrooke (QC) has been postponed in October 2021. We hoped for a physical event, but the situation was so uncertain that we preferred an online format for this conference.

For this year, papers for the conference are provided on a purely voluntary basis, and only abstracts and short videos are mandatory. This has been proposed in order to motivate people to participate and to lighten the workload for everyone in this particular context. The online event represents an opportunity for students to present their work in a lightning presentation style, and have a chance to win one of the Best Student Presentation awards.

The lightning presentation style has been chosen to give more place to online exchange and discussions instead of long monologues that can be tedious in an online format. These 3-minute concise and efficient presentations are intended to grab the attention of the audience, so that people will join later on to discuss online using the *gather* platform.

Each day will have a general theme: acoustics and structures – acoustics and living beings – acoustics and computers to simplify and gather the community on general topics instead of dispatching participants in small sub-areas. Three plenary lectures and an update on the NoiseCanada21 challenge (setting up a participative Canada noise map during AWC21) will start each of the three half-days of the conference.

We sincerely hope that all members of CAA will seize that opportunity to regroup in 2021 despite the adversity of this never-ending pandemic and we look forward to a successful and -in presence- event in St-John's, Newfoundland in September 2022!

Olivier Robin, Conference Chair
Patrice Masson
Sebastian Ghinet

Conférence en ligne

Nous sommes heureux de vous présenter dans ce numéro de septembre de la revue Acoustique canadienne, la liste des résumés acceptés et des articles de deux pages pour la conférence en ligne AWC2021. Comme la plupart d'entre vous le savent, en raison de la situation COVID-19, la Semaine canadienne de l'acoustique (AWC) initialement prévue en octobre 2020 à Sherbrooke (QC) a été reportée en octobre 2021. Nous espérons pouvoir organiser une conférence en présentiel, mais les incertitudes persistantes nous ont amenés à préférer un format en ligne pour cette conférence.

Pour cette année, les communications pour la conférence sont fournies sur une base purement volontaire, et seuls les résumés et les vidéos sont obligatoires. Ceci est proposé afin de motiver les gens à participer et d'alléger la charge de travail de chacun dans ce contexte si particulier. L'événement en ligne représente une occasion pour les étudiants de présenter leur travail dans un style de « présentation éclair » et d'avoir une chance de gagner l'un des prix de la meilleure présentation étudiante.

Ce type de présentation a été choisi pour donner plus de place aux discussions en ligne plutôt qu'aux longs monologues qui peuvent être lassants dans un format en ligne. Ces présentations de 3 minutes, concises et efficaces, sont destinées à attirer l'attention du public, afin que les personnes participantes se joignent ensuite pour discuter en ligne à l'aide de la plate-forme *gather*.

Chaque journée aura un thème général : acoustique et structures – acoustique et êtres vivants – acoustique et informatique, afin de rassembler la communauté sur des sujets généraux au lieu de répartir les participants en petits sous-groupes. Trois conférences plénières et une mise à jour sur le défi NoiseCanada21 (mise en place d'une carte participative du bruit du Canada lors de l'AWC21) viendront démarrer chacune des trois demi-journées de la conférence.

Nous espérons sincèrement que tous les membres de l'ACA saisiront cette occasion de se regrouper en 2021, malgré l'adversité de la pandémie actuelle. Nous espérons que l'événement qui se tiendra à St-John's (NL) en septembre 2022 sera couronné de succès et se déroulera en présence de toutes et tous !

Olivier Robin, Directeur de conférence
Patrice Masson
Sebastian Ghinet



CONTROL NOISE

LOWER PROJECT COSTS

IMPROVE SPEECH PRIVACY
BOOST COMFORT & WELLNESS

QUICK ROI

INCREASE PRODUCTIVITY

FACILITY FLEXIBILITY

ENHANCE WORKPLACE CULTURE

SUPPORT FOCUS

LogiSon[®]
ACOUSTIC NETWORK
SOUND.
THAT WORKS.[™]

Sound masking is more than a product. It's a service provided by professional technicians who know the effect isn't achieved from the moment they power the system, but by tuning the sound to an independently-proven curve. Designed right, tuned right—that's our motto. And the result is more consistent, comfortable and effective sound masking.

www.logison.com

© 2021 KR MOELLER ASSOCIATES LTD. LOGISON IS A REGISTERED TRADEMARK OF 777388 ONTARIO LIMITED. PHOTO BY VINCENT LIONS.



General Planning / Plenaries / virtual rooms

Three 'half-days' will be structured around three general themes from October, 05 to October, 07 (noon to 5:30pm to accommodate Canada's time zones). Day 1 is devoted to 'Acoustics and structures' (involving room acoustics, building acoustics, vibroacoustics, ultrasound, shock and vibration), Day 2 to 'Acoustics and living beings' (psychoacoustics, hearing, bioacoustics, musical acoustics, education in acoustics) and Day 3 focuses on 'Acoustics and computers' (computations, simulations, signal processing applied to any acoustics domain).

Our first plenary speaker (Day 1 – Acoustics and structures) will be Stephen Hambric. Dr Hambric is a Research Professor in the Fluid Dynamics and Acoustics Office at the Applied Research Lab (Penn State University, USA), a Professor in the Penn State Graduate Program in Acoustics and the Director of Penn State's Center for Acoustics and Vibration. Dr. Hambric has directed many numerical and experimental flow, structural acoustics, and noise/vibration control research and development programs.

Our second plenary speaker (Day 2 – Acoustics and living beings) is Catherine Guastavino. Dr Guastavino is Associate Professor and William Dawson Scholar (School of Information Studies - McGill University), associate Member of Schulich School of Music (McGill) and member of the Centre for Interdisciplinary Research in Music Media and Technology (CIRMMT). Her research concentrates on soundscapes. The project « Sound in the city » that includes partners from McGill University, the City of Montreal, and the professional realm aims to position Montreal as a leader in urban noise management and soundscape by connecting research and practice

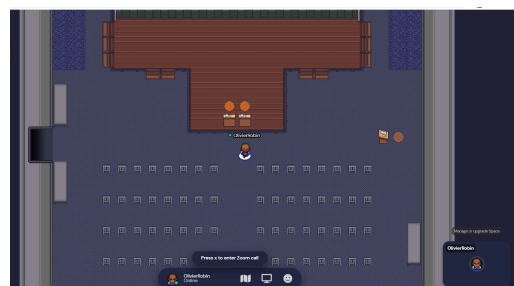
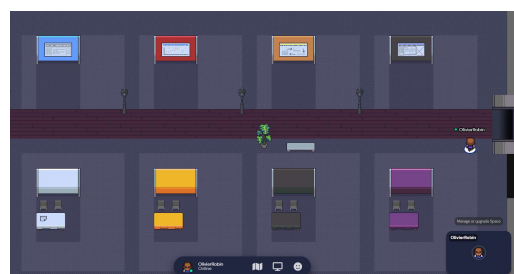
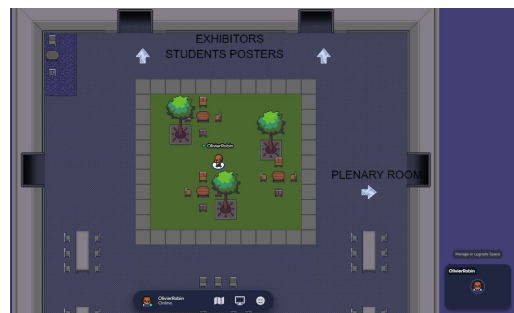
The third speaker is still to be confirmed at the time of publication.



Gather.town is a 2D web-conferencing software which allows you to meet others in virtual rooms with the ability to move around and interact with other participants (chat or video). In Gather.town, you use your avatar to walk around, to sit down at tables or start a conversation with other attendees.

In the AWC21 gather.town platform, participants will find :

- A main room in which the plenary lectures and lightning sessions will be streamed,
- A virtual room including researchers, students and exhibitors to discuss/exchange after video presentations, including poster presentations and booths
- A virtual room to meet / discuss with people in private spaces
- A virtual room dedicated to employment (CV and job offers).



Planification générale / conférences plénières / carte virtuelle

Trois « demi-journées » seront structurées autour de trois thèmes généraux du 5 octobre au 7 octobre (de midi à 17h30 pour s'adapter aux fuseaux horaires du Canada). Le thème du jour 1 est « Acoustique et structures » (impliquant l'acoustique des salles, l'acoustique du bâtiment, la vibroacoustique, les ultrasons, les chocs et les vibrations), celui du jour 2 est « Acoustique et êtres vivants » (psychoacoustique, audition, bioacoustique, acoustique musicale, éducation à l'acoustique) et celui du jour 3 est 'Acoustique et informatique' (calculs, simulations, traitement du signal appliqué à n'importe quel domaine de l'acoustique).

Notre premier conférencier (Jour 1 – Acoustique et structures) sera Stephen Hambric. Dr Hambric est professeur-chercheur au *Fluid Dynamics and Acoustics Office - Applied Research Lab* (Penn State University, États-Unis), professeur au *Penn State Graduate Program in Acoustics* et directeur du *Penn State's Center for Acoustics and Vibration*. Le Dr Hambric a dirigé de nombreux programmes de recherche et développement sur les écoulements numériques et expérimentaux, l'acoustique structurelle et le contrôle du bruit et des vibrations.

Notre deuxième conférence (Jour 2 – Acoustique et êtres vivants) sera Catherine Guastavino. Dr Guastavino est professeure agrégée et boursière William Dawson (École des sciences de l'information - Université McGill), membre associée *Schulich School of Music* (McGill) et membre du *Centre for Interdisciplinary Research in Music Media and Technology* (CIRMMT). Ses recherches portent sur les paysages sonores. Le projet « Sound in the city » qui regroupe des partenaires de l'Université McGill, de la Ville de Montréal et du monde professionnel vise à positionner Montréal comme un leader en gestion du bruit urbain et paysage sonore en reliant recherche et pratique

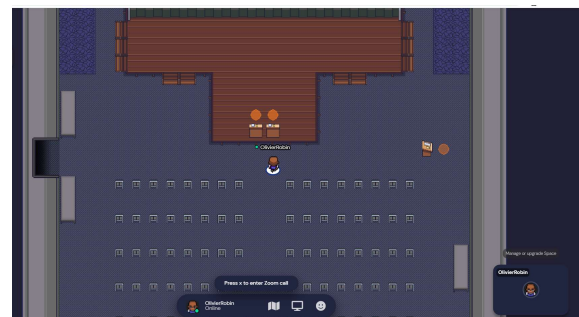
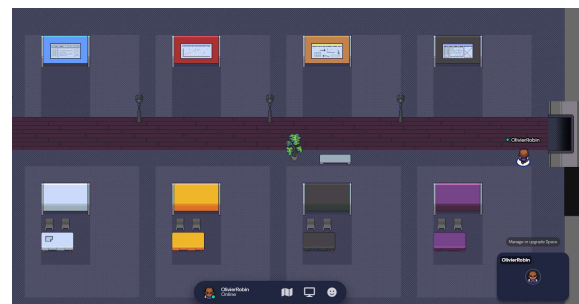
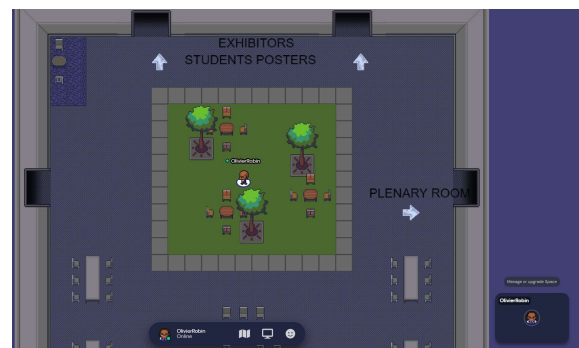
La troisième personne intervenante doit encore être confirmée au moment de la publication.



Gather.town est un logiciel de webconférence 2D qui permet de rencontrer d'autres personnes dans des salles virtuelles avec la possibilité de se déplacer et d'interagir avec les autres participants (chat ou vidéo). Dans Gather.town, vous utilisez un avatar pour vous promener, vous asseoir à des tables ou entamer une conversation avec d'autres participants.

Sur la plateforme de rassemblement AWC21, les participants trouveront :

- Une salle principale dans laquelle seront retransmises les conférences plénières et les sessions éclair,
- Une salle virtuelle comprenant des chercheurs, des étudiants et des exposants pour discuter/échanger après les présentations vidéo, y compris les présentations d'affiches et les stands
- Une salle virtuelle pour rencontrer/discuter avec des personnes dans des espaces privés
- Une salle virtuelle dédiée à l'emploi (CV et offres d'emploi).





NOISE MONITORING BUILT FOR ANY SITE

METER 831C & SYSTEM NMS044

NOISE MONITORING SOLUTIONS

- Connect over cellular, WiFi or wired networks
- Control meter and view data via web browser
- Receive real time alerts on your mobile device
- Monitor continuously with a solar powered outdoor system



Dalimar
instruments

450 424 0033 | dalimar.ca



MTS Sensors, a division of MTS Systems Corporation (NASDAQ: MTSC), vastly expanded its range of products and solutions after MTS acquired PCB Piezotronics, Inc. in July, 2016. PCB Piezotronics, Inc. is a wholly owned subsidiary of MTS Systems Corp.; IMI Sensors and Larson Davis are divisions of PCB Piezotronics, Inc.; Accumetrics, Inc. and The Modal Shop, Inc. are subsidiaries of PCB Piezotronics, Inc.



The network of research organizations
Le réseau des organismes de recherche

An information system with academic CV management, expertise inventory and networking capabilities for research institutions and associations.

Un système d'information avec gestion de CV académique, un inventaire de l'expertise interne et des capacités de réseautage pour des organismes de recherche.

With UNIWeb, researchers can:

Avec Uniweb, les chercheurs peuvent:

Streamline

funding applications with Canadian Common CV integration

Simplifier

les demandes de financement grâce à l'intégration au CV commun canadien

Reuse

CCV data to generate academic CVs and progress reports

Réutiliser

les données du CVC pour générer des CV académiques et des rapports de progrès

Mobilize

knowledge by creating engaging webpages for research projects

Mobiliser

les connaissances en créant des pages Web attrayantes pour les projets de recherche

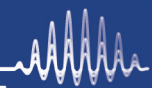
<http://uniweb.network>

THEME 1 - ACOUSTICS AND STRUCTURES - THÈME 1 - ACOUSTIQUE ET STRUCTURES

Evolution Of The Acoustical Provisions Within The Model National Building Code Of Canada <i>Todd Busch</i>	8
Measurement Of Acoustic Resistance Of Perforated Plates Subjected To A Pulsated Grazing Flow <i>Jean Michel Coulon, Xukun Feng, Zacharie Laly, Noureddine Atalla</i>	10
Noise Reduction In Ducts Using Helmholtz Resonators <i>Sourabh Dogra, Arpan Gupta, Umberto Berardi</i>	12
The Effects Of Acoustical Ceiling Panel Type And Penetrations For Services On Vertical Sound Isolation Inside Buildings <i>Gary S. Madaras</i>	14
Bio-Inspired Flow Velocity Microphone: Acoustic Simulation Of Possible Encapsulating Packages <i>Kiran Vadavalli, Frédéric Lepoutre, Stephane Leahy, Jérémie Voix</i>	16
Separation Of Wind Turbine Infrasound Acoustics From Wind Noise Using Cross-Spectra <i>John Vanderkooy</i>	18
Abstracts for Presentations without Proceedings Paper - Résumés des communications sans article	21

Scantek, Inc.

Calibration Laboratory



Scantek offers traceable, high quality and prompt periodic calibration of any brand of sound and vibration instrumentation

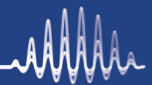
Calibration and Service Capabilities:

- Microphones
- Preamplifiers
- Acoustical Calibrators
- Sound Level Meters & Analyzers
- Accelerometers & Vibration Meters
- Vibration Calibrators and more

ISO 17025:2005 and ANSI/NCSL Z-540-1: 1994 Accredited Calibration Laboratory

Scantek, Inc.

Sales, Rental, Calibration



www.ScantekInc.com/calibration

800-224-3813

EVOLUTION OF THE ACOUSTICAL PROVISIONS WITHIN THE MODEL NATIONAL BUILDING CODE OF CANADA

Todd Busch *^{1,2}

¹Soft dB Acoustical Consulting, Etobicoke, Ontario, Canada

²Invited Committee Member, Canadian Commission of Building and Fire Codes, Sound and Vibration Task Force

1 Introduction

This paper explores the evolution of the model National Building Code of Canada (NBCC). Starting in 1941, the NBCC required a sound transmission loss between dwelling units of 45 dB or higher. There were prohibitions on the attachment of fixtures. Refuse chute construction was described. In 1954, references to compromising air leaks were introduced. In 1965, sound transmission class (STC) 45 performance was added including a variety of service rooms. ASTM E90-61T was introduced. In 1970, a table was added showing “sound ratings” of assemblies. Minor changes occurred in the 1975, 1977, and 1985 versions. In 1980, STC 50 was adopted for elevator shafts. In 1990, STC 50 between dwellings was adopted along with an STC 55 provision for elevator shafts and refuse chutes. In 1995, a larger table of expected laboratory STC ratings was included. No significant changes occurred for the 1995 or 2005 versions. The 2010 edition saw language added for secondary suites where an STC 43 rating was stipulated. The 2015 version added in the option of demonstrating either an apparent STC (ASTC) performance of 47 or STC 50. Additional reference was made to ISO standards in regards to flanking paths. Future changes are being considered for impact insulation class (IIC), exterior noise control, and low-frequency sources.

2 NBCC 1941

Starting in 1941, the NBCC required walls and floors between dwellings to be sound transmission loss of 45 dB or higher and transmission loss (TL) was defined. There were prohibitions on the attachment of fixtures to walls separating dwelling units including plumbing, water-supply pipe, drainage pipe or mechanical equipment. Refuse chute construction was described by specifying a minimum 2.156 lb/ft² (No. 18 Gauge) surface weight.

3 NBCC 1954

In 1954 references to compromising air leaks were introduced. Specifically, “The required sound insulation can not be obtained if air leaks exist in any layer of the intervening construction.” The 45 dB rating requirement between dwelling units was retained unchanged.

4 NBCC 1965

In 1965, STC 45 performance was added for a variety of

service rooms to the effect that, “Every service room or space such as storage room, laundry, workshop or building maintenance room and garages ... when not located in a dwelling unit, shall be separated from the dwelling units by a construction providing ... [an STC rating of 45 or greater].” ASTM E90-61T, “Laboratory Measurement of Airborne Sound Transmission Loss of Building Partitions and Elements,” was introduced as an acceptable methodology for measuring the TL and obtaining STC ratings.

5 NBCC 1970

In 1970, a table was added for the first time showing “sound ratings” of acceptable assemblies, classified as either I or II, and distinct from the stipulated STC 45 rating between dwellings. ASTM E-90-66T was introduced.

6 NBCC 1975

Minor changes occurred in the 1975 version. ASTM E90-70 was introduced.

7 NBCC 1977

Minor changes occurred in the 1977 version. ASTM E90-75 was introduced.

8 NBCC 1980

More change occurred in the 1980 version. Now in addition to STC 45 between dwellings, “Where a dwelling unit is adjacent to an elevator shaft or a refuse chute, the separating construction shall have [an STC] rating of at least 50, or shall have a “sound rating” of I or II as described [in the accompanying table].” ASTM E90-75 was retained and ASTM E336-77, “Standard Test Method for Measurement of Airborne Sound Attenuation between Rooms in Buildings,” was introduced. The table of acceptable assemblies had no fewer than twenty-eight fire and “sound ratings” indicated for various wall constructions and no fewer than eleven for floors, ceilings, and roofs.

9 NBCC 1985

Minor changes occurred in the 1985 version. Newly introduced language stated that, “Building services located in an assembly required to have [an STC] rating shall be installed in a manner that will not decrease the required rating of the assembly.” ASTM E90 and ASTM E336 were now referenced to their most-recent versions in different sections of the NBCC document.

*t.busch@softdb.com

†toddbusch@hotmail.com

10 NBCC 1990

In 1990, the increased performance of STC 50 between dwellings was introduced for separations between dwelling units along with an STC 55 provision for elevator shafts and refuse chutes. ASTM E413, "Classification for Rating Sound Insulation," was introduced to accompany ASTM E90 and ASTM E336. More performance specificity was added by stipulating compliance with measurements that were conducted in terms of the relevant ASTM standards or as could be found in the table of fire and STC ratings. So-called "sound ratings" were dropped.

11 NBCC 1995

No significant changes occurred for the 1995 version although reference was now clearly made to ASTM E492-90, "Standard Test Method for Laboratory Measurement of Impact Sound Transmission Through Floor-Ceiling Assemblies Using the Tapping Machine," and E1007-97, "Standard Test Method for Field Measurement of Tapping Machine Impact Sound Transmission Through Floor-Ceiling Assemblies and Associated Support Structures," as they pertain to impact insulation class (IIC) testing which was heretofore not included. Despite references to these standards, neither design nor performance testing for IIC was required in this version of the NBCC. The overall number of tabulated assemblies for walls along with floors, ceilings and roofs was greatly increased from prior versions of the NBCC and the associated information modified to include fire-resistance ratings, STC ratings, and IIC performance ratings.

12 NBCC 2005

No significant changes occurred for the 2005 version.

13 NBCC 2010

The 2010 edition saw language added for secondary suites where either an STC 43 rating was stipulated or specific construction utilized, to the effect that "Where a house contains a secondary suite, each dwelling unit shall be separated from every other space in the house in which noise may be transmitted by construction:

- 1) whose joist spaces are filled with sound-absorbing material of not less than 150 mm nominal thickness,
- 2) whose stud spaces are filled with sound-absorbing material,
- 3) having a resilient channel on one side spaced 400 or 600 mm o.c., and
- 4) having 12.7 mm thick gyms having 12.7 mm thick gypsum board on ceilings and on both sides of walls."

14 NBCC 2015

The 2015 version added in the option of demonstrating either an apparent STC (ASTC) performance of 47 or laboratory tested STC 50 for dwellings (or greater when flanking is also

considered). It was noted that, "An ASTC measurement or calculation will always yield a value equal to or lower than the STC for the same configuration, as the ASTC includes flanking transmission." The National Research Council of Canada (NRCC) software soundPATHS® was referenced as an acceptable tool for analyzing future performance when flanking is considered as required. Additional reference was made to ISO standards in regards to flanking paths, including ISO 15712-1, "Building acoustics — Estimation of acoustic performance of buildings from the performance of elements — Part 1: Airborne sound insulation between rooms," and ISO 10848 which is comprised of five separate standards. Supplemental tabulations were incorporated providing, "Options for Design and Construction of Junctions and Flanking Surfaces to Address Horizontal and/or Vertical Sound Transmission Paths." Furthermore, limitations on sound ratings of fans in terms of "sones" was incorporated through reference to CAN/CSA-C260-M, "Rating the Performance of Residential Mechanical Ventilating Equipment," and HVI publication 915, "Loudness Rating and Testing Procedure."

15 Discussion

The Canadian Commission of Building and Fire Codes (CCBFC) is the organization reviewing further changes to the NBCC. At this time, there are a number of topics of interest. Future changes are being considered for impact insulation class (IIC) in terms of making performance testing mandatory, for making controls over the construction of exterior facades a topic area that would allow for greater control of exterior noise intrusion, and other methods of design and construction that would limit problematic experience of dwelling residents due to the low-frequency sources that are typically found within service rooms such as mechanical rooms. An additional possibility involves the extension of the STC provisions to both educational and healthcare facilities nationwide which would greatly expand the scope of application of the acoustical provisions of the NBCC to a wider range of buildings.

16 Conclusion

The progression of the NBCC from 1941 through to the most recently adopted version in 2015 contains a steady progression of the acoustical requirements for residential dwellings. From the earliest point in time, a minimum of sound transmission performance was stipulated as a means to limit intrusive noise between dwellings. Further investigation is underway to determine if and when further additions and refinements of the NBCC are favoured which could occur within the next publication expected in the year 2025.

Acknowledgments

The author would like to thank Morched Zeghal of Codes Canada for sharing the historical information about the past versions of the model NBCC that are the basis for this paper, and for ongoing coordination of CCBFC activity pertaining to the NBCC 2025 code cycle.

MEASUREMENT OF ACOUSTIC RESISTANCE OF PERFORATED PLATES SUBJECTED TO A PULSATED GRAZING FLOW

Jean-Michel Coulon ^{*1}, Xukun Feng ¹, Zacharie Laly ¹ and Nouredine Atalla ¹

¹CRASH, Centre de Recherche Acoustique-Signal-Humain, Université de Sherbrooke, Canada

1 Introduction

High porosity macro-perforations can be found in the silencers of the intake and exhaust systems of various fluid machines. In linear acoustics, because their dimensions are much larger than viscous boundary layer, their impedance is mainly reactive. At high amplitude non-linear effects [1-5] are associated with an additional resistance, proportional to the acoustic velocity in perforations. In presence of a grazing flow, the resistance increases linearly and the reactance decreases with friction velocity in the main pipe [6-8]. In highly pulsated flows the two problems are coupled. It is admitted [5] that when the mean velocity of the flow is higher than the acoustic velocity in perforates this tends to linearized the impedance (Goldman criteria). Most of these results were based on experiments limited to 160 dB. However, in some practical applications, levels can reach 180 dB, Mach number can reach 0.3 and porosity from 5% to 40%. These are the orders of magnitude of pulsated flow that we propose to explore in this study.

As described in the section 2, an electropneumatic source was built specially for this application. In section 3, the impedance extraction method is presented. In section 4, the results are analyzed as function of the mean flow velocity in main pipe and the acoustic velocity in perforations. The aim is to understand the balance between these two parameters for high porosity macro-perforations.

2 Experimental set-up

The experimental set up illustrated in Fig. 1 consists of a harmonic acoustic pneumatic source [9]. Compressed air flows from a plenum chamber through the entire line which is made of a rotating control valve, a flow chopper and the grazing flow section. The air in the plenum is generated by a compressor and a venturi flowmeter measures the mass flow rate q_m . The alimentation pressure P_{alim} in the plenum is regulated by a regulator placed upstream. The flow chopper constituted by a wheel with 6 or 8 apertures is driven in rotation by a brushless motor. The apertures generate noise at a frequency of six or eight times the rotation frequency of the motor. Four dynamic pressure sensors are used to measure the transfer matrix of the grazing flow section using the two-load method [10]. The first measurement is made with an anechoic termination as shown in Fig. 1 and the second

measurement is made with an opened termination. Four different 250 mm long plates were tested, perforated with 3mm diameter holes with different porosities (5%, 10%, 23% and 40%). They were backed with eight cavities 50 mm long.

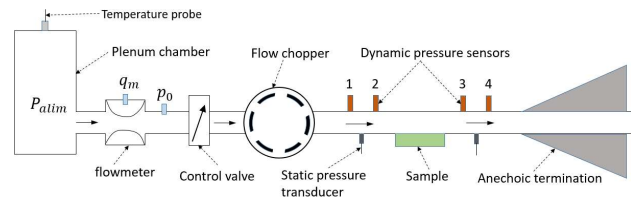


Figure 1: Experimental set up using harmonic acoustic pneumatic source

3 Determination of the grazing impedance

After the measurement of the transfer matrix using the two-load method, the grazing flow impedance of the perforated plate is calculated using an indirect method. In a first step, the two axial wavenumbers are calculated from the experimental transfer matrix. Afterward using Ingard-Myers boundary condition [11], an overdetermined system with 4 equations and 2 unknowns, is obtained. This can be solved using a least square method and the surface impedance of the perforates can be calculated. The transfer impedance is calculated by removing the impedance of the backing cavities.

4 Experimental data analysis

In this chapter, the measured impedance is analyzed as function of the mean flow velocity in main pipe and the acoustic velocity in the perforations. Because this parameter cannot be measured directly, it was decided to compute it numerically with GT-POWER [12]. The whole set-up was modeled in 1D, as compressed air flowing from a reservoir through a periodically fluctuating orifice area before entering into the grazing flow section and finally emerges into the atmosphere. By averaging the acoustic velocity in front of all the 8 cavities, the acoustic velocity across the grazing flow section was computed.

Because reflection coefficients of both terminations were quite close in low frequency, only results above 400 Hz were considered and averaged in the frequency range [400Hz, 800Hz]. With the different configurations of diaphragm, vessel pressure and plate porosity, different combinations (Flow Mach number, Acoustic Mach number) are obtained. Flow Mach number is ranging from 0.025 to 0.275 and acoustic Mach number from 0.027 to 0.245. Considering the

* jean-michel.coulon@cta-brp-udes.com

noise levels that were measured in the section, non-linear effects can be expected. In order to quantify them, the linear component of the resistance has to be removed from the experimental data. Because the linear resistance was not measured directly, the Cummings model [7] were used. Once the non-linear resistance was extracted, it was interpolated as a linear function of the acoustic velocity in perforates, as it is admitted in literature. As shown in Fig. 2, it is possible to compare the linear component of the resistance with the non-linear component as functions of the flow and acoustic Mach numbers. As it was stated by Goldman but for low porosity [5], when the flow in the main pipe decreases, the non-linear effects tend to appear much “faster”. It is possible to draw a line separating the dominance of both domains.

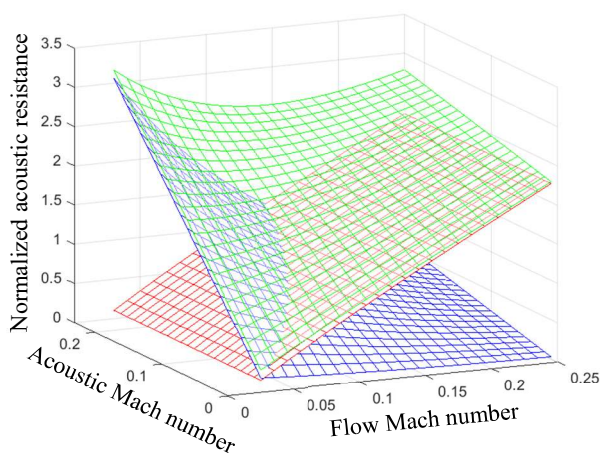


Figure 2: Acoustic resistance and its components as function of the acoustic Mach number and the flow Mach number. □ Total resistance, □ Nonlinear component, □ linear component.

5 Conclusion

The objective of this study was to investigate the behavior of a macro-perforated plate subjected to a pulsated grazing flow. In order to explore noise levels up to 180dB, an electropneumatic source was built. By changing the flow, the acoustic output of the source and the plate porosity, it was possible to tune acoustic Mach number in perforates between 0.023 and 0.245 and main flow Mach number between 0.025 and 0.275. The transfer matrix of the section was measured using a two-load method, then the impedance of the plate was calculated using a least square method. In order to highlight possible non-linear effects, the results were compared to an existing linear model. The measured acoustic resistance is much higher than the linear one for low Mach numbers, showing the competition between nonlinear effects and the main flow. These results agree qualitatively with the Goldman criteria defined for micro-perforated plates.

Acknowledgment

This study was supported by the Natural Sciences and Engineering Research Council of Canada (NSERC) and Bombardier Recreational Products (BRP)

References

- [1] Z. Laly, N. Atalla & S.-A. Meslioui, “Acoustical modeling of micro-perforated panel at high sound pressure levels using equivalent fluid approach,” *J. Sound. Vib.*, 427 (201/8),134-158.
- [2] U. Ingard, H. Ising, “Acoustic nonlinearity of an orifice,” *J. Acoust. Soc. Am.*, 42 (1) (1967) 6–17.
- [3] A. Komkin, A. Bykov, M. Mironov, “Experimental study of nonlinear acoustic impedance of circular orifices.” *J. Acoust. Soc. Am.*, 148 (3), September 2020.
- [4] N. S. Dickey, A. Selamet, “The effect of high-amplitude sound on the attenuation of perforated tube silencers” *J. Acoust. Soc. Am.*,108 (3), Sept 2000
- [5] L. Goldman, R. L. Panton, “Measurement of the acoustic impedance of an orifice under a turbulent boundary layer,” *J. Acoust. Soc. Am.*, Vol. 60, No. 6, Dec, 1976
- [6] J. W. Kooi and S. L. Sarin, “An experimental study of the acoustic impedance of Helmholtz resonator arrays under a turbulent boundary layer” *AIAA Pap.*, 1981–1998 ~1981.
- [7] A. Cummings, “The effects of grazing turbulent pipe-flow on the impedance of an orifice,” *Acta Acustica*, 61, 233–242 ~1986.
- [8] R. Kirby and A. Cummings, “The impedance of perforated plates subjected to grazing gas flow and backed by porous media,” *J. Sound. Vib.*, 217, 619–636 ~1998
- [9] A. Allard, N. Atalla & P. Micheau, “The equivalent fluctuating area for modelling harmonic acoustic pneumatic sources (HAPS),” *Applied Acoustics*, 172 (2021) 107602
- [10] M.L. Munjal, A.G. Doige, “Theory of a two source-location method for direct experimental evaluation of the four-pole parameters of an aeroacoustics element,” *J. Sound. Vib.*, 141(2) (1990), 323-333.
- [11] D. Hervé, D. Wim, D.R. Wim, “Indirect measurement of liner impedance under grazing flow using the two-port reduction method,” *Inter noise Congress*, Madrid, 2019.
- [12] Y. Mochkaai: “GT-POWER as a tool for acoustic and dynamic optimization of exhaust systems,” *GT-SUITE User Conference 2009 Frankfurt – Nov 2009*

NOISE REDUCTION IN DUCTS USING HELMHOLTZ RESONATORS

Sourabh Dogra ^{*1}, Arpan Gupta ^{†1}, Umberto Berardi ^{‡2}

¹Indian Institute of Technology Mandi, Himachal Pradesh, India.

²Ryerson University, Toronto, Ontario, Canada

1 Introduction

Ducts are an important part of the modern-day building. Ducts are used to circulate the fresh air in the buildings. The movement of the air in the duct creates noise throughout the building. People residing in these building are exposed to these noises for a very long time and leads to various health issues like tinnitus, hypertension and loss of hearing [1,2]. Various researches are being carried out around the world on this issue. Helmholtz resonators are often utilized in the literature to address these issues [3,4]. Helmholtz resonators attenuate the sound of the desired frequency by properly designing the geometry. But the attenuation band is very narrow. In this paper we have designed an arrangement of different Helmholtz resonators which are able to produce large amount of the transmission loss over large number of frequencies. These theoretical studies are validated with numerical results.

2 Methodology

2.1 Theoretical analysis

Helmholtz resonators are analysed as lumped mass system and modelled as spring mass system. The natural frequency of the lumped mass system is given by:

$$\omega_0 = \frac{c}{2\pi} \sqrt{\frac{A}{vL}}$$

Here ω_0 is natural frequency, c is the speed of the sound, A is the area of the neck, v is the volume of the back cavity and L is the length of the neck.

The Helmholtz resonators fitted over the ducts are shown in the Figure 1. These types of the configuration are analysed by using classical transfer matrix (TM) theory. According to this theory the transfer matrix of the Helmholtz resonator fitted over the duct is written as:

$$\begin{bmatrix} p_0 \\ u_0 \end{bmatrix} = \begin{bmatrix} 2 \times 2 \\ \text{TM}_{Duct} \end{bmatrix} \begin{bmatrix} 2 \times 2 \\ \text{TM}_{HR} \end{bmatrix} \begin{bmatrix} 2 \times 2 \\ \text{TM}_{Duct} \end{bmatrix} \begin{bmatrix} p_d \\ u_d \end{bmatrix} \quad (1)$$

P and u are the pressure and velocity at inlet (0) and outlet (d) of the Helmholtz resonator.

The transfer matrix for the uniform duct is given by [5]

$$\begin{bmatrix} p_0 \\ u_0 \end{bmatrix} = \begin{bmatrix} \cos(kh) & jY \sin(k_0h) \\ jY \sin(k_0h) & \cos(kh) \end{bmatrix} \begin{bmatrix} p_d \\ u_d \end{bmatrix} \quad (2)$$

For the Helmholtz resonator the mounted over the duct the transfer matrix is

$$\begin{bmatrix} p_0 \\ u_0 \end{bmatrix} = \begin{bmatrix} 1 & 0 \\ \frac{1}{Z_{HR}} & 1 \end{bmatrix} \begin{bmatrix} p_d \\ u_d \end{bmatrix} \quad (3)$$

Here, Z_{HR} denotes the impedance of the Helmholtz resonator and is calculated as

$$Z_{HR} = \frac{\omega^2}{\pi c} + j\omega\lambda \frac{l_e}{A} + \frac{c^2}{j\omega v}, \quad l_e = l + 0.85d$$

Finally, Transmission loss (TL) is calculated using the elements of the Eq (1) as:

$$TL = 20 \log_{10} \left| \frac{T_{11} + \frac{T_{12}}{\rho c} + T_{21} \rho c + T_{22}}{2e^{jkd}} \right| \quad (4)$$

2.2 Numerical analysis

The numerical analysis is carried in the Finite Element Software COMSOL Multiphysics 5.0. The frequency domain under pressure acoustic study in COMSOL are used to perform the analysis. The acoustic model of the different Helmholtz resonators mounted over the duct is shown in fig.1(a). The domain is discretized using tetrahedron element. The maximum size of the mesh element is kept $\lambda/15$ time the maximum investigated frequency. The acoustic analysis is performed by normally incidenting on the plane sound wave field of pressure 1 Pascal through sine sweep at one end. The transmission loss with in the duct is analysed using the expression.

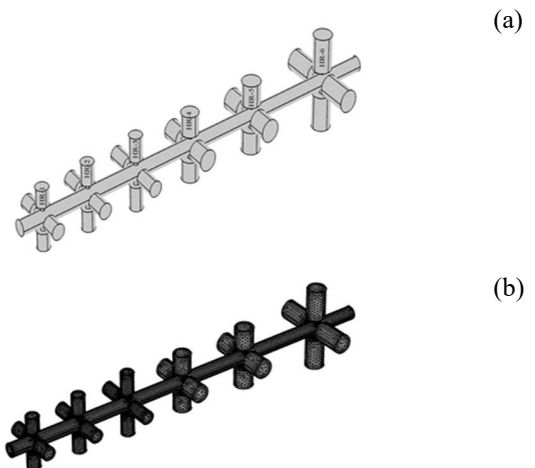


Figure 1: (a) Geometry of the different Helmholtz resonators mounted over the duct. (b) Mesh image of the different Helmholtz resonators in series.

* sourabh.sd47@gmail.com

† agupta@iitmandi.ac.in

‡ uberardi@ryerson.ca

3 Results

A 3D model of the Helmholtz resonators fitted over the duct is prepared in COMSOL. Twenty-four Helmholtz resonators of six different sizes are analyzed. The diameter of the duct is 22.5 mm. The size of the Helmholtz resonators is chosen is such that low range frequencies can be analyzed. The geometry and the natural frequencies of the different Helmholtz resonators are given in the Table 1. Plane wave radiation condition is used at the two ends of the duct. The rest of the boundaries of the duct and the Helmholtz resonator are assumed to be hard so that no sound transmission takes place through these boundaries.

Table 1: Geometric parameters of resonators.

Configuration	Cavity		Natural frequency (Hz)
	Radius(mm)	Height(mm)	
HR-1	22.5	50	530
HR-2	22.5	60	480
HR-3	22.5	70	442
HR-4	30	60	364
HR-5	32.5	65	322
HR-6	32.5	102	354

The system is analyzed in the frequency range of 50 to 1500 Hz. The theoretical transmission loss is calculated by using the Eq (4). The length of the neck is 15 mm whereas the radius of the neck is 7.5 mm. The dimension of the neck is same for all configurations.

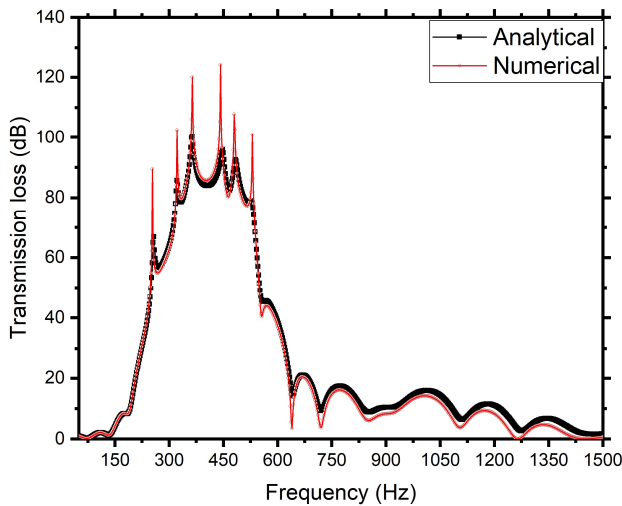


Figure 2: Comparison of theoretical and numerical Transmission loss.

Plugging the various parameters in the Eqs. (2) (3) transfer matrix for the duct and Helmholtz resonators is estimated. Finally multiplying these transfer matrices as given in Eq (1) gives the transfer matrix for one pair of the resonators. Similarly finding the transfer matrix of all the resonators pairs and then multiplying all gives the transfer matrix of the proposed arrangement.

4 Discussion

Transmission loss for the different Helmholtz resonators is given in the table. 2. The theoretical transmission loss is in good agreement with the numerical results as shown in Figure 2. The large increase in the transmission loss can be observed from the table corresponding to the natural frequency of different Helmholtz resonators. There is a widening of the transmission loss over the frequency near by the natural frequencies. This is mainly due to the combined effect of absorption of the sound waves due to the Helmholtz resonators and Bragg reflection phenomenon due to the periodic arrangement of the array of the Helmholtz resonators.

Table 2: Transmission loss corresponding to various HR.

Configuration	Transmission loss
HR-1	89 dB
HR-2	102 dB
HR-3	120 dB
HR-4	124 dB
HR-5	107 dB
HR-6	100 dB

5 Conclusion

In this paper we have designed a system of Helmholtz resonators to control the noise generated from the moving air in the duct. Helmholtz resonator can absorb the sound of the desired frequency by properly designing its geometry. We have used different Helmholtz resonators in the combination of the serial and parallel arrangements. The system is analysed numerically in COMSOL and validated by a theoretical model. The theoretical and numerical results both are in good agreement. The proposed model provides a significant amount of transmission loss. There is broadband low frequency attenuation due to combine effect of the Bragg reflection and Helmholtz resonance. These types of the model are very useful where the space is not a constrain.

Acknowledgments

This research is supported by DST India and IC-IMPACTS, Canada under project DST/INT/CAN/P-04/2020.

References

- [1] Rajalakshmi, R., John, N. A., and John, J., 2016, "Review on Noise Pollution and Its Associated Health Hazards," *Sch. J. Appl. Med. Sci.*, **4**(ISSN 2347-954X), pp. 500–503.
- [2] Waddington, D. C., and Oldham, D. J., 2007, "Noise Generation in Ventilation Systems by the Interaction of Airflow with Duct Discontinuities: Part 1 Bends," *Build. Acoust.*, **14**(3).
- [3] Cai, C., and Mak, C. M., 2016, "Noise Control Zone for a Periodic Ducted Helmholtz Resonator System," *J. Acoust. Soc. Am.*, **140**(6), pp. EL471–EL477.
- [4] Wang, X., and Mak, C.-M., 2012, "Wave Propagation in a Duct with a Periodic Helmholtz Resonators Array," *J. Acoust. Soc. Am.*, **131**(2), pp. 1172–1182.
- [5] Fahy, F., 2001, *Foundations of Engineering Acoustics*.

THE EFFECTS OF ACOUSTICAL CEILING PANEL TYPE AND PENETRATIONS FOR SERVICES ON VERTICAL SOUND ISOLATION INSIDE BUILDINGS

Gary S. Madaras*¹

¹ Rockfon 4849 S. Austin Ave., Chicago, IL 60638, United States of America.

1 Introduction

Preventing noise from transmitting between enclosed rooms is important inside buildings. Inter-room noise isolation applies to enclosed rooms horizontally adjacent to one another on the same floor as well as between vertically adjacent rooms on different floors. Much is known about constructing partitions to achieve the desired level of noise isolation. There have been multiple, comprehensive studies on the noise isolating performance of partitions.¹ There is far less information and test data about the noise isolation performance of floor-ceiling assemblies, especially in nonresidential buildings with concrete floors and suspended acoustic panel ceilings below them.

Without these tests, architects and acousticians have resorted to a few general 'rules of thumb.' One of these is to achieve greater vertical noise isolation—the acoustic ceiling panels suspended below the concrete slab should,

1. be made of a certain material, such as mineral fiber;
2. have a certain minimum weight of 5 kg/m² (1 psf); and
3. have a minimum ceiling attenuation class (CAC) of 35.

Recent testing used a consistent, baseline, concrete floor slab and three suspended acoustic panel ceilings of different material types, weights, and acoustic performances to investigate the potential effects acoustic ceilings have on the noise isolation performance of floor-ceiling assemblies.

2 Method

Acoustic testing was performed at NGC Testing Services in Buffalo, New York, in January 2020 by a senior test engineer. The laboratory is accredited by the National Voluntary Laboratory Accreditation Program (NVLAP) (Laboratory Code 200291-0). STC tests were performed according to ASTM E90, *Standard Test Method for Laboratory Measurement of Airborne Sound Transmission Loss of Building Partitions and Elements*, and E413, *Classification for Rating Sound Insulation*.

A baseline STC test was performed on a 133-mm (5 1/4-in.) thick, normal weight, concrete floor slab (293 kg/m²/60 psf) poured onto a steel deck with 38-mm (1 1/2-in.) deep flutes (20 kg/m²/2 psf). Vinyl composite tile (VCT, 4 kg/m²/0.80 psf) flooring was adhered to the top of the concrete slab. The total weight of the floor construction was 307 kg/m² (62.8 psf). There was no acoustic panel ceiling suspended below the floor construction for the baseline test. Following the baseline test, a standard, 24-mm (15/16-in.), metal, tee-bar, ceiling grid was installed 508 mm (20 in.)

below the concrete floor and remained in place for all subsequent STC tests.

Three different types of acoustic ceiling panels were installed in the suspension grid and tested independently. All three ceiling panel types were 610 mm (24 in.) wide (nominal) x 610 mm (24 in.) long (nominal) x 19 mm (3/4 in.) thick (nominal) with painted white finishes and square, lay-in edges. The main differences between the ceiling panel types were the core material types, panel weights, and acoustic performances.

	Material	Weight
Ceiling panel type 1	Mineral fiber	5.37 kg/m ² (1.10 psf)
Ceiling panel type 2	Stone wool	3.37 kg/m ² (0.69 psf)
Ceiling panel type 3	Glass fiber	1.86 kg/m ² (0.38 psf)

CAC is a measure of a ceiling panel's ability to attenuate noise transmitting through a room's acoustic ceiling, over a partition terminating in height at the level of the suspended ceiling (creating a shared plenum space above the ceiling) and back down through the acoustic ceiling in the adjacent room. It is a double-pass rating as the sound passes through the ceiling two times. While CAC is not applicable directly to single-pass vertical noise isolation in the presence of a contiguous concrete slab, ratings are provided because industry rules of thumb, even though not technically accurate, include the use of CAC 35+ panels to help with controlling vertical transmission of noise through floor-ceiling assemblies. The CAC ratings of the ceiling panels ranged from 20 to 35, representing the most common performance range used in the industry.

The noise reduction coefficient (NRC) is the amount of sound absorbed by a surface like an acoustic ceiling panel. It varies between 0.0 (no sound absorption) and 1.0 (a lot of sound absorption). Ceiling panels with higher NRC ratings decrease noise levels and reverberation, making speech in enclosed rooms more intelligible and preventing noise from traveling farther distances in open spaces. The NRC ratings of the ceiling panels ranged from 0.75 to 0.95. This range represents the mid to high range available in the industry. Low performing panels of NRC 0.70 and below were excluded.

Two series of STC tests were performed. For the first series, all suspension grid modules were filled with only the acoustic ceiling panels. There were no light fixtures or air distribution devices implemented into the ceiling systems. For the second series of tests, nine ceiling panels were replaced by six recessed light troffers, two plaque-style supply air diffusers, and one eggcrate-style return air grille. These two series of tests, with and without building service penetrations, were conducted so that any effects of the noise leaking through the penetrations on overall vertical noise

*gary.madaras@rockfon.com

isolation, such as would be the case in real buildings, would be documented.

3 Results

TL and STC results are provided in Figure 1 (no penetrations in the ceilings for building systems devices) and Figure 2 (penetrations in the ceilings for building systems devices). The baseline concrete on steel deck with VCT flooring on top rated STC 47, which is three points below the minimum STC 50 requirement in standards such as the Facility Guidelines Institute (FGI) for healthcare buildings and ANSI/ASA S12.60, *Acoustical Performance Criteria, Design Requirements, and Guidelines for Schools*.

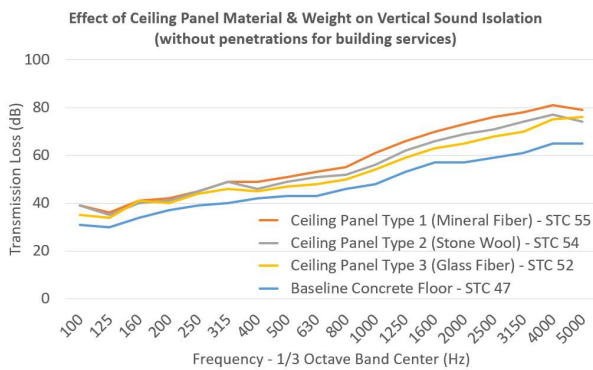


Figure 1: All three acoustic ceiling panel types increase noise isolation performance (STC 52-55) compared to the concrete floor slab alone (STC 47) and higher than the STC 50 rating in the standards. Without penetrations in the ceiling for building services, the variance in performance amongst the three ceiling types (3 STC points) was only slightly larger than when the penetrations were included (2 STC points).

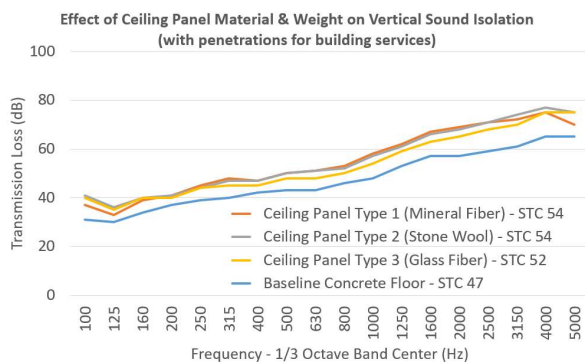


Figure 2: All three acoustic ceiling panel types increase noise isolation performance (STC 52-54) compared to the concrete floor slab alone (STC 47) and higher than the STC 50 rating in the standards even with the penetrations for building systems.

Adding an acoustic ceiling to the baseline floor increased the STC rating of the assembly, on average, six and a half STC points. Adding any of the three acoustic ceiling panel types resulted in assembly ratings that were two to five STC points higher than the minimum STC 50 in the standards. The three ceiling panel types varied by only three STC points when there were no penetrations for building systems and

differed by only two STC points when the penetrations for lights, supply air, and return air were present.

4 Discussion

The results in Figures 1 and 2 show that, while adding a suspended acoustic ceiling below a concrete slab makes a significant improvement in noise isolation (STC), the actual type of ceiling panel (core material, weight, CAC rating, NRC rating) does not have a meaningful impact. While some might initially consider the two STC point difference for panel type 1 compared to panel types 2 and 3 meaningful, the author suggests the difference is immaterial and imperceptible, especially when considering the precision and bias of the test method as defined in the standard.

Adding an acoustic panel ceiling below the slab, on average, increases the vertical noise isolation six-and-a-half STC points. Since absorption in the rooms below may also be required to comply with maximum permissible reverberation times or minimum ceiling NRC ratings in the standards, the addition of an acoustic panel ceiling appears to be the wise approach for complying with both the vertical noise isolation and interior room acoustic requirements.

Since the acoustic ceilings, on average, increase the noise isolation performance of the floor-ceiling assembly to STC 53 to 54, three to four STC points higher than the goal STC 50 minimum in the standards, the thickness and weight of the concrete slab used in these tests could be decreased.

5 Conclusions

Testing shows current design rules of thumb, namely that acoustic ceiling panels should be of a certain material type, weight, or CAC rating for improved vertical noise isolation, do not hold true. In fact, these rules may be leading to worse overall acoustic conditions for building occupants and noncompliance with the absorption or reverberation time requirements if the ceiling panels have a low NRC of 0.70 or less.

While selecting and specifying acoustic ceiling panels for buildings, design professionals should focus on selecting the appropriate high NRC rating.² As long as the acoustic panel ceiling is included in the design, architects can be confident the ceiling panel material, weight, and CAC rating is not important to the overall floor-to-floor, airborne, noise isolation performance of the floor-ceiling assembly.

Acknowledgements

Gratitude is extended to Rockfon® and ROCKWOOL® for taking an interest in and dedicating resources toward furthering our industry-wide understanding of how sound and architecture interact.

References

- [1] California Department of Health Services, *Catalogue of STC and IIC Ratings for Wall and Floor/Ceiling Assemblies*, Western Wall and Ceiling Contractors Association.
- [2] Madaras, G. Specifying Ceiling Panels with a High NRC. *The Construction Specifier*, February 2020.

BIO-INSPIRED FLOW VELOCITY MICROPHONE: ACOUSTIC SIMULATION OF ENCAPSULATING PACKAGES

Kiran Vadavalli^{*1}, Jérémie Voix^{†1}, Frédéric Lepoutre^{‡2}, and Stephane Leahy^{§2}

¹Université du Québec, École de technologie supérieure, Montréal, QC, Canada

²Soundskrit Inc, 1751 Rue Richardson #5102, Montreal, Quebec, Canada H3K 1G6

1 Introduction

With the emergence of voice assisted devices like smart speakers and wireless earbuds, there is a need to design voice capture systems that are more robust to background noise and reverberation. Current directional far field audio capture systems are based on omnidirectional microphone arrays or pressure gradient microphones that provide bidirectional polar pickup patterns. The array microphones suffer from lower sensitivities and directionality limited to few bands. The fundamental sensing mechanism of such systems is based on ‘acoustic pressure’ sensing which is scalar in nature, with no directional information. On the contrary, the use of thin bio-inspired nano hair follicles as sensors (for eg : mimicking the moving spider auditory sensing) enable “acoustic particle velocity” sensing that is vectorial quantity carrying spatial information. This inherent directional nature of acoustic particle velocity enables the development of novel directional microphones.

The current research focuses on the optimal acoustic design of sound ports and signal paths to integrate this kind of velocity microphone into various consumer use cases by retaining or improving the acoustic performance of the bare (a.k.a. un-encapsulated flow sensing element. For comparison of simulation models, two case studies (closed pipe & open pipe) were presented. A multiphysics FEM software was used to model these cases in pressure & thermoviscous acoustic modules. The key acoustic performance targets for these cases, such as resonant frequencies, sensitivity and directivity were presented with theoretical validation.

2 Bio-inspired velocity microphone

The innovative technology behind the velocity microphone was invented by Professor Ronald N. Miles [1] at Binghamton University. Soundskrit and Professor Miles collaborated [2] to advance the design of nano sensors for consumer industry applications. Soundskrit has leveraged this novel bio-inspired flow velocity microphone to overcome the directional audio capture challenge, while maintaining high fidelity audio at a broad range of frequencies in its latest generation microphone. Fundamentally the sensing technology is based on how insects perceive sounds even at longer distances in the presence of background noise as shown in Figure 1. Acoustic sensitivity of these latest generation microphones have been tested at Soundskrit’s labs as shown in Figure 1 with PCB, two pressure microphones and a speaker source. In an “out-

of-plane”, acoustic flow in the plane of sensor fiber is ignored and out of plane signal is only captured. A schematic representation of a basic “out-of-plane” MEMS package, in a Figure 2, show the sensor fibers and the resulting acoustic flow.

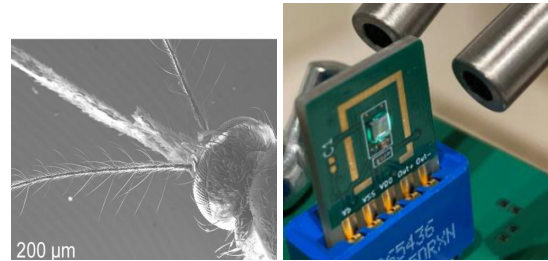


FIGURE 1 – Closeup view of insect hair (Left) [2], Soundskrit Mic (Right)

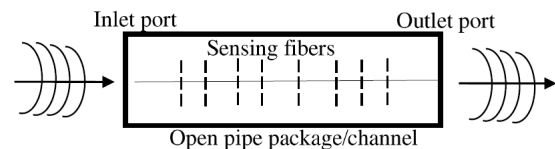


FIGURE 2 – Basic schematic of Soundskrit sensing mechanism

2.1 Acoustic modeling and simulation setup

Two simulation cases were modelled in COMSOL Multiphysics v5.6 (COMSOL AB, Stockholm, Sweden) to predict and compare the key acoustic performance parameters. The first case is a closed pipe (single port), which is a representative of sound path for a pressure microphone with diaphragm. The second case is an open pipe (dual port), which is a representative of sound path for a flow velocity microphone package. The open-pipe case falls under “out of plane” sensing mode as described in Section 2. A computationally efficient 3D hybrid model comprising of pressure model for inlet & outlet acoustic domains and thermoviscous acoustic model for pipe cavity were developed in COMSOL, as illustrated in Figure 3. In an open pipe model, both inlet and outlet acoustic domains were modelled to excite the pipe with unit pressure background field on both ports. In case of a closed pipe model, only inlet acoustic domain is used to excite the inlet port with hard wall termination at other end. For a fair comparison between two cases, the dimensions of the closed pipe & the open pipe cases were similar with a length of 10 mm and diameter of 2 mm. The size of acoustic domains is equal to six times the diameter of pipe. Acoustic flow velocity of sensor fiber and air velocity are almost similar with very tiny sensory fiber in

*. kvadavalli@critias.ca

†. jeremie.voix@etsmtl.ca

‡. frederic.lepoutre@soundskrit.ca

§. stephane.leahy@soundskrit.ca

the order of nanometers as per [3]. The acoustic simulations predicted the air velocity spectrum at the center of the open pipe, as well as the pressure at the closed end of the pipe near diaphragm for the closed pipe.

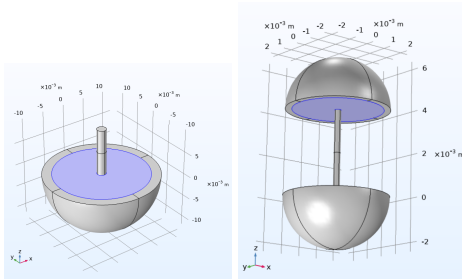


FIGURE 3 – 3D COMSOL model of closed pipe(left) & open pipe(right)

3 Results and Discussion

3.1 Sensitivity response

Resonant frequency for a closed pipe pressure response can be observed around 7.5 kHz which is close to theoretical value of 8.5 kHz from organ pipe theory as in Figure 4. Similarly for an open pipe resonant peak can be seen around 17 kHz close to its theoretical value of 17.1 kHz and therefore validating the mode developed. For similar pipe dimensions, an open pipe case has a higher value of resonant frequencies. In fact, the velocity sensitivity of the open pipe case has a higher gain and much flatter response over a wide range of frequencies compared to the pressure response from a closed pipe case.

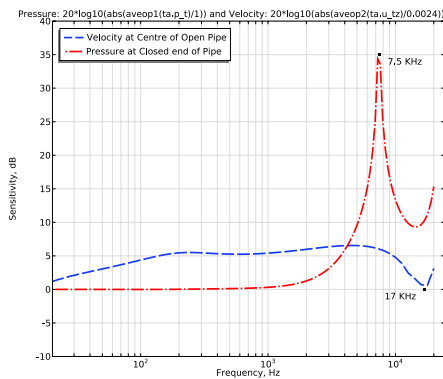


FIGURE 4 – Sensitivity for Closed pipe and Open pipe

3.2 Directivity pattern

The omni-directional nature of a pressure microphone near and above 8 kHz is lost due to the presence of a resonant peak as shown in Figure 5. Above that resonance, it becomes subcardioid and even supercardioid at much higher frequencies. Unlike a pressure microphone, the directivity of an open pipe case for a velocity microphone in Figure 6 maintains the so-called “figure 8” directivity pattern even at a higher frequency of 16 kHz with 20 dB off-axis rejection, which is beneficial for far-field audio capture.

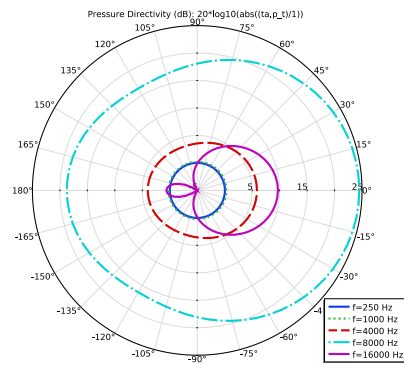


FIGURE 5 – Pressure Directivity at the closed end of pipe

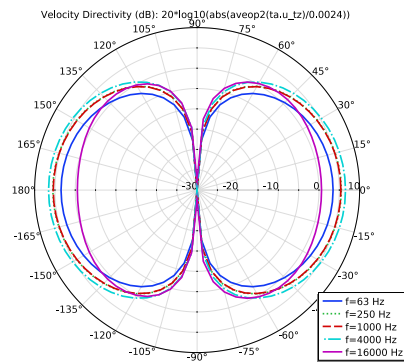


FIGURE 6 – Velocity Directivity at the center of open pipe

4 Conclusions

The directivity of a closed pipe for a pressure microphone has an omni-directional nature as expected with a resonant peak well ahead in comparison with an open pipe for the same dimensions. Resonant frequencies compare well with theory, validating the simulation. Directivity of an open pipe case for a velocity microphone shows a perfect “figure 8” pattern even at higher frequencies as well as a moderate boost in sensitivity depending on the dimensions of the open pipe. Finally, this simulation methodology can be extended to more complicated sound path configurations that can utilize in-plane sensing and aesthetic placement of sound ports for various use-cases.

Acknowledgments

The authors would like to acknowledge funding received from Soundskrite through the MITACS Accelerate program (IT# 20227) and software support from CMC Microsystems.

References

- [1] RN Miles, Q Su, W Cui, M Shetye, FL Degertekin, B Bicen, C Garcia, S Jones, and N Hall. A low-noise differential microphone inspired by the ears of the parasitoid fly *ormia ochracea*. *The Journal of the Acoustical Society of America*, 125(4):2013–2026, 2009.
- [2] Ronald N. Miles, Mahdi Farahikia, Stephane Leahy, and Ahmed Abdel Aziz. A flow-sensing velocity microphone. In *IEEE SENSORS*, pages 1–4, 2019.
- [3] Jian Zhou and Ronald N Miles. Sensing fluctuating airflow with spider silk. *Proceedings of the National Academy of Sciences*, 114(46):12120–12125, 2017.

ACOUSTICS OF INFRASOUND FROM WIND TURBINES USING CROSS-SPECTRA

John Vanderkooy*¹,

¹Dept. of Physics and Astronomy, University of Waterloo, Waterloo ON Canada N2L3G1

1 Introduction

Measured wind turbine (WT) infrasound near homes often contains mostly wind noise, not the true acoustic signature of the WTs. With appropriately-spaced multiple microphones, the wind noise is essentially random, while the blade pass frequency (BPF) signals are largely coherent, allowing a determination of the total acoustic power (pressure²) from the WTs, as well as the remaining random wind-induced noise.

Exterior and interior microphone signals will be strongly affected by both wind noise and true WT acoustic signals. Turbulent eddies and random air parcel motion may display spectral maxima around 0.2 Hz, but there is enough energy at frequencies up to 10 Hz or so that it often blankets the true infrasonic WT acoustic signals, which are produced by the fluctuations from the moving blades interacting with the supporting pylon. In what follows we distinguish the pseudo-noise caused by the wind itself, from the true acoustic WT signals that propagate at sound speed.

Earlier we have shown [1] that the total infrasound level can be up to 20 dB above the acoustic pulse level from the nearest WT, and even 10-15 dB higher than a whole wind farm of 100 units. The present paper shows how the acoustic power from the WTs can be separated from the often dominating wind noise, using appropriate microphone arrangements and specific processing. As a byproduct, the acoustic transmissibility from outside to inside a house can also be determined.

2 Experiments and analysis

An important experiment for this work was the measurement of infrasound for a typical 2-storey home with a microphone on the porch at the front door, well covered with fiberfill and a blanket, and another about 15m away at the back deck, similarly screened from the wind. It was a moderately windy day and there were no WTs within at least 30 km from the home. GRAS 40AZ microphones with CC preamplifiers had a response down to 0.3 Hz, as measured in a sealed calibration box. The two signals were measured over a 1-hour period, sampled at 800 Hz to encompass all infrasound components and some LF audio as well. Figure 1 shows the spectra of the two signals. The microphone responses fall off below 0.3 Hz, but the true spectra actually rise even more at lower frequencies. A similar experiment with two separated microphones was carried out over flat terrain.

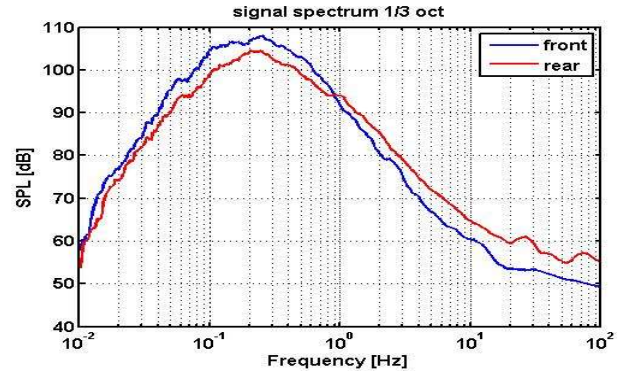


Figure 1: Spectra of the microphone signals at the front and back doors of a home far from any wind turbines.

When the two 2.88 million microphone data samples are analyzed in overlapping windowed blocks, the coherence between them is shown in Figure 2. Notice that there is little coherence between these wind-induced signals above about 0.2 Hz, which is where BPFs from WTs reside.

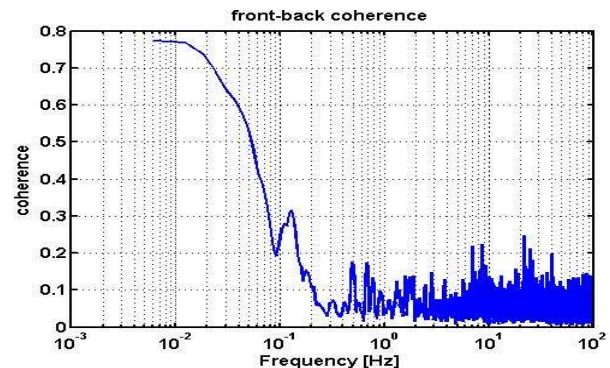


Figure 2: Coherence between the microphone signals at the front and back of a residence, with no nearby WTs.

Turbulent wind eddies that are larger than the 15m microphone separation would show coherence between them, but with random air velocities of say 5 m/s, these would not have spectral components above about 5/15 or 0.3 Hz, consistent with the plot in Figure 2. Higher frequencies such as 0.5-10 Hz would be associated with eddies smaller than 15m, so the wind noise would show no coherence in the BPF regime.

True acoustic waves from the WT blade-pylon interaction travel at 340 m/s, and at the very low BPF of WTs, signals will be almost coincident and coherent in microphones spaced only 15m apart. Thus the coherence between outside microphones at infrasonic frequencies above 0.5 Hz will be predominantly due to the true net acoustic signals from the WTs. This fortunate separation is due to the nature

*jv@uwaterloo.ca

of wind eddies, and the large difference between typical random air velocities of 2-5m/s and the speed of sound, 340m/s. The wind induced noise may be significant at BPFs, but it will not be coherent, and appropriate processing can control it.

3 Signal processing and discussion

The signals x and y at the outside microphones consist of differing random wind-induced components rx and ry , together with fluctuating WT true acoustic signals, a , which are nearly the same. We thus can model this as:

$$x = rx + a, \quad y = ry + a. \quad (1)$$

Our major goal is to determine the power of the acoustic component, a . Cross-spectral density function terms [2] between rx , ry , and a will be essentially zero (except perhaps at extremely low frequencies), but the common WT acoustic a signal in both x and y results in a nonzero component. It is easily shown that the cross-spectral density from two properly-spaced microphones will give an unbiased estimate of the acoustic spectral power $Pa(f)$ of the WT farm in either microphone:

$$G_{xy}(f) \approx G_{aa}(f) = Pa(f). \quad (2)$$

If there is also a microphone inside the residence, the acoustic amplitude transfer function T from outside to inside can also be obtained as a secondary goal. We can also describe T by its impulse response, t .

Let's continue the assumption that the two acoustic WT outside signals a are equal, that no noise is generated inside the house, and that the outside random wind signals all around the house leak in to produce an interior random signal, ri , that is also uncorrelated with rx and ry . Thus the inside microphone gets a signal z ,

$$z = ri + t**a, \quad (3)$$

where the $**$ operation is a time convolution. The averaged cross-spectrum, between the exterior and interior signals x and z , becomes

$$G_{xz}(f) \approx T G_{aa}(f) = |T| Pa(f). \quad (4)$$

Thus the ratio $|G_{xz}(f)/G_{xx}(f)|$ gives $|T|$, the frequency-dependent transmissibility. Figure 3 shows the transmissibility of a home adjacent to a wind farm of about 100 WTs. The cross-spectra displayed strong BPF lines and we implemented Eq. 4 by selecting cross-spectral data near each harmonic, joining the points between the harmonic frequencies with straight lines. Measurements were taken during the spring, so a window may have been open. The data point that exceeds unity transmissibility may indicate a resonance condition, but could also be due to some residual noise.

The total spectral power of the cross-correlation is some 9dB lower than the spectral power of either outside microphone, substantially removing the random wind noise, but not affecting the spectrum of the BPF components.

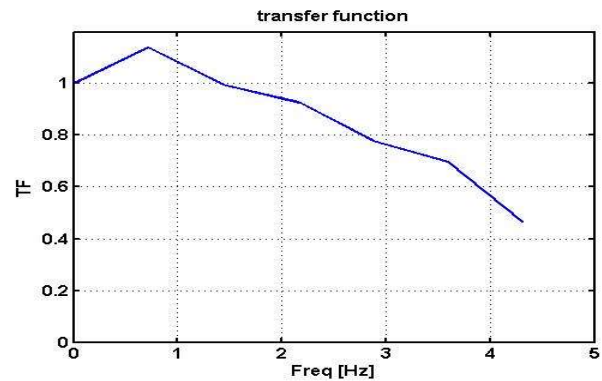


Figure 3: Transmissibility of the subject house determined from the amplitude ratios of the BPF cross-spectra.

A high-pass filter could also have been used to reduce the wind noise power, but the cross-spectral method also removes such noise in the BPF region. The random wind noise is not produced by the WTs, so the major conclusion is that infrasound from WTs may be much less than that deduced from single microphone measurements.

4 Summary

By making appropriate measurements with two exterior and one interior microphones, we can determine the total WT acoustic infrasound level, and also get a reasonable estimate of the acoustic inside/outside transmissibility. Measurements of a few wind farms show that the wind-induced infrasound is often considerably larger than the acoustic signal. If we wish to impute health effects to infrasound level, we should use these lower acoustic levels, since the wind-induced noise occurs anyway, even away from the wind farm.

Acknowledgements

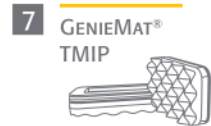
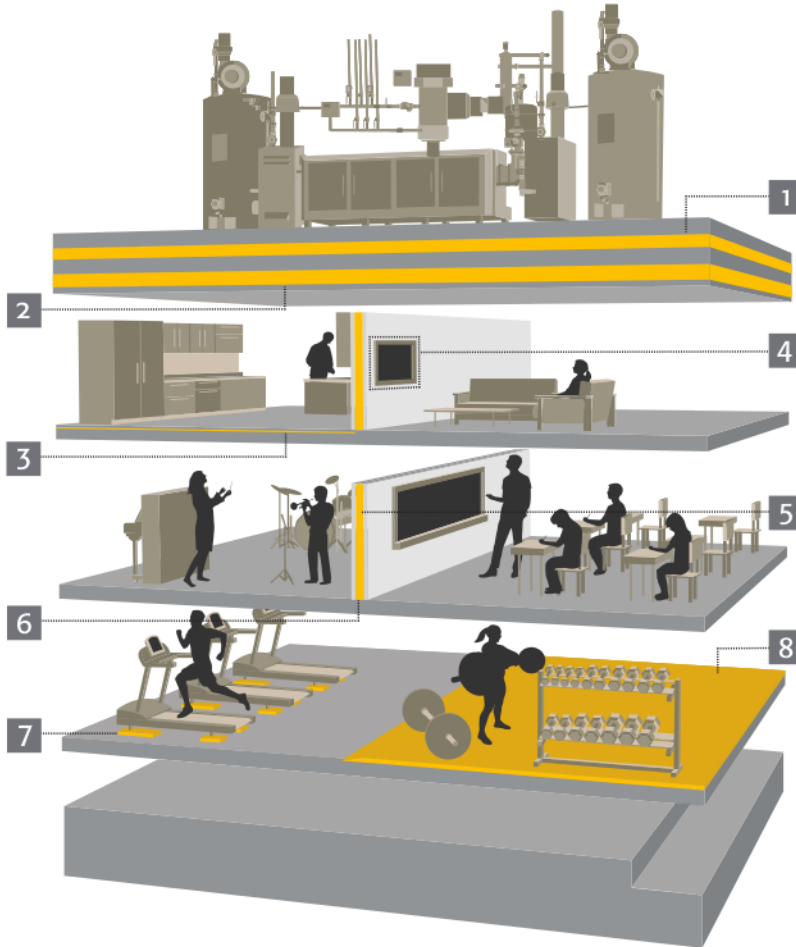
I thank Richard Mann and Kevin Krauel for participating in earlier measurements and discussions. Andy Metelka has supplied much of the data and impetus for the multi-microphone measurements.

References

- [1] J. Vanderkooy and R. Mann, "Measuring Wind Turbine Coherent Infrasound", 6th International Conference on Wind Turbine Noise (WTN2015), Glasgow 20-23 April 2015.
- [2] J. S. Bendat and A. G. Piersol, "Engineering Applications of Correlation and Spectral Analysis", Wiley, 2nd edition, 1993.



It's not magic, it's engineering.®



SOUND AND VIBRATION ISOLATION

We are a team of experienced engineers focused on developing high-performing, cost effective acoustical products to ensure building code is met for sound transmission (STC/IIC).

Innovative by design, simple to install, **GenieClip®** and **GenieMat®** are the trusted brands of architects, builders and acoustical consultants worldwide.



WWW.PLITEQ.COM | 416-449-0049 | INFO@PLITEQ.COM

ABSTRACTS FOR PRESENTATIONS WITHOUT PROCEEDINGS PAPER RÉSUMÉS DES COMMUNICATIONS SANS ARTICLE

Thin Multi-Resonant Metamaterial As Broadband Noise Absorber

Gauthier Bezancon, Olivier Doutres, Thomas Dupont

Low frequency noise absorption can be obtained with a thin multi-resonant material as the subwavelength pancake absorber which is composed of thin annular pores periodically arranged in series and connected through a central perforation. This type of acoustic metamaterial has a first absorption peak at low frequencies and thin secondary peaks at medium frequencies, making it more suitable for tonal noise absorption. This work investigates a geometrical variation of the central perforation within the material thickness to broaden the material sound absorption efficiency. An analytical approach based on lumped elements and transfer matrix approach is used to predict the material behavior and investigate multiple profiles of the main pore. The analytical model is verified by comparison with a thermo-visco-acoustic finite element model of the material. It is shown that the main pore profile can be designed so that the secondary absorption peaks are moved closer to each other, thus creating an efficient broadband noise absorber at both low and medium frequencies.

Identification Of The Dispersion Curves And The Damping Loss Factor Using Hybrid Inhomogeneous Wave Correlation – Green’s Function Method

Muhammad Najib Bin Fazail, Nouredine Atalla, Jean-Daniel Chazot, Gautier Lefebvre

This paper presents a method to identify the vibro-acoustics dynamic behavior of orthotropic structures such as sandwich honeycomb panels and stiffened panels. The harmonic measured or calculated spatial field is used as the primary input and correlated to a well-defined inhomogeneous wave in a wavenumber space domain or k-space domain to evaluate at first the dispersion relation as a function of the heading angle. Next, the damping loss factor is estimated using a spatial correlation with a Green’s function based model of the propagation in the structure. The validity of the proposed method is investigated numerically using the Finite Element Method (FEM) and experimentally by using scanning laser vibrometer measurements on several structures. The identified dispersion curves are compared with theoretical models and the measured damping is compared with widely used methods such as 3dB method, the decay rate method and the power input method over a large frequency band. The validity and the limitations of the method are discussed in the paper.

Transfer Path Analysis: Application Of The Inverse Hybrid Method On A Noise Abatement Isolators

WaFaa El Khatiri

Transfer Path Analysis TPA has demonstrated its strength in solving NVH problems. Whatever the nature of the mechanical systems (coupled or decoupled), TPA methods can accurately represent vibroacoustic behaviors of noise. Aerospace vehicles are made up of several mechanical elements, among them we cite isolation systems. These are designed to reduce the transmission of vibrations and reduce interior noise. This article discusses the experimental characterization of an isolator using transfer path analysis (TPA). The Inverse method of the Classic TPA is presented and compared with the direct method on a set up made up of a mass coupled by an isolator on an aluminum plate embedded in a concrete cavity, the characterization is carried out by considering a single transfer path and four transfer paths. Several parameters are studied and discussed such as the effects of the coupling vs decoupling of the two connected structures, the number of transfer paths, the degrees of freedom and the completeness of the connection points or the absence of the inverted transfer function matrix. A CTPA method was developed “Inverse Hybrid” to be able to characterize the system on an internal test bench in order to go back to the reference. CTPA Inverse Hybrid is shown to be a practical method when In-Situ measurements of the coupled system are not plausible.

Measurement Of Acoustic Resistance Of Perforated Plates Subjected To A Pulsated Grazing Flow

Xukun Feng, Jean-Michel Coulon, Zacharie Laly, Nouredine Atalla

Linear and non-linear properties of perforations have been studied extensively. High porosity macro-perforations are normally considered linear, while many of these experiments were limited to noise levels below 160 dB. To reproduce more representative conditions met in some internal combustion engine exhaust systems, a new

electro-pneumatic source was built and used. The new test bench is capable of generating single-pulse up to 180 dB with a low harmonic distortion under stationary grazing flow with Mach number up to 0.3. A two-load method based on the transfer matrix method is used in the experiment. From the measured transfer matrix, the transmission loss can be determined and the transfer impedance can be further extracted using an indirect method. The presented test bench is shown to be a practical tool to investigate how extremely high amplitude single-frequency acoustic excitation affects the transfer impedance of perforated panels using in various industrial applications.

Vibrational Response Of Finite Size Microperforated Plate

Lucie Gallerand, Mathias Legrand, Thomas Dupont, Philippe Leclaire

MicroPerforated Plates (MPP) are widely used in the industry for their advantageous acoustic absorption properties. These structures involve viscous and thermal exchanges in the boundary layers near the perforated walls that can result in sound absorption. Initially developed for their acoustic properties, it is theoretically shown in this work that these structures can also induce significant added mechanical damping. As light solutions, they also offer the possibility to replace heavy layers of viscoelastic rubber commonly implemented to damp vibrating structures. They can also have high damping capacities in the low frequency range. The aim of this work is to investigate the vibration damping performance of microperforated structures. Analytical derivations highlighting the viscous damping in the boundary layers near the perforation walls are proposed. A parametric study shows the existence of a characteristic frequency, identical to the characteristic frequency, for which the added damping of the perforations reaches a maximum. Preliminary results also show that the damping of a microperforated structure is several orders of magnitude greater than that of an equivalent homogeneous plate. The level of damping can be optimised by adjusting the geometric parameters of the perforations (diameter, perforation rate) to make the resonance frequency of the plate coincide with the characteristic frequency. **Keywords** MicroPerforated Panel — Vibration — Mechanical damping — Viscous boundary layers

Numerical Prediction Of The Local Flat Bottom Hole Linear And Non-Linear Resonance In An Aluminum Plate

Biaou Jean-Baptiste Kouchoro, Anissa Meziane, Phillippe Micheau, Mathieu Renier, Nicolas Quagebeur

Numerous experimental and numerical studies have shown the interest of the local defects resonance (LDR) for the non-destructive testing of composite materials and thin plates. A non-linear contact mechanism involving "clapping" phenomenon can predominate during the propagation of a guided wave in the damaged area. Thus, the analysis of the non-linear behaviors of a defect excited at its LDR would allow to optimize its characterization. This work presents a numerical Finite Element in 2 dimensions of the local resonance of a 12 mm long and 8 mm deep Flat Bottom Hole (FBH) in a 9 mm thick aluminum plate, excited by a guided wave of type A0. The analysis of the transient part of the FBH vibratory response enables the precise determination of its resonance frequencies and the associate modal deformation. In a second time, a linear parametric study varying the thickness of the plate for the same thickness under FBH has highlighted the sensitivity of the resonance efficiency to the size of the plate. It shows that the resonance effect disappears when the ratio between the thickness of the FBH and the thickness of the plate is too small. Finally, nonlinear behaviour of the FBH has been considered and studied. Experimental studies in progress will allow to validate this numerical study. The results of this study are promising and allow to consider more realistic defects such as delamination in composite materials.

Design Considerations For Mass Timber Supportive Housing Projects

Banda Logawa

With the latest changes to the height limit restriction for newly constructed wood buildings in British Columbia, there has been a growing interest in mass timber construction projects for the supportive housing market. In supportive housing projects, it is quite common to have a combination of amenity spaces, meeting rooms, counseling or support service rooms, office spaces, and residential units in the same building. Furthermore, it is not unusual to see relatively small volume rooms with less opportunity to alter the floor plan around to avoid noise transmission issues altogether. Each space will require different acoustic treatment to meet the relevant guidelines and building code requirements. This paper will highlight the various challenges and design considerations that are being encountered in recent mass timber supportive housing projects in British Columbia as well as exploring solutions for noise control and treatments to maximize the design intent required for multi-use occupancy.

Acoustical Modelling Of A Metamaterial By A Mass-Spring Analogy

Maël Lopez, Thomas Dupont, Raymond Panneton

Acoustic absorption and noise reduction, at low frequencies, are of interest for different industrial sectors: building and transport. Porous materials and acoustic resonators are conventional solutions used. Nevertheless, their effectiveness is limited by their thickness and are not suitable at low frequencies. For this purpose, studies have been oriented towards metamaterials. Metamaterials are materials with an engineered structure. The engineered structure governs their effective parameters such as density and compressibility. Here, the metamaterial is called multi-pancake. Its structure is composed of a main pore with repetition of thin annular cavities along its axis. Previous studies have shown that such a periodic structure increases the effective compressibility of the perforated material. However, a better understanding of the physics is needed to optimize its engineered structure with a view to maximize its low-frequency acoustic absorption. This study presents a theoretical model based on a mass-spring analogy. The losses are considered by an equivalent fluid model which is integrated in the mass and stiffness matrices. The mass-spring analogy makes it possible to determine the sound absorption of the material, the velocity profile, and the resonance frequencies. Results are in good agreement with results obtained by the finite element and the transfer matrix methods.

Acoustics Of Infrasound And Audible Noise Inside Homes Near Wind Turbines Using Multichannel Spectral Processing

Andy Metelka

Previous measurements inside homes show presence of BPF's (Blade Pass Frequencies) below 10Hz as far away as 120km from the nearest Wind Turbine. This holds true for measurements inside homes, yet outside measurements become more challenging at all frequencies due to Wind Turbulence. Random wind turbulence occurs at the microphone screening devices as well as adjacent structures predominantly at lower frequencies. The homes, both near and far, act as windscreens in these low frequency settings, un-masking the BPFs that appear inside. This paper discusses both near and far field measurements in different locations inside homes while making simultaneous spectral measurements outside. Measurements inside, being free from wind turbulence, indicate BPF's are clear and distinct below audible levels at all times of day and year.

Ultrasonic Assessment Of Young's Modulus In Pipes Using Lamb Waves Dispersion Curves

Sebastien Perrier

Echologics' acoustic condition assessment was the industry's first non-invasive solution for measuring the structural wall thickness of buried water mains. The method relies on accurate estimation of the Young's modulus of the pipe material. This is currently estimated from the pipe specifications or measured from exhumed coupons in accordance with applicable standards. The goal of this project was to determine whether the Young's modulus could be assessed by measuring Lamb waves in-situ and fitting the actual phase dispersion in the pipe to the theoretical phase dispersion using Multichannel Analysis Surface Waves (MASW). In the lab, the Lamb wave dispersion curves were obtained by exciting the pipe wall along the pipe axis and measuring the longitudinal wave propagation using a laser vibrometer. The resultant symmetric and antisymmetric Lamb mode velocities were found to fit the dispersion curves well. The test methodology was subsequently adapted for in-situ measurements on empty and pressurized pipes. Specifically developed wedges and a viscous coupling agent were used to ensure that the pulse was refracted along the longitudinal axis of the pipe wall where both Lamb wave modes of vibration were excited. The results of this study are presented in this paper.

Band Gap Study Of Metamaterials

Anil Pundir, Arpan Gupta, Umberto Berardi

Investigations in the field of solid-state physics show metamaterial, a kind of periodic material, can produce a band of frequency gap. When the frequency of a sonic-wave falls into the frequency gap, it cannot propagate in the sonic crystal. Enlightened by the concept of frequency gap, various metamaterials are in evolution. Search for band(s) gap holds the key to such innovations. In the present paper, the band(s) of frequency gap are obtained for two-component and three-component 2D period materials by using Finite Element Method. The influences of geometrical parameters on the band gap are analysed for the pre-selected material of the core (Aluminium) and the coating (Natural Rubber). For the specified value of the lattice constant, with the increasing size of the core, band gap increases. General effect of the coating leads to flattening of the dispersion curve. Peculiarly, multiple frequency

band gap appears (comparatively of substantial sizes) at the threshold size of the core or core with coating vis-à-vis lattice size i.e. when net diameter of the core is equal to half of the lattice constant (for circular core and square lattice). Keywords: Sonic Crystal; Periodic Material; Band of Frequency Gap; Two and Three Component Systems; Threshold Scatterer Size.

Characterization Of An Isolation Interface Between Two Structures Through The Measurement Of The Dynamic Transfer Stiffness

Rabii Slimane, Nouredine Atalla

Unwanted vibrations could be mitigated by simply improving the characterization and design of vibrating systems, receiving structures, and the interfaces between them. This project focuses on the characterization of an isolation interface between two structures through the measurement of the dynamic transfer stiffness. Unlike current methods, that primarily rely on removing the resilient element from its original assembly, two in-situ methods allowing an independent and over a considerable frequency range characterization have been studied: a "direct" method and a "remote" method allowing the use of remote measurement positions and the over-determination of the problem. In order to test the performance of both methods, a numerical and experimental validation through transfer path analysis approaches is carried out. First, a simple Mass/Isolator-Mass system is used to validate the direct method by comparing it to the resonance method. Then, a more realistic test rigs (Mass/Beam-Isolator-Plate) are constructed to further test and validate the methods on more resonant structures. Finally, an analysis of transferability is performed in which an obtained dynamic transfer stiffness value is used to predict the response of a separate system containing the same resilient element. In both cases, the response is predicted with considerable accuracy, verifying that the identified dynamic stiffness is a system independent quantity.

Discussion On Characterization Of Apparent Dynamic Stiffness Of Elastic Interlayer Materials Used In Floating Floors

Jianhui Zhou, Zijian Zhao

Dynamic stiffness is a key factor which affects the impact sound insulation performance of a floating floor assembly. However, recent studies revealed that the standard test method in ISO 9052-1 raises challenges on the measurement precision of this material property. This study will first discuss the assumption of single degree of freedom model and its impact on the measurement and selection of the resonant frequency, and then investigate the effect of static load and the air cavity in the elastic material on the measured apparent dynamic stiffness through experimental testing. Different steel plates representing the common range of mass per unit area will be used to conduct the tests. Elastic interlayers with waving profile with a polycarbonate frame is designed to restrain the air flow during the test. The results will provide some new insights on the characterization of apparent dynamic stiffness of elastic interlayer materials used in floating floors.

ACOustics begins with ACO™

SLARMSuccesses™
Red Rocks & ATPAC, Dallas

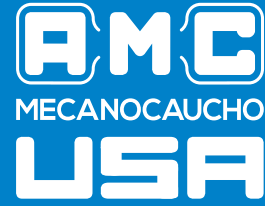


TEL: (416) 754.7008 | FAX: (416) 754.2351
EMAIL: SALES@A-TECH.CA | WWW.A-TECH.CA
P.O. BOX 252 | SCARBOROUGH | ONTARIO M1E 4R5

Exclusive Canadian Agent
ACO Pacific, Inc.

www.acopacific.com sales@acopacific.com

BIM FOR AKUSTIK+SYLOMER® ACOUSTIC HANGERS AND FLOATING FLOOR MOUNTS.



Manufacturing solutions
for architectural acoustics
and vibration problems
since 1969.



HOW TO
DOWNLOAD
AMC BIM
MODELS

Akustik 1 +Sylomer® acoustic hangers.

Akustik 1 +Sylomer® acoustic hangers. Available drawings.

DRAWINGS

Akustik 1 + Sylomer®15 Type A Akustik 1 + Sylomer®15 Type B Akustik 1 + Sylomer®15 Type B M-8 Akustik 1 + Sylomer®30 Type A
Akustik 1 + Sylomer®30 Type B M-6 Akustik 1 + Sylomer®30 Type B M-8 Akustik 1 + Sylomer®50 Type A Akustik 1 + Sylomer®50 Type B
Akustik 1 + Sylomer®75 Type A Akustik 1 + Sylomer®75 Type B M-6 Akustik 1 + Sylomer®75 Type B M-8

Type	SUMMARY	LOAD kg MAX	Weight (kg)	Code	BIM	CE
Akustik 1 + Sylomer®15 type A	Metal armor of the Akustik 1 secured to the ceiling with two holes and an M6 male fixing type (Type A)	15	0.133	23651	<input type="button" value="BIM"/>	<input type="button" value="CE"/>

Akustik + sylomer®

Change country or language Downloads Business Agents Contact Home E2B area | L+1 964-662-3732

About us Products Acoustic results Long term behaviour APP References Wooden structures

BIM

AKUSTIK 1 + SYLOMER®	Code	DWG	STP	IFC	RFA
Akustik 1 + Sylomer®30 Type A	23501	23501.dwg	23501.stp		
Akustik 1 + Sylomer®30 Type B M-6	23509	23509.dwg	23509.stp		
Akustik 1 + Sylomer®75 Type A	23517	23517.dwg	23501.stp		
Akustik 1 + Sylomer®75 Type B M-6	23525	23525.dwg	23509.stp		
Akustik 1 + Sylomer®50 Type A	23502	23502.dwg	23502.stp	23502.ifc	23502.rfa
Akustik 1 + Sylomer®50 Type B	23520	23520.dwg	23520.stp	23520.ifc	23520.rfa
Akustik 1 + Sylomer®30 Type B M-8	23603	23603.dwg	23603.stp		
Akustik 1 + Sylomer®75 Type B M-8	23604	23604.dwg	23604.stp		
Akustik 1 + Sylomer®15 type A	23651	23651.dwg	23651.stp	23651.ifc	23651.rfa
Akustik 1 + Sylomer®15 type B	23652	23652.dwg	23652.stp	23652.ifc	23652.rfa
Akustik 1 + Sylomer®15 type B M-8	23653	23653.dwg	23653.stp	23653.ifc	23653.rfa

ABOUT US PRODUCTS TESTS BUSINESS AGENTS FOLLOW US IN

AMC Mecanocaucho General Quality Contact Akustik + Sylomer® References Comparative tests Behaviour at high and low frequencies Long term behaviour Laboratory tests See Business-agents All News Youtube Facebook LinkedIn

By clicking on the button "BIM" drawings in RFA extension on Revit® from Autodesk version 2018 can be downloaded as well as IFC, DWG or STP.

ADAPTED FOR USA/CANADA

Adapted for 1-1/2" CRC and 7/8" DWF furring channels or wire. Akustik+Sylomer Hangers are easier to install now in the US/Canada.



Wilmer J. Acuña
Technical Sales Manager

www.mecanocaucho.com
www.akustik.com
 wilmer@amcsa.es

837 Coldbrook Drive.
Greer, SC 29651
 +1 215.910.1029

Pascalex Inc.
160-3755, Place Java
Brossard, QC J4Y 0E4
 +1 450.659.3700



THEME 2 - ACOUSTICS AND LIVING BEINGS - THÈME 2 - ACOUSTIQUE ET ÊTRES VIVANTS

The Acoustics Of Guttural Fricatives In Three Languages <i>Koorosh Ariyae, Chahla Ben-Ammar, Talia Tahtadjian, Alexei Kochetov</i>	28
Coronal Fricatives Among L1 And L2 Hul'q'umi'num' Speakers <i>Sonya Bird, Phil Howson</i>	30
In-Ear Noise Dosimetry : Field Method Using Earmuffs' Noise Reduction <i>Arthur Colombier, Chahinez Hocine, Cécile Le Cocq, Olivier Doutres, Franck Sgard, Jérémie Voix</i>	32
Effects Of Timbre And Pitch Register On Perceived Emotion In Melodies <i>Ange-Dominique A. Akesse, Michael D. Hall</i>	34
Speaking Versus Smiling: The Labiodentalization Of Bilabials In Korean <i>Elisabeth H Kang, Yadong Liu, Annabelle Purnomo, Melissa Wang, Bryan Gick</i>	36
Biomechanical Simulation Of Lip Compression And Spreading <i>Connor Mayer, Chenhao Chiu, Bryan Gick</i>	38
The Effect Of Place Of Articulation On The Extent Of Velopharyngeal Opening In Quebecois French Nasal Consonants <i>Jacqueline Ama Murray, Melissa Wang, Jahurul Islam, Gillian De Boer, Bryan Gick</i>	40
Development Of An Intra-Aural Protective Device For Hearing-Impaired Individuals Working In Noisy Environments <i>Solenn Ollivier, Jérémie Voix, Rachel Bouserhal, Christian Giguère, Fabien Bonnet, Hugues Nélisse</i>	42
Computer Assisted Segmentation Of Tongue Ultrasound And Lip Videos <i>Pertti Palo</i>	44
The Contextual Effects Of Nasal Vowels On Velopharyngeal Opening In Quebecois French <i>Charissa Y. Purnomo, Linda X. Wu, Gillian De Boer, Jahurul Islam, Bryan Gick</i>	46
Speaker Accommodations Towards Vui Voices On The Dimensions Of Voice Onset Time And Pitch Range <i>Gracellia Purnomo, Chloë Farr, Charissa Y Purnomo, Nicole Ebbutt, Amanda Cardoso, Bryan Gick</i>	48
The Effects Of Microgravity On Tongue Height <i>Arian Shamei, Bryan Gick</i>	50
3d Finite Element Model Of The Human Thorax To Study Its Low Frequency Resonance Excited By An Acoustic Harmonic Excitation Onto The Chest Wall <i>Arife Uzundurukan, Philippe Micheau, Sébastien Poncet, Pierre Grandjean, Daria Camilla Boffito</i>	52
Prosodic Differences In Mandarin Speakers With Alzheimer's Disease <i>Linda Xianglin Wu, Arian Shamei, Yadong Liu, Bryan Gick</i>	54
Abstracts for Presentations without Proceedings Paper - Résumés des communications sans article	57

THE ACOUSTICS OF GUTTURAL FRICATIVES IN THREE LANGUAGES

Koorosh Ariyaee¹, Chahla Ben-Ammar¹, Talia Tahtadjian¹, & Alexei Kochetov¹

¹University of Toronto, Toronto, Ontario, Canada

1 Introduction

Gutturals, consonants produced in the posterior portion of the vocal tract, are considered to include uvulars (e.g., /q, ɢ, ʁ, ʁ/, pharyngeals (/ħ, ʕ/), and, by some accounts, laryngeals (/ʔ, h/) [1]. Unlike consonants of other places of articulation, gutturals have been relatively phonetically understudied, with previous acoustic investigations being limited to a handful of languages and often few speakers. The existing acoustic work has been done mainly on guttural fricatives, /ɣ, ʁ, ħ, ʕ, h/, in Modern Standard Arabic ([2-4]). These works have established that duration of fricative noise distinguishes voiced from voiceless fricatives, as well as /h/ from the other fricatives. Noise spectra, on the other hand, were found to play an important role in differentiating place, as, for example, centre of gravity of noise correlates with the relative posteriority of the constriction. Spectral properties were also noted to differentiate voicing.

The goal of this study is to provide an acoustic analysis of voiceless and voiced guttural fricatives in three languages: Emirati Arabic (EA, Semitic), Iraqi Central Kurdish (IK, Iranian, Indo-European), and Lebanese Western Armenian (LA, Armenian, Indo-European). The first two languages contrast voiceless and voiced uvulars /ɣ, ʁ/ (which are in some sources described as velars /x, ɣ/), voiceless and voiced pharyngeals /ħ, ʕ/, and the voiceless laryngeal /h/ ([5] on EA; [6] on IK). LA contrasts voiceless and voiced uvulars /ɣ, ʁ/, and the voiceless laryngeal /h/ [7-8]. All these languages/varieties are relatively understudied phonetically, or hardly studied at all.

2 Method

The study involved 59 participants: 18 speakers of EA, 20 speakers of IK, and 21 speakers of LA, residing predominantly in Abu Dhabi and Dubai (UAE), Sulaymaniyah and Kirkuk (Iraqi Kurdistan), and Beirut (Lebanon), respectively. The participants were roughly balanced by gender (32 females, 27 males) and were of similar age - mainly in their 20s. In addition to their L1, they also spoke English and, for LA, Arabic. They were recruited through personal networks and local contacts in respective countries, and paid an equivalent of 15 CAD for their participation. Audio recordings were performed using an online experiment platform Gorilla.sc [9] and recording devices of participants' choice.

The materials included real words with the target consonants /ɣ, ʁ, (ħ, ʕ) h/, embedded in a carrier phrase. Care was taken to keep the stimuli and phrases as similar as possible across the languages. Each utterance (1 word per fricative in intervocalic position) was repeated 3 times, giving 9 to 15 tokens per speaker, depending on the language.

The data were annotated in Praat [10], with boundaries set manually to indicate onsets and offsets of fricatives and adjacent vowels. Measurements were extracted using a script and included fricative duration and spectral moments taken at the midpoint of the fricative. Among the spectral measurements, we will here be concerned with only one - centre of gravity (COG), higher or lower frequency of which corresponds to the relative posteriority of the fricative constriction (i.e., expected to be lower for, e.g., /ħ/ than /ɣ/).

3 Results

To examine differences among fricatives, Linear Mixed Effects Models were performed for duration and COG separately for each language, as well as by Place in voiceless fricatives and Voicing in uvular and pharyngeal fricatives. The results, summarized in Table 1, revealed robust differences across 3-way (EA and IK) and 2-way (LA) place contrasts, as shown in the table. They also revealed consistent voicing differences. With the exception of the duration difference for uvulars and pharyngeals between EA and IK, all observed differences were the same across three languages.

Table 1: A summary of statistical results for Place (uvular, pharyngeal, laryngeal) and Voicing (voiceless, voiced) by language; '>' indicates higher values.

Parameter	Place (voiceless)			Voicing (non-/h/)
	EA	IK	LA	All
Duration	phar > uvu > lar	uvu > phar > lar	uvu > lar	vls > vd
COG	uvu > phar > lar		uvu > lar	vls > vd

To illustrate these results, Figure 1 presents fricative duration and centre of gravity ((a) and (b) respectively) by consonant and language. For duration, we can see a clear difference in voicing for uvular (red) and pharyngeal (green) sounds: the voiced consonants are much shorter. We can also see that /h/ is shorter than its voiceless counterparts. Turning to COG, recall that lower values of this variable indicate a greater posteriority of the consonant, reflecting the highest concentration of spectral energy along frequencies. Considering voiceless fricatives first, we can see in the plot that their COG values decrease from uvulars (red) to pharyngeals (green), and then to laryngeals (blue). This is consistent for all three languages (but note that LA lacks pharyngeals). The same is observed for voiced sounds of two places. In terms of voicing, voiced sounds show lower COG, given the low-frequency voicing energy, and likely frequent approximant-like realizations (due to lenition).

* koorosh.ariyaee@mail.utoronto.ca

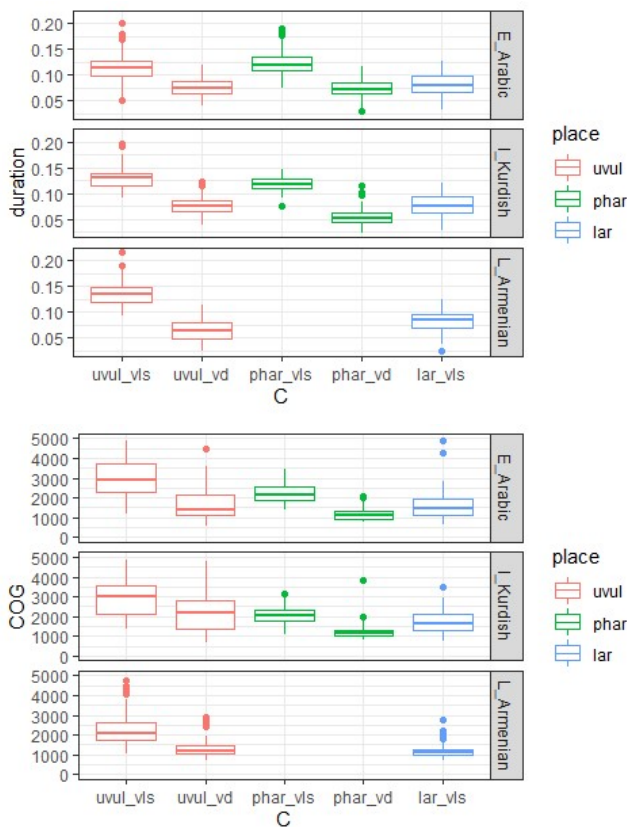


Figure 1: Boxplots for duration (sec; top plot) and COG (Hz; bottom plot) by consonant (voiceless and voiced uvulars and pharyngeals, voiceless laryngeal) and language.

4 Discussion

The results obtained in this study are similar to previous findings for Standard Arabic. Taking voiceless fricatives, for example, we can see in Figure 2 that COG values reported in several previous studies of Arabic fricatives (N1983 [2], AK2005 [4], AAM2005 [3]) were lower for pharyngeals and laryngeals, which is also the case obtained for EA, IK, and (in part) LA in this study. The lower COG for /h/ in our results is also consistent with the findings of [3]. There is also considerable agreement in mean values for the fricatives across the studies, despite the very different recording conditions.

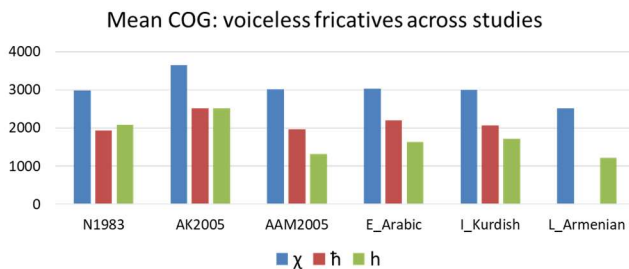


Figure 2: A comparison of mean COG (Hz) values across previous studies of Arabic voiceless fricatives (see text) and current results.

As a next step, we are planning to investigate additional variables, such as standard deviation, skewness, kurtosis, and

intensity of fricative noise, as well as vowel transitions to/from fricatives (as these could further clarify place of articulation differences). The analysis will also be extended to word-initial and word-final positions, for which we have also obtained the data.

5 Conclusion

To conclude, this study contributes to the phonetic documentation of guttural sounds by covering new languages/varieties and using relatively large speaker samples. This study also serves to confirm the validity of the online audio recording method, which has been increasingly used in phonetics during the pandemic of COVID-19.

Acknowledgments

Thanks to the participants; to Asiya Majid & Aram Salih for language consultation; to Farnaz Younessi, Dasyar Ali, & Lara Keshishian for assistance with recruitment of participants. The work was supported by Social Sciences & Humanities Research Council of Canada Insight grant and the UofT Linguistics Department funding.

References

- [1] J. J. McCarthy. Semitic gutturals and distinctive feature theory, In B. Comrie & M. Eid (eds.), *Perspectives on Arabic linguistics III*, 63-91. Amsterdam: Benjamins, 1991
- [2] K. Norlin. Acoustic analysis of fricatives in Cairo Arabic. Working papers/Lund University, Department of Linguistics and Phonetics, 25, 1983.
- [3] A. S. Abu-Al-Makarem. The acoustics of fricative consonants in Gulf Spoken Arabic. PhD dissertation. Bowling Green State University, 2005.
- [4] M. A. Al-Khairy. Acoustic characteristics of Arabic fricatives. PhD dissertation. University of Florida, 2005.
- [5] T. T. C. Leung, D. Ntelitheos, and M. Al-Kaabi. *Emirati Arabic: A comprehensive grammar*. Routledge, 2020.
- [6] W. M. Thackston. *Sorani Kurdish: A reference grammar with selected readings*. Harvard University, 2006.
- [7] D. Sakayan. *Western Armenian for the English-speaking world: A contrastive approach*. Yerevan State University Press, 2012.
- [8] Vaux, B. *The phonology of Armenian*. Oxford University Press, 1998.
- [9] A. L. Anwyll-Irvine, J. Massonnié, A. Flitton, N. Kirkham, J. K. Evershed. Gorilla in our midst: An online behavioral experiment builder. *Behavior research methods*; 52(1):388-407, 2020.
- [10] P. Boersma, and D. Weenink. Praat: doing phonetics by computer [Computer program]. Version 6.1.50, retrieved 20 June 2021 from <http://www.praat.org/>, 2021.

CORONAL FRICATIVES AMONG L1 AND L2 HUL'Q'UMI'NUM' SPEAKERS

Phil J. Howson¹ and Sonya Bird^{*1}

¹University of Victoria, Department of Linguistics, Canada

1 Introduction

Hul'q'umi'num' (Central Salish) is spoken along the Salish sea on the southeastern side of Vancouver Island and the adjacent Gulf Islands in British Columbia (BC), Canada. Hul'q'umi'num' has fewer than forty L1 speakers but increasing numbers of L2 speakers of all ages, with the language revitalization movement rapidly gaining momentum across Hul'q'umi'num' territory [1]. The research project reported on here is part of a SSHRC-funded community-university partnership to support L2 speakers fine-tune their pronunciation and achieve what they think of as "authentic" pronunciation [2].

Hul'q'umi'num' has 37 consonants, including a robust series of coronal fricatives: /t, s, ʃ, θ/. The goal of this project is to examine the acquisition trajectories of these fricatives by L2 learners and compare them to L1 speech.

2 Method

2.1 Participants

Two Hul'q'umi'num' L1 speakers (both female: H1L1 & H2L1) and three L2 speakers (2 female, 1 male: H1L2, H2L2, & H3L2) took part in our study. The L1 speakers were born in 1932 and 1941, respectively. The L2 speakers were aged 30-50.

2.2 Procedure and analysis

Data come from a pronunciation test that were carried out in 2016 and again in 2019, in Duncan, BC. Both times, the test was conducted in groups that included an Elder, an instructor/researcher, and 2-3 learners. One learner performed the test while the other(s) monitored the audio recorder. They switched roles after completion of the test.

Each word on the pronunciation test was first read by the Elder and then repeated by the learner. This was done twice for each word on the list. Recordings were made in Audacity with a Yeti USB microphone connected directly to a laptop computer.

All of the coronal fricatives /t, s, ʃ, θ/ were represented in the pronunciation test, in a range of syllable and word positions. The dataset included a total of 148 L1 tokens and 222 L2 tokens. In some cases, learners either mispronounced the target sound or the target word was accidentally skipped (52 tokens, or approximately 14%), leading to a total of 370 tokens analysed, including 114 /s/ tokens, 64 /ʃ/, 137 /t/, and 55 /θ/.

We segmented the fricatives in Praat [3] and extracted the four spectral moments – center of gravity (COG), stand-

ard deviation (SD), skewness, and kurtosis [4] – at 10 equally spaced intervals over the time-course of each target segment. Our analysis included a total of 7 data sets, 1 for each L1 speaker and 2 for each L2 speaker (1 for 2016 and 1 for 2019). In R [5], we used GAMMs to analyze each fricative's median COG trajectory, comparing L2 speakers to each other and to L1 speakers. Based on [6], we compared COG in CV and VC position, but found no noticeable differences, so omitted syllable position effects from our analysis. Additionally, we performed a principal components analysis (PCA) using median value of each spectral measure at vowel midpoint to investigate how all four spectral moments contributed to distinguishing fricatives from one another.

3 Results

3.1 COG results

Figure 1 presents the COG results for the L1 speakers, H1L1 and H2L1. The results revealed different COG peak values and trajectories for most segments. Most significant was the difference between H1L1 and H2L1 for /θ/: H1L1 had a much lower peak COG (~4,000 Hz) with a gradual increase until 75% duration, while H2L1 had a sharp increase to ~8,000 Hz at 25% and a gradual increase after that to ~9,000 Hz at 75%. COG differences indicate an interdental fricative (/θ/) for H1L1 and a dental one for H1L2 (closer to [θ̟]), reflective of dialectal variation previously documented by other Hul'q'umi'num' and Coast Salish scholars [6, 7]. H1L1 had no significant COG difference between /t, ʃ/, but H2L1 had lower COG and a flatter trajectory from /ʃ/ compared to /t/.

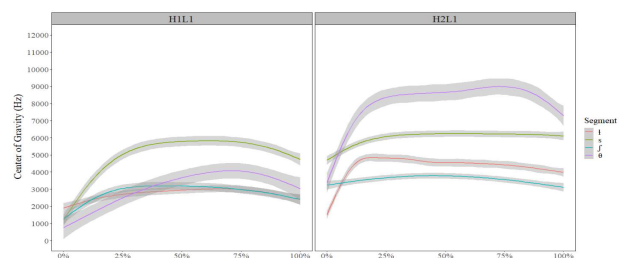


Figure 1: Dynamic COG measures for H1L1 (left) and H2L1 (right). /t/ is orange, /s/ is green, /ʃ/ is blue, and /θ/ is purple.

Figure 2 presents the dynamic COG measures for H1L2, H2L2, and H3L2 for 2016 and 2019. H1L2 showed a lowering of COG in 2019 compared to 2016 for /t, ʃ, θ/, along with a general compression of the COG space; /s/ revealed no significant change. H2L2 also had a compression in COG space, but it was the result of an increase in COG for /t, ʃ, θ/ and a decrease of /s/ in 2019 compared to 2016. All learners had a relatively low COG for /θ/ in 2016, similar to H1L1. In 2019, H3L2's /θ/ was closer to H2L1; their COG for /t/ was also higher in 2019 compared to 2016, generating a shift towards

* sbird@uvic.ca

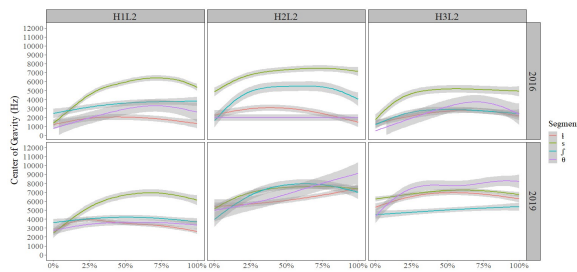


Figure 2: Dynamic COG measures for H1L2 (left), H2L2 (center), and H3L2 (right) in 2016 (top) and 2019 (bottom). /s/ is green, /f/ is blue, and /θ/ is purple.

H2L1 overall, at least for these two fricatives. Neither H1L2 nor H2L2 had clear shifts from one L1 speaker to the other from 2016 to 2019.

3.2 PCA results

Figure 3 presents the PCA individuals for H1L1 and H2L1. The data revealed that the acoustic space formed by the four spectral moments creates an isosceles trapezoidal shape. For both speakers, two segments were much closer together than the other segments. For H1L1, it was /t, θ/, but for H2L1, it was /t, f/. The placement of /θ/ in particular reflects the COG results across speakers (Figure 1). For both speakers, skewness and kurtosis played a major role in dimension 1, but H1L1 also had a strong contribution from SD, while H2L1 had a strong contribution from COG instead. For both H1L1 and H2L1, the weakest measure in dimension 1 was the strongest for dimension 2, COG for H1L1 and SD for H2L1, while the remaining spectral moments had a weak contribution to dimension 2.

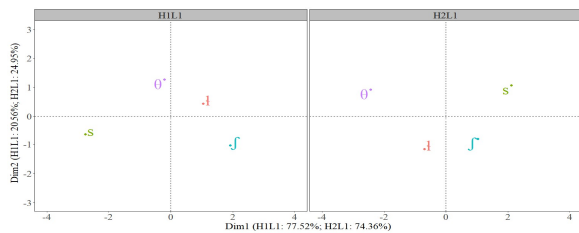


Figure 3: PCA Individuals for H1L1 (left) and H2L1 (right). /s/ is green, /f/ is blue, and /θ/ is purple.

Similar to the L1 speakers, each of the learners had two segments that were closer to each other than the others, although they often changed from 2016 to 2019. For example, Figure 4 shows that H2L2 had /t, f/ closer in 2016 (similar to H2L1) and /t, θ/ in 2019 (similar to H1L1).

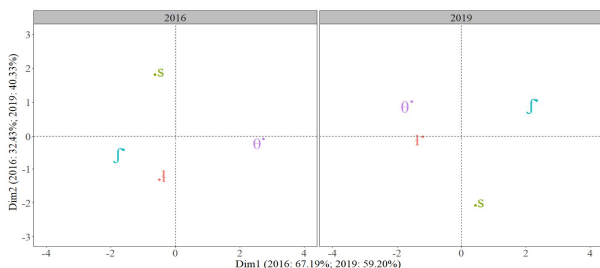


Figure 4: PCA Individuals for H2L2 in 2016 (left) and 2019 (right). /s/ is green, /f/ is blue, and /θ/ is purple.

We observed a similar contribution pattern for L2 speakers as for L1 speakers, but there were differences. Specifically, in 2016 all speakers had large contributions on dimension 1 for skewness, kurtosis, and one of SD or COG. But in 2019, we observed that H2L2 had large contributions of kurtosis, SD, and COG for dimension 1 and a large contribution from skewness to dimension 2.

4 Discussion

The data revealed that both L1 and L2 Hul'q'umi'num' speakers produce sound contrasts in their own way, although the overall acoustic distributions of the coronal fricatives share similarities. H1L1 and H1L2 differed most substantially in their realization of /θ/, reflecting dialectal differences between them. While learners' fricatives differed in 2016 and 2019, there is no clear pattern of moving towards more L1-like realizations as a whole. Perhaps this is because L1 speakers do not provide consistent models, differing even amongst themselves. At least one learner, H3L2, seems to have shifted, becoming more similar to H2L1 than to H1L1 over time. It would be interesting to look into such shifts further, to determine whether and how much individual L1 speaker models affect the speech of L2 learners.

Overall, the data supports the notion that L2 speakers can acquire novel segments, even as adults, and that L2 speakers arrange their acoustic space to achieve a similar dispersion as L1 speakers, even though they may do this in different ways, by manipulating different acoustic parameters.

Acknowledgments

We are grateful to the Hul'q'umi'num' Language and Culture Society and to the speakers who contributed to this work, as well as SSHRC grants #756-2020-0100 (to first author) and #890-2017-0026 (to second author). We would especially like to acknowledge late Dr. Sti'tum'at Ruby Peter for her contributions to our work and so much more.

References

- [1] Dunlop, B., Gessner, S., Herbert, T., & Parker, A. (2018). Report on the status of B.C. First Nations languages (3rd ed). Brentwood Bay, Canada: First Peoples' Cultural Council.
- [2] Bird, S. & Kell, S. (2017). The role of pronunciation in SENCOFEN Language Revitalization. *Canadian Modern Language Journal* 73(4), 538-569.
- [3] Boersma, P., & Weenink, D. (2021). Praat: doing phonetics by computer. Computer program. <http://www.praat.org/>.
- [4] Jongman, A., Wayland, R., and Wong, S. (2000). "Acoustic characteristics of English fricatives," *J. Acoust. Soc. Am.* 108(3), 1252-1263. [4] R Core Team (2021). R: A language and environment for statistical computing. <http://www.R-project.org/>.
- [5] R Core Team (2020). R: A language and environment for statistical computing. Vienna: R Foundation for Statistical Computing. <http://www.R-project.org/>
- [6] Mellesmoen, G. & Babel, M. (2020). Acoustically distinct and perceptually ambiguous: /ay/ajuTəm (Salish) fricatives. *J. Acoust. Soc. Am.* 147(4), 2959-2973.
- [7] Suttles, W. (2004). *Musqueam Reference Grammar*. Vancouver BC: UBC Press.

IN-EAR NOISE DOSIMETRY: FIELD METHOD USING EARMUFFS' NOISE REDUCTION

Arthur Colombier^{*1}, Chahinez Hocine^{†1}, Cécile Le Cocq¹, Franck Sgard², Olivier Doutres¹, and Jérémie Voix^{‡1}

¹Université du Québec, École de technologie supérieure, Montréal, Québec, Canada

²Institut de Recherche Robert-Sauvé en santé et en sécurité du travail, Montréal, Québec, Canada

1 Introduction

Precisely assessing the noise dose reaching the eardrum is key for proper hearing loss prevention program (HLPP). However, measuring this dose under hearing protection devices (HPD) is complex, especially for earmuffs, due to (1) their difficult instrumentation especially when considering the placement of the microphone under the HPD, (2) measurements artefacts - referred to as wearer's induced disturbances (WID) - that adds noise to the in-ear microphone (IEM) measurements [1] and (3) the necessity to precisely estimate individualized acoustic corrections. Such issues were addressed in previous studies that aimed either to remove WIDs [1] or to neglect their contribution on earplugs [2]. The proposed method designed for earmuffs will predict the noise dose at the eardrum based on continuous measurements of noise reduction (NR) through the earcup and measurement from the outer-ear microphones (OEM) only.

2 Method

The proposed approach aims to address the three aforementioned issues by relying on sound pressure measurements outside the earcanal to make the WIDs contributions negligible. Thus, it relies on the estimation of four acoustic transfer functions (TF) in order to determine an individualized insertion loss (IL) : the transfer function of the open ear (TFOE), the noise reduction NR^* , the external transfer function TF'_{ext} and the transfer function of the earcanal TF'_{canal} .

$$IL = 20 \log_{10} \left(\frac{p_t}{p'_t} \right) = L_{p_t} - L'_{p_t} \quad (1)$$

The necessary measurement locations are showed on Fig. 1 (top). The prime symbol ("'") indicates that the measurement is done with worn earmuffs. L_{p_0} is the sound pressure level (SPL) measured without the head being present. These TFs illustrate the link between the SPLs measured at the eardrum while the hearing protector is worn and the SPL L_{p_0} . It is illustrated in Fig. 1 (bottom) and can be written as follow :

$$IL = NR^* + TFOE + TF'_{canal} - TF'_{ext} \quad (2)$$

The proposed approach is detailed in the flowchart of Fig. 2. The *first step* consists in assessing three TFs for calibration purposes. First, the TFOE, specific to the wearer, needs to be assessed. On top of classical microphone in real ear (MIRE) method, several alternatives are possible

[3–5]. Second, the TF'_{canal} , which is wearer specific, depends mostly on the earcanal geometry [6]. This function can be estimated using finite element methods (FEM) that allow to evaluate easily several ear canal geometries and vary the microphone placement [7]. Third, the TF'_{ext} depends on the precise position of the OEM. The estimate of this function and its variability can be measured once for each specific model of HPD.

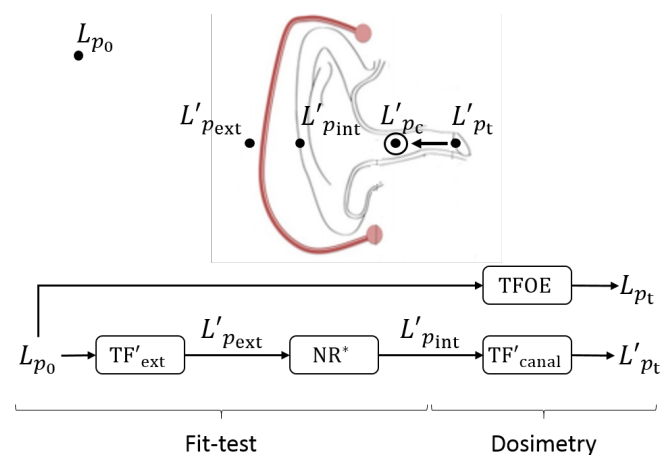


Figure 1 – Sound pressure level measurement locations of the proposed approach (top). The circled dot represents the alternate position used in the experimental validation. Transfer functions used to compute the effective sound pressure level at the eardrum L'_{p_t} as well as the insertion loss (bottom).

The *second step* consists in using the optimal microphone pair (see recommendation from [8]) to estimate the NR^* and define a baseline specific to the evaluated earmuff. This function serves as reference for real-time measurement of the attenuation. The calculated uncertainties are used to define two error factors : NR_{min} and Δ_{th} . The first factor is used in the *third step* to ensure that the attenuation is sufficient in all frequency bands. This step is also used to monitor the fit of the earmuff (fit-test) and warn the wearer if needed. The *fourth step* calculates the difference between the baseline and the measured attenuation. This difference is compared to the threshold Δ_{th} . When above this threshold it is necessary to assess whether this difference is due to WIDs contribution. If so, the method developed by [1] to remove such energetic contributions can be used. In the *fifth step*, when no WIDs are detected, the noise reduction estimate NR^* is updated. Finally, the precise noise dose under HPD can be calculated from the accumulated values of L'_{p_t} in the *sixth step*. The steps 3 to 6 are looped and allow for the continuous estimation and monitoring of the NR^* , while the estimation of L'_{p_t} enables the calculation of the noise dose under the earmuff.

*. acolombier@critias.ca
 †. chocine@critias.ca
 ‡. jeremie.voix@etsmtl.ca

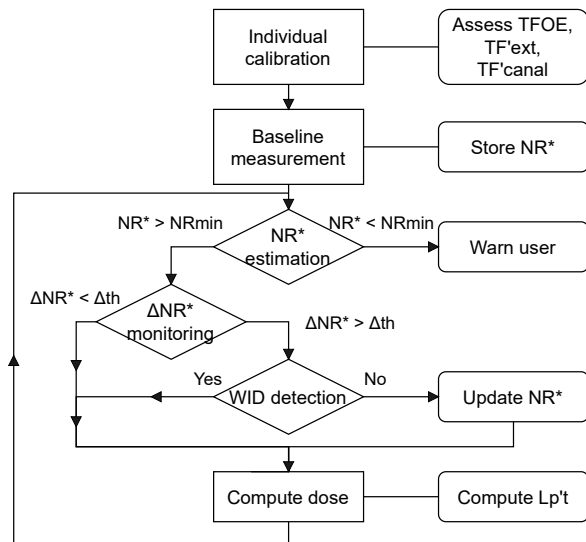


Figure 2 – Flowchart of the proposed approach, L'_{pt} from continuously updated values of NR^*

All SPLs measurements and TF assessment previously described were conducted on the Optime 98 earmuffs (3M, U.S.A.) on 23 participants, in both free-field and diffuse-field, and under three conditions [8].

3 Results

Fig. 3 shows the mean and standard deviations (STD) of the noise reduction NR^* for the optimal microphone pair (identified as the one giving the smallest STDs over all evaluated pairs in [8]).

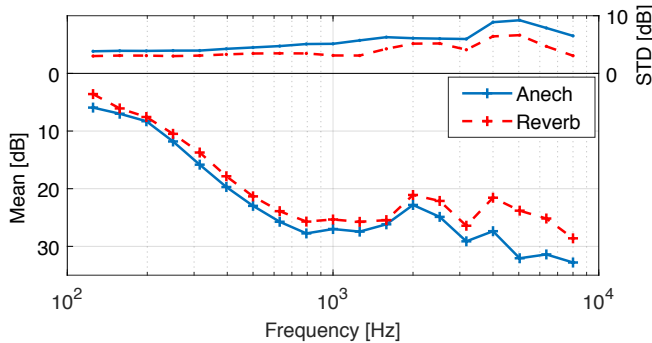


Figure 3 – Mean and standard deviation values of the NR^* measured on 23 human participants in diffuse-field (reverberant chamber in red) and in free-field under 24 incidences (anechoic chamber in blue)

Fig. 4 presents the insertion loss, IL^* , calculated based on the following equation 3 :

$$IL^* = NR^* + TFOE^* + TF_{canal}^{*'} - TF_{ext}^{*'} \quad (3)$$

The " * " symbol used for IL^* , TF_{canal}^{*}' and $TFOE^*$ indicates that one of the required measurement is not located at the eardrum (see circled dot in Fig. 1). All TFs in equation 3 are computed based on the same dataset used for the fourth required TF plotted in Fig. 3.

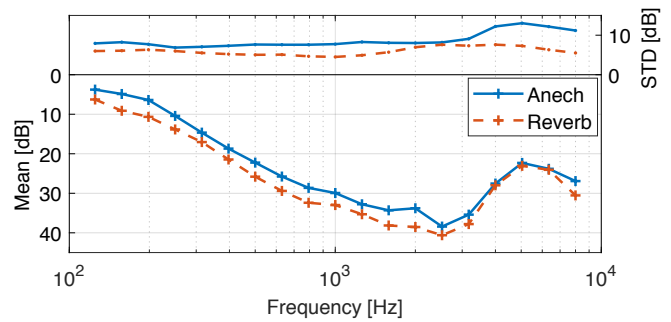


Figure 4 – Mean and standard deviation values of the IL^* computed from the four transfer functions based on equation 3 in both acoustic fields.

4 Discussion and conclusions

While the proposed method, relying on the assessment of the noise dose at the eardrum based on continuous microphone measurements outside the HPD has already been done for earplugs [2], the proposed adaptation for earmuffs was validated off line from experimental measurements conducted on 23 human subjects. The validation confirmed that on the one hand, NR^* measurements showed on Fig. 3 should enable the definition of the baseline (see Fig. 2) while the STDs will help in defining the NR_{min} and Δ_{th} factors. On the other hand, this validation showed that the indicator IL^* computed from equation 3 would give promising results with regards to estimating the noise dose at the eardrum under earmuffs, pending that some individual acoustic correction could be determined from FEM models.

Acknowledgments

The authors would like to acknowledge the financial support received from EERS Global Technologies Inc., through the NSERC-EERS Industrial Research Chair in In-Ear Technologies (CRITIAS).

References

- [1] F. Bonnet et al. In-ear noise dosimetry under earplug : method to exclude wearer-induced disturbances. *International Journal of Industrial Ergonomics*, 74, 2019.
- [2] V. Nadon et al. Method for protected noise exposure level assessment under an in-ear hearing protection device : a pilot study. *International Journal of Audiology*, 60(1) :60 – 69, 2021.
- [3] D.J. Hurley et al. The Ear as a Biometric. In A.K. Jain et al., editors, *Handbook of Biometrics*, pages 131–150. Springer US, Boston, MA, 2008.
- [4] P. Bilinski et al. HRTF magnitude synthesis via sparse representation of anthropometric features. In *2014 IEEE ICASSP*, pages 4468–4472, Florence, Italy, May 2014.
- [5] K. Iida et al. Personalization of head-related transfer functions in the median plane based on the anthropometry of the listener's pinnae. *JASA*, 136(1) :317–333, July 2014.
- [6] F. Bonnet et al. Individual in-situ calibration of in-ear noise dosimeters. *Applied Acoustics*, 157, 2020.
- [7] F. Sgard et al. Développement d'outils et de méthodes pour mieux évaluer et améliorer la protection auditive individuelle des travailleurs. Technical Report R-901, IRSST, 2016.
- [8] C. Hocine. Instrumentation de casques anti-bruit : mesures expérimentales sur sujets humains. Master's thesis, Ecole de Technologie Supérieure, Montréal, July 2021.

EFFECTS OF TIMBRE AND PITCH REGISTER ON PERCEIVED EMOTION IN MELODIES

Ange-Dominique A. Akesse¹ and Michael D. Hall^{*2}

¹Departments of Graduate Psychology James Madison University, Harrisonburg, Virginia, USA

²Departments of Psychology, James Madison University, Harrisonburg, Virginia, USA

1 Introduction

Timbre perceptually interacts with pitch. Examples include pitch shifts in tones without the fundamental [1, 2], and in Shepard tones as a function of the spectral envelope's center (e.g., [3]). Also, timbre and pitch are perceptually integral, as indicated by influences of each dimension on the other in speeded classification tasks [4].

Fewer studies have examined the related question of whether timbre contributes to the perception of emotion in music. It has been revealed that emotional interpretations of isolated tones change with the instrument producing them [5], though it might be argued that timbre's influence on emotion could be overcome by complex pitch relationships in melodies. Evidence on this issue is very limited, though changes in timbre can be enough to impact the emotional interpretation of melodic excerpts [6].

The current investigation sought to confirm timbre's contribution to the emotional interpretation of melodies while clarifying its role. In light of timbre-pitch interactions, influences on perceived emotion might be altered with changes in pitch register, which can impact timbre [7]. This experiment therefore manipulated octave/pitch register directly. The summarized experiment also extended previous work by establishing whether emotional interpretations could specifically be predicted by spectral characteristics of timbre.

2 Method

2.1 Participants

Twenty-five students with self-reported normal hearing from introductory psychology courses at JMU participated in partial fulfillment of course requirements. Data from nine were not analyzed due to configuration errors (5), missing or invalid responses (2), and premature responses (2). Age ranged from 18.8 to 21.7 years ($M = 19.6$; $SE = 0.27$). Musical experience ranged from 0 to 11 years ($M = 4.75$; $SE = 1.07$) as determined by responses to a questionnaire (see below).

2.2 Stimuli

Twelve, eight-bar, melodic excerpts were isolated from repositories of MIDI transcription files [8 - 10]. Lab staff selected excerpts from classical compositions that were unfamiliar, with six characterized as joyful, and six as sad.

Register varied by transposing melodies an octave (down for joyful, up for sad). Since transpositions exceeded the pitch range of instruments for two joyful and two sad melodies, their keys were adjusted until all notes were obtained.

Stimuli were rendered (at 44.1 kHz (16-bit)), using sampled instruments from Ableton's *Live Suite* [11]. Excerpts were separately produced by Bb clarinet, trumpet, and violin. To assess perceived emotion without an instrument, sinewave versions were produced by our own plug-in (with 20 ms linear amplitude ramps for isolated onsets/offsets). Stimuli were equated for mean RMS amplitude and presented through a 4-pole, low-pass filter with an 11 kHz cut-off over Sennheiser HD 25-SP II headphones in a sound-attenuated chamber.

2.3 Procedures

After consent, participants completed a musical training and experience survey followed by the experimental task. The experiment was controlled by Empirisoft's *DirectRT* software [12]. Participants judged the strength of the intended emotion ("happy" or "sad") following each melody on a 7-point scale and made their responses using a button box.

All iterations of a melody occurred in one block of trials. Blocks began with a sinewave original melody, a standard for judging subsequent stimuli, followed by randomized timbre-register combinations. Block order varied across listeners.

Ratings for each emotion were hypothesized to decrease with transpositions, consistent with incongruent spectral shifts. Ratings were expected to (1) vary with instrument around the sinewave condition according to energy across the spectrum, and (2) to be reversed for joyful and sad melodies.

3 Results

Mean ratings of the strength of intended emotions were calculated as a function of register and timbre and are summarized in Figure 1. To assess how transposed melodies were influenced by instrument timbre relative to sinewaves, ANOVAs for joyful and sad melodies were conducted with timbre (clarinet, trumpet, violin, sinewave) as the factor. To assess influences of the critical variables, a 2x3 ANOVA for each intended emotion was conducted with register (original, transposed) and instrument (clarinet, trumpet, violin) as factors. Bonferroni pair-wise comparisons clarified effects, and Greenhouse-Geisser corrections are reported as applicable.

Perceived emotion changed with register and instrument for joyful melodies (panel A of Figure 1). Ratings decreased with transposition, producing a main effect of register, $F(1, 95) = 63.843$, $p < .001$, $\eta^2 = .402$. Ratings also were higher for violin and trumpet relative to clarinet, producing a main effect of instrument, $F(1.808, 171.790) = 18.473$, $p < .001$, $\eta^2 = .163$; p 's $< .001$ for pair-wise comparisons. Furthermore, for the low register perceived joy was greater for trumpet and violin relative to the sinewave condition. This tendency contributed to an effect of timbre, $F(3, 285) = 12.432$, $p < .001$, $\eta^2 = .116$; all p 's $< .001$ for pair-wise comparisons.

* hallmd@jmu.edu

Register and instrument likewise affected ratings for sad melodies (panel B of Figure 1). Transpositions decreased perceived sadness for trumpet and violin, contributing to a main effect of register, $F(1, 95) = 6.102, p = .015, \eta^2 = .060$. Also, ratings were higher for violin and clarinet relative to trumpet, producing an instrument main effect, $F(1.671, 158.792) = 4.493, p = .018, \eta^2 = .045$; p 's $< .031$ for pair-wise comparisons. Finally, transposition conveyed more sadness for instruments than sinewaves (p 's $< .033$), contributing to a timbre effect, $F(2.746, 260.848) = 13.137, p < .001, \eta^2 = .121$.

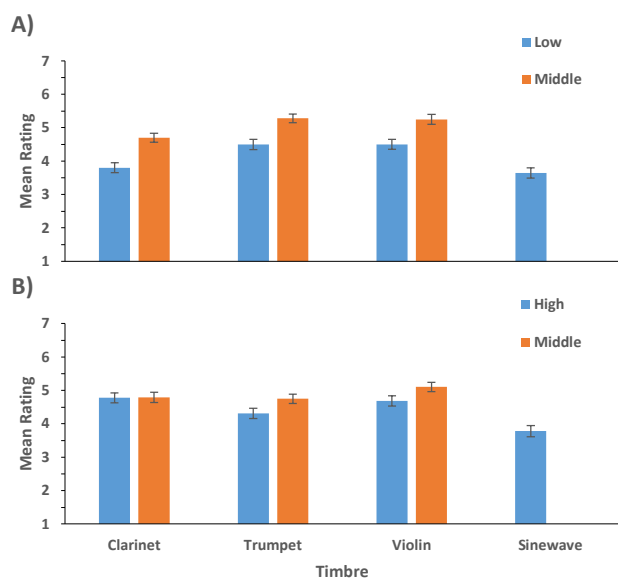


Figure 1: Mean ratings of the strength of intended emotions (along with standard errors) as a function of timbre and octave for initially joyful and sad melodic excerpts (panels A and B, respectively).

4 Discussion

The anticipated effects of timbre and octave generally were observed. Higher registers were more joyful/less sad, as were trumpet and violin trials relative to clarinet (see Figure 1)].

What timbre dimension(s) might be responsible for these primary findings? One measure used to distinguish spectra [13] that may reveal timbre-pitch interactions [2] is the spectral centroid, the frequency representing the center of spectral energy, which contributes to tonal brightness. We calculated the centroid for each excerpt's average spectrum.

Since pitch and timbre interact, changing register could influence emotion by changing timbre. Centroids increased across instruments for higher octaves, paralleling register effects, except for clarinet, where sad ratings did not change with register. Perhaps shifts in low centroids were insufficient to defeat pitch-based interpretations over a small pitch range.

Centroids provide a partial account of timbre effects. Centroids increased from clarinet to trumpet to violin, and were positively, though weakly related to ratings for joyful melodies, $r = .382, p = .011$. A corresponding correlation was absent for sad stimuli, $r = -.025, p = .443$. Listeners may have relied on another attribute, such as rise time, when rating sad violin melodies. After all, rise times were very long in these bowed samples (> 300 ms). We are pursuing this.

If adding parameters better predicts our findings, then future studies could benefit from manipulating timbre characteristics in combination. For now, results from this study confirm timbre's influence on perceived emotion, as found for individual tones and an alternative set of melodies [5, 6]. Furthermore, it appears that some of this contribution could be due to changes in perceived brightness, at least for joyful melodies. Thus, researchers should avoid assumptions that the emotional interpretation of melodic information can be evaluated independently of the timbre used to express it.

Acknowledgments

Thanks to assistants Ram Srinivas, Robin LaHaye, Riley Herr, and Morgan Wilkinson for data and stimulus help.

References

- [1] Seither-Preisler, A., Krumbholz, K., Patterson, R., Johnson, L., Nobbe, A., Seither, S., & Lütkenhöner, B. (2007). Tone sequences with conflicting fundamental pitch and timbre changes are heard differently by musicians and nonmusicians. *J Exp Psychol Hum Percept Perform*, 33(3), 743–751. <https://doi.org/10.1037/0096-1523.33.3.743>
- [2] Becker, C. J. & Hall, M. D. (2014). Effects of fundamental frequency removal and low-pass filtering on pitch comparisons. *Psychomusicology*, 24(3), 195–206. <https://doi.org/10.1037/a0037933>
- [3] Deutsch, D. (1987). The tritone paradox: Effects of spectral variables. *Percept & Psychophys*, 41(6), 563–575. <https://doi.org/10.3758/bf03210490>
- [4] Pitt, M. A. (1994). Perception of pitch and timbre by musically trained and untrained listeners. *J Exp Psychol Hum Percept Perform*, 20(5), 976–986. <https://doi.org/10.1037/0096-1523.20.5.976>
- [5] Eerola, T., Ferrer, R., & Alluri, V. (2012). Timbre and affect dimensions: Evidence from affect and similarity ratings and acoustic correlates of isolated instrument sounds. *Music Percept*, 30(1), 49–70. <https://doi.org/10.1525/mp.2012.30.1.49>
- [6] Hailstone, J. C., Omar, R., Henley, S. M., Frost, C., Kenward, M. G., & Warren, J. D. (2009). It's not what you play, it's how you play it: Timbre affects perception of emotion in music. *Quart J Exp Psych*, 62(11), 2141–2155. <https://doi.org/10.1080/174702109.02765957>
- [7] Hall, M. D. & Rohaly, T. (2018). Predicting pitch's influence on instrument timbres and vowels. Poster presented at the 17th annual Auditory Perception, Cognition, and Action Meeting (APCAM 2018), New Orleans, Louisiana.
- [8] kunstderfuge.com: The largest resource of classical music .mid files. (2021). Retrieved from <http://www.kunstderfuge.com/>
- [9] midiworld.com. (2021). Retrieved from <https://www.midiworld.com/classic.htm>
- [10] mfiles. (2021). Retrieved from <https://www.mfiles.co.uk/classical-midi.htm>
- [11] Ableton AG. (2021, February 23). Ableton Live Suite 11 (Version 11.0.1). Ableton AG. <https://www.ableton.com/>
- [12] Jarvis, B. G. (2018). DirectRT (v2018.1.109). Empirisoft Corporation. https://www.empirisoft.com/download_old.aspx
- [13] McAdams, S., Winsberg, S., Donnadieu, S., De Soete, G., & Krimphoff, J. (1995). Perceptual scaling of synthesized musical timbres: Common dimensions, specificities and latent subject classes. *Psych Res*, 58, 177–192. <https://doi.org/10.1007/BF00419633>

SPEAKING VERSUS SMILING: THE LABIODENTALIZATION OF BILABIALS IN KOREAN

Elisabeth H. Kang ^{*1}, Yadong Liu ^{†1}, Annabelle Purnomo ^{‡1}, Melissa Wang ^{♦1}, and Bryan Gick ^{#1,2}

¹Department of Linguistics, University of British Columbia, Canada

²Haskins Laboratory, New Haven, Connecticut, United States of America

1 Introduction

Speech production generates many instances of conflict between synchronous movements in opposing directions. With the various processes that occur in the production of different sounds, suppression of certain movements over others is likely to occur. Previous research exploring this conflict focused on the labiodentalization of bilabial sounds (i.e., /p/ → [f]) during smiled speech in English. The conflict between the lip spreading/opening that occurs when smiling and the compression/closing of the lips required to form bilabial stop sounds (/p/, /b/, /m/) was found to result in labiodentalized variants of English bilabial stops [1].

While conflict between opposing movements occurring simultaneously has been found to occur in the production of English bilabials, it remains unclear whether this resolution is the result of a physiological or phonological (i.e., learned substitution) process, considering that the English inventory contains labiodental tokens. The present study thus undertakes an investigation of Korean, a language containing no labiodental tokens in its inventory. More specifically, the exploration of this language in particular presents an opportunity to explore whether labiodentals are naturally emergent or if they are learned over time. Moreover, whether the body resolves conflict between opposing movements through an additive mechanism (i.e., tug-of-war) or suppression of certain movements remains unclear. If labiodentalization were to occur in Korean, the ways in which speech postures interact with and conflict with speech sounds may be further explored.

2 Method

2.1 Video

Twenty-four videos of 26 native Korean speakers were selected from the video platform YouTube and examined for production of /m/, /b/, /p^h/, and /p/. YouTube was chosen for its abundance of interviews and vlogs (i.e., video blogs), which provided a clear headshot of each speaker’s face for natural running speech. All videos met the following criteria: only one speaker’s face was shown per frame, each speakers’ native language was Korean, and there were instances of both smiling and neutral faces while producing a bilabial sound. Portions of speech were manually coded as “smiled” or “neutral” based on the video.

* ehkang@student.ubc.ca

† yadong@alumni.ubc.ca

‡ apurnomo@student.ubc.ca

♦ mjw10@student.ubc.ca

gick@mail.ubc.ca

2.2 Analysis

Videos converted into WAV Audio files and transcripts containing bilabial phonemes were manually aligned at the sentence level using *Praat* [2]. Bilabial tokens were also manually aligned and annotated with their condition (i.e., neutral or smiled), phoneme, and token number.

The facial behavior analysis software *OpenFace 2.0* [3] detects facial action units (FAU) and calculates the degree of intensity of these FAUs. Using the timestamps extracted from *Praat* annotations, the degree of activation of the FAUs “lip corner puller” (which is activated during smiling) and “lip tightener” (which is activated during bilabial closures) were analysed using *OpenFace 2.0*. The annotated tokens were then extracted and manually coded as bilabial or labiodental.

3 Results

A total of 308 productions of labial phonemes were found from the 26 speakers, with 165 in the neutral condition and 143 in the smiled condition. Among the 143 labial phoneme productions found in the smiled condition, there were 26 cases produced as labiodental stops.

Table 1 summarizes the number of bilabial and labiodentalized realizations of each phoneme including /m/, /b/, /p^h/, and /p/ produced in both neutral and smiled conditions. Figure 1 illustrates the ratio of labiodentalization of /m/, /b/, /p^h/, and /p/.

Table 1: The number of each phoneme realized as a bilabial or labiodentalized closure in neutral versus smiled conditions.

Condition	Closure	/m/	/b/	/p ^h /	/p/
Neutral	# of Bilabials	98	51	15	1
	# of Labiodentals	0	0	0	0
Smiled	# of Bilabials	89	38	13	3
	# of Labiodentals	18	7	1	0
	Ratio of labiodentalization	0.2	0.18	0.08	0

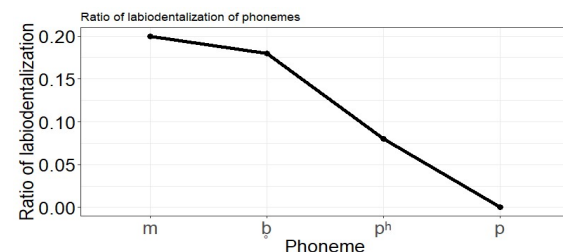


Figure 1: Ratio of labiodentalization of /m/, /b/, /p^h/, and /p/.

The “lip corner puller” intensity 200 ms prior to and 130 ms following the release of labial productions, as seen in Figure 2, shows the greatest intensity when producing a labiodentalized closure in the smiled condition. Less intensity was observed when producing a bilabial closure in the smiled condition, and the lowest intensity was evident when producing a bilabial closure in the neutral condition. Additionally, Figure 3 presents the “lip tightener” intensity during the same period as shown in Figure 2. The greatest intensity was observed when a bilabial closure was achieved in the smiled condition. A lesser intensity was observed when producing a labiodentalized closure in the smiled condition and a bilabial closure in the neutral condition.

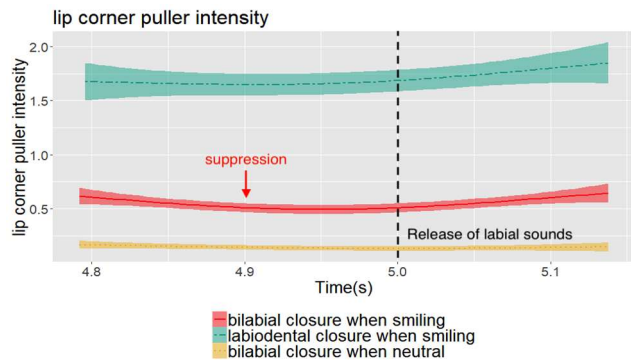


Figure 2: “Lip corner puller” intensity surrounding the release of labial closures.

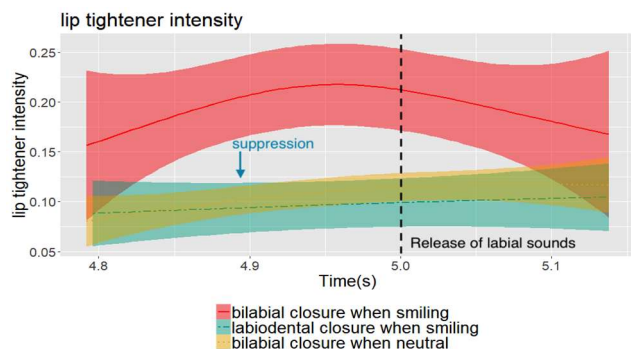


Figure 3: “Lip tightener” intensity surrounding the release of labial closures.

4 Discussion

Results shown in Table 1 reveal that labiodentalized bilabials are evident in Korean speech, which suggests that the smiling versus lip-closing conflict is resolved as a physiological process. Figure 1 further indicates that the greatest ratio of labiodentalization is observed in /m/ followed by /b/ and /p/, while no labiodentalized /p/ was observed. Previous research found various intraoral pressures [4] and muscle activations [5] for /m/, /b/, and /p/ closures in an increasing order. Our results suggest that the frequency of labiodentalization decreases when stronger muscle force and intraoral pressures are required for bilabial segment production in Korean, which is consistent with the previous findings for English [6].

FAU intensity results indicate greater “lip tightener” intensity when producing bilabial closures in the smiled condition compared to the neutral condition, indicating that augmented lip closing force is required when smiling. Furthermore, greater “lip tightener” intensity is found in bilabial closures compared to labiodentalized closures produced when smiling, suggesting a suppression of lip closing force when a labiodental variant is produced while smiling. Regarding “lip corner puller” intensity, decreased intensity is observed when producing bilabial closures compared to labiodentalized closures in the smiled condition, indicating that the force of smiling gets suppressed with stronger lip closing force.

Regarding the limitations of this study, whether intensity of FAU could represent activation of certain muscles accurately remains unknown, and further studies could investigate the correlation between facial muscle activation and FAU.

5 Conclusion

Labiodentalization of bilabial stops when smiling in Korean points to a physiological rather than phonological resolution process. Our FAU results corroborate findings from the previous study in English, further suggesting that the smiling versus lip-closing conflict could be resolved via suppression of one or the other movement.

Acknowledgments

This work was supported by the National Institutes of Health grant number DC-002717 to Haskins Laboratories and NSERC Discovery grant RGPIN-2021-03751 to the last Author.

References

- [1] Chan, T., Taylor, R. C., Wong, E. Y., & Gick, B. (2018). Coarticulation of speech and smile movements. *The Journal of the Acoustical Society of America*, 144(3), 1903-1904.
- [2] Boersma, P., & Weenink, D. (2021). Praat: doing phonetics by computer [Computer program]. Version 6.1.51, retrieved 22 July 2021 from <http://www.praat.org/>.
- [3] Baltrusaitis, T., Zadeh, A., Lim, Y.C., & Morency, L. (2018). OpenFace 2.0: Facial Behavior Analysis Toolkit. 13th IEEE International Conference on Automatic Face & Gesture Recognition (FG 2018), 59-66.
- [4] Lubker, J. F., & Parris, P. J. (1970). Simultaneous Measurement of Intraoral Pressure, Labial Pressure, and Labial Electromyographic Activity During Production of the Bilabial Sops/p—/b. *The Journal of the Acoustical Society of America*, 47(1A), 104-104.
- [5] Gick, B., Chiu, C., Flynn, C., Stavness, I., Francis, N., & Fels, S. (2012). Producing whole speech events: Differential facial stiffness across the labial stops. *Mentalis*, 15, 15.
- [6] Liu, Y., Chan, T., Purnomo, G., & Gick, B. (2021). Talking while smiling: Suppression in an embodied model of coarticulation. *Proceedings of the International Seminar on Speech Production*, 130-133.

BIOMECHANICAL SIMULATION OF LIP COMPRESSION AND SPREADING

Connor Mayer ^{*1}, Chenhao Chiu ^{†2}, and Bryan Gick ^{‡3,4}

¹Department of Language Science, University of California, Irvine, United States of America

²Graduate Institute of Linguistics, National Taiwan University

³Department of Linguistics, University of British Columbia, Canada

⁴Haskins Laboratories, New Haven, United States of America

1 Introduction

Researchers have proposed that human movements exploit regions of biomechanical stability, allowing targets to be reliably achieved in the face of noisy, everyday conditions [1]. Such regions produce quantal biomechanical effects [2], whereby a wide range of muscle activations can generate a similar outcome. Quantal effects have been observed in a number of articulatory regions relevant to speech, including the lips [3, 4], tongue [5], and larynx [6].

Previous biomechanical simulation studies investigating quantal properties of labial speech movements [3, 4] have omitted two cross-linguistically common lip postures. The first is lip compression, or exolabial rounding, where the aperture between the lips is narrowed without or with limited accompanying protrusion [7]. Lip compression frequently accompanies front rounded vowels and some back unrounded vowels. The second is lip spreading, where the corners of the lips are drawn apart. Spreading often accompanies high front vowels such as /i/.

Previous empirical work has attempted to identify the muscle activations used in producing compression and spreading. Spreading is most clearly associated with activation of the buccinator (BUC), risorius (RIS), and zygomaticus (ZYG) muscles, all of which serve to draw back the corners of the mouth [8]. The muscle activations driving lip compression have proven to be more difficult to identify, but orbicularis oris (OO) has been implicated in constricting the lips, while mentalis (MENT), depressor anguli oris (DAO), and BUC have been suggested to help check the constriction generated by OO and produce compression rather than protrusion [9, 10]. A challenge for such studies, however, is that the lip muscles are heavily interdigitated, making measurement of individual muscle activations using techniques such as electromyography difficult [11].

In the current study, we present biomechanical simulation results using a 3D finite-element method face model. With these simulations, we attempt to identify muscle groupings that are sufficient to generate lip compression and spreading and also to examine the biomechanical stability of these two postures.

2 Methods

Simulations of lip compression and spreading were performed using the Artisynt platform [12]. Artisynt is a bio-

mechanical simulation platform that combines finite-element and multibody methods to allow the rigid and deformable structures in the human body to be modeled. For the present simulation we used a model containing the skull, jaw, lips, and face. This model is described in more detail in [4]. Simulations were performed by specifying groupings of muscles and their relative maximum activation stress, then activating them from 0% to 100% of the maximum muscle stress in 1% increments. Lip aperture was measured using the same green-screen technique described in [4], with pixel area measurements converted to mm².

Lip spreading was achieved by activating BUC (50 kPa) as the main agonist muscle. Only simulations including BUC were able to generate lip spreading that did not result in complete closure. Simulations that incorporated RIS and ZYG at low levels generated similar postures and are not reported here.

Lip compression was achieved by activating peripheral orbicularis oris (OOP; 70 kPa), DLI (45 kPa), BUC (30 kPa), levator labii superioris (LLS; 30 kPa), and levator labii superioris alaeque nasi (LLSAN; 20 kPa). OOP was activated to reduce lip aperture and induce a certain degree of lip protrusion. The remaining muscles serve to check the constriction generated by OOP: DLI counteracts this for the lower lip, LLS and LLSAN for the upper lip, and BUC along the horizontal dimension. Simulations without these antagonist muscles tended to generate excessive closure.

3 Results

The end-state configurations of the model are shown in Fig. 1. Rest posture and the approximant posture from [4] are included for reference. The postures achieved for spreading and compression align well with expected visual outcomes.

Fig. 2 (left) shows lip aperture as a function of muscle activation for the spreading movement. These results show that the activation of BUC decreases the overall lip opening and induces a consistent lip spreading posture. Furthermore, activation between approximately 50% and 100% results in little change in resulting lip aperture. This quantal region is shaded in Fig. 2.

Fig. 2 (right) shows lip aperture as a function of muscle activation for the compression movement. These results show that activation of the muscles OOP, DLI, BUC, LLSAN, and LLS in the proportions listed in Table 1 is sufficient to produce lip compression. The graph also highlights the existence of a quantal region between approximately 75% and 100% muscle activation, though this region is smaller than that produced by spreading.

* cjmayer@uci.edu

† chenhaochiu@ntu.edu.tw

‡ gick@mail.ubc.ca

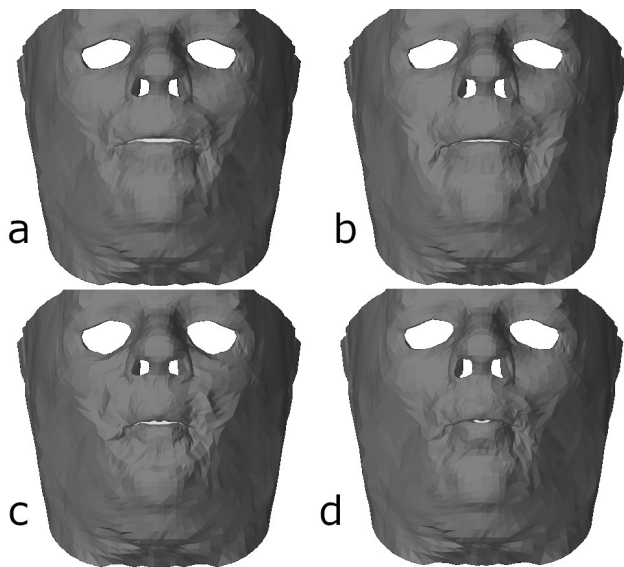


Figure 1: End-state configurations for (a) rest posture; (b) lip spreading; (c) lip compression; and, for reference/comparison, (d) lip rounding.

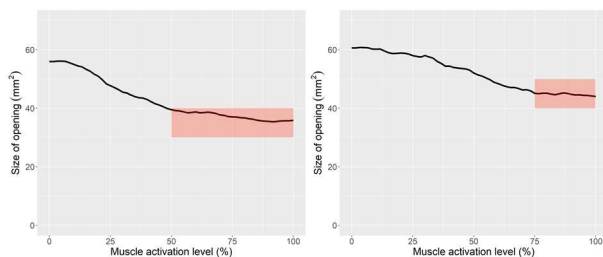


Figure 2: Lip aperture in the simulations of spreading (left) and compression (right). The shaded area marks the quantal region.

4 Discussion

Our results identify groupings of muscles that are sufficient to produce both lip spreading and lip compression. Further, these muscle configurations exhibit quantal properties, indicating that they exploit regions of biomechanical stability that allow targets to be met under a range of different muscle activations.

These results supplement previous work in several ways. Though earlier studies have discussed these two lip postures, they have either focused only on lip aperture without much discussion of muscle activations driving these movements [13, 14], or have reported muscle activation measured using EMG with no corresponding lip opening data [10]. In addition, attributing EMG signals to particular muscles is difficult due to factors described above [11]. The present study uses a 3D biomechanical model to predict muscle groupings that are sufficient to produce lip spreading and rounding, as well as to predict their effect on lip aperture as muscle activation increases.

This study also supports the claim that the functional groupings of muscles that drive the movements used in speech are chosen in part due to their quantal properties: both sets of muscles generate quantal relationships between muscle activation and lip aperture.

It is not the case that the groupings identified in these simulations are the only viable strategies for producing these movements. Further simulation studies should investigate the role of jaw opening in lip compression, as well as other strategies that have been proposed in the literature, such as differential activation of different areas of the OOP [9, 10].

Acknowledgments

This work was supported by the National Institutes of Health grant number DC-002717 to Haskins Laboratories.

References

- [1] G.E. Loeb. Optimal isn't good enough. *Biol. Cybern.*, 106: 78–94, 2012.
- [2] O. Fujimura. Comments on 'On the Quantal Nature of Speech,' by K.N. Stevens. *J. Phon.*, 17: 87–90, 1989.
- [3] I. Stavness, M.A. Nazari, P. Perrier, D. Demolin, and Y. Payan. A biomechanical modeling study of the effects of the orbicularis oris muscle and jaw posture on lip shape. *JSLHR*, 56(3): 878–890, 2013.
- [4] B. Gick, C. Mayer, C. Chiu, E. Widing, F. Roewer-Després, S. Fels, and I. Stavness. Quantal biomechanical effects in speech postures of the lips. *J. Neurophysiol.*, 124(3): 833–843, 2020.
- [5] K. Honda, S. Takano, and H. Takemoto. Effects of side cavities and tongue stabilization: Possible extensions of the quantal theory. *J. Phon.*, 38(1): 33–43, 2010.
- [6] S.R. Moisiuk and B. Gick. The quantal larynx: The stable regions of laryngeal biomechanics and implications for speech production. *JSLHR*, 60(3): 540–560, 2017.
- [7] J.C. Catford. *Fundamental problems in phonetics*. Bloomington and London: Indiana University Press, 1982.
- [8] A. Marchal. *From speech physiology to linguistic phonetics*. London: Wiley.
- [9] S. Ohman, R. Leanderson, and A. Persson. Electromyographic studies of facial muscles during speech. *Speech Trans Lab, Status Report*, 3: 1–11, 1965.
- [10] K. Hadding, H. Hirose, and K.S. Harris. Facial muscle activity in the production of Swedish vowels: An electromyographic study. *J. Phon.*, 4(3): 233–245, 1976.
- [11] C. Blair and A. Smith. EMG recording in human lip muscles: can single muscles be isolated? *JSLHR*, 29(2): 256–266, 1986.
- [12] J.E. Lloyd, I. Stavness, and S. Fels. ArtiSynth: A fast interactive biomechanical toolkit combining multibody and finite element simulation. In Y. Payan (ed), *Soft Tissue Biomechanical Modeling for Computer Assisted Surgery*. Berlin: Springer: 355–394, 2012.
- [13] W. Linker. Articulatory and acoustic correlates of labial activity in vowels: A cross-linguistic study. *UCLA Working Papers in Phonetics*, 56, 1982.
- [14] J.C. Catford. *A practical introduction to phonetics*. Oxford: Clarendon Press, 1988.

THE EFFECT OF PLACE OF ARTICULATION ON VELOPHARYNGEAL OPENING IN QUÉBÉCOIS FRENCH NASAL CONSONANTS

Jacqueline A. Murray ^{*1}, Melissa Wang¹, Jahurul Islam¹, Gillian de Boer¹ and Bryan Gick^{1,2}

¹Department of Linguistics, University of British Columbia, Canada.

²Haskins Laboratory, New Haven, United States of America.

1 Introduction

There has been previous literature demonstrating an interaction between place of articulation (PoA) and velopharyngeal opening (VPO). Rochette & Grégoire (1983) [1] found that there is a greater extent of opening in the production of the French bilabial nasal consonant than the palatal. They did not however compare the alveolar PoA, and used only 2 speakers, one male and one female. This continues from a small literature suggesting that there may be a continuum of VPO targets for nasal sounds [1 - 3] as opposed to the frequently understood binary nature ([+nasal] vs. [-nasal]).

Other studies looking at VPO in French have compared phonemically nasal vowels versus consonants, and contextually nasalized vowels versus oral segments [1, 2]. However, there is still more to be explored as it relates to place of articulation. Furthermore, previous findings demonstrate differences in velar anatomy between males and females [4 - 6], leading to the consideration of potential effects of sex on VPO.

The present study seeks to explore whether PoA influences the VPO uniformly across speakers and whether sex is a contributing factor to the extent of the opening. To expand on previous research, this study will include measurements of /n/, and a greater number of sentences and speakers, which will allow consideration of potential sex effects.

2 Methods

From the Munhall et al. (1995) [7] X-ray film database, nine native speakers (five males and four females) of Québécois French at the Université Laval were selected. All of these speakers were between the ages of 19 and 30 years old.

The X-ray films, originally created by Dr. Claude Rochette, were adjusted by Munhall et al. (1995)[7], the details of which can be found in his paper. The nine speakers produced a total of 24 films with about 4000 frames each. We quantified the VPO using ImageJ [8] by counting black pixels present between the pharyngeal wall and the upper surface of the velum. This region intersects the “path of the velum” making full contact with the pharyngeal wall is a complete closure and coded as VPO = 0. Maximal opening

for each individual speaker was coded as VPO = 1. Therefore, each speaker was compared to themselves for their ratio per segment as opposed to each other.

For analysis, we ran linear mixed-effects models to assess the parameters of the research question. The p-value for significance was set at .05.

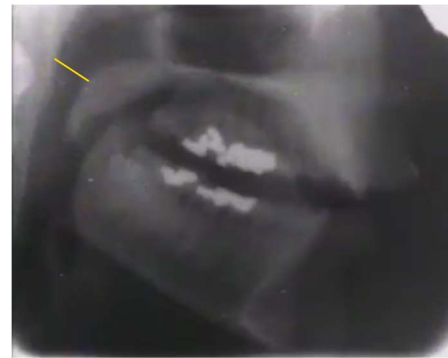


Figure 1: X-ray image of a speaker at sagittal view. The yellow line demonstrates the location of VPO measurement along the “path of the velum”.

3 Results

Figure 2 indicates the average VPO ratios in each of the three phones. The y-axis represents the ratio of opening from 0 to 1 and the places of articulation are represented along the x-axis. The palatal nasal /ɲ/ is represented by ‘gN’. As the figure indicates, bilabials have a higher VPO compared to palatals or alveolars while there does not appear to be a difference between the alveolars and palatal nasals.

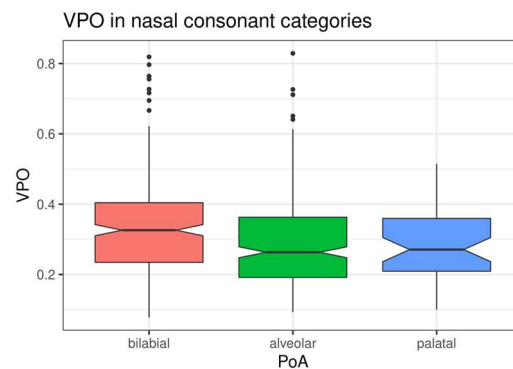


Figure 2: Boxplot of VPO in [m] ($N = 285$), [ɲ] ($N = 48$), and [n] ($N = 304$).

* j.murray96@hotmail.com

To determine if PoA was a significant contributor to the VPO ratio in nasal consonants, we performed a linear mixed effects analysis in R [9] using *lmerTest* [10]. We fit a null model with the fixed effect of sex and a predictor model with an added fixed effect of PoA; both models included random i

ntercepts for speakers as random effects. P-values were obtained via likelihood ratio test comparing the predictor model against the null model.

Results revealed a significant effect of PoA on VPO ($\chi^2 = 25.27$, $p < .001$, $df = 2$). An ANOVA of the predictor model also confirmed the significant fixed effect of PoA ($F(2, 630) = 12.89$, $p < .001$). The model summary indicated that [m] was significantly different than [n]; however, no other differences were found significant.

We also investigated the fixed effect of sex as well as the interaction effect of PoA and sex on VPO; neither of them, however, were found significant.

4 Discussion

The findings of this study could not confirm a significant difference between the bilabial and palatal nasals, as reported in Rochette & Grégoire (1983)[1]. On the other hand, our study found a significant difference between bilabial and alveolar nasals, a comparison which was not examined before. One caveat about these results is that, though significantly larger than Rochette & Grégoire (1983), we had a small number of tokens for the palatal category compared to bilabials and alveolars. Future studies should include a balanced number of tokens for all the categories.

The lack of significant interaction between sex and VPO indicate that VPO is most likely a linguistic phenomenon and is less likely affected by physiological differences of the vocal tract. Further, sex we cannot from the current study say if the impact of PoA is articulatory or phonetic. It could be due to articulatory reasons that the more anterior closure enables a greater opening in the velum. It could also be a phonetic target that production of /m/ requires greater nasal resonance than /n/ or /ɲ/. Further studies would need to be conducted, including to determine if the difference in VPO between /m/ and more posterior nasals is cross-linguistic.

Though this study was conducted on continuous speech rather than elicited tokens, a limitation is that it was based on sentences that were read in the lab as opposed to completely natural speech. An area of further study could be to run such analyses on spontaneous speech in naturalistic settings.

5 Conclusion

The analysis through ANOVA and the likelihood ratios revealed that there is indeed an effect of PoA on the VPO within the category of nasal consonants. No effect of sex

or speaker was found to provide an interaction. These results support previous literature where gradation of VPO across conditions was investigated, and it builds onto existing research by filling the gap of whether there is an effect of speaker or sex.

Though significant results were found, future research could seek to elucidate whether this difference can be explained as deriving from biomechanical or acoustic factors.

Acknowledgements

The authors would like to thank Hillary Smith, Ernest Tse, Chiachih Lo, and Erin Mawhinney for their assistance with data preparation and Charissa Y Purnomo for assistance with editing and formatting. This work is funded by NIH grant number DC-002717 to Haskins Laboratories and NSERC Discovery Grant RGPIN-2021-03751 to Bryan Gick.

References

- [1] Rochette, C. E., & Grégoire, L. (1983). Contribution à l'étude des coarticulations de consonnes occlusives et de voyelles en français à l'aide de la radiocinématographie et de l'oscillographie. Québec QC, Canada: Centre international de recherches sur le bilinguisme. (International Center for Research on Bilingualism).
- [2] Rochette, C. E. (1973). Les groupes de consonnes en français: étude de l'enchaînement articulaire à l'aide de la radiocinématographie et de l'oscillographie. Paris, France: P C. Klincksieck.
- [3] Benguerel, A., Hirose, H., Sawashima, M., & Ushijima, T. (1977). Velar coarticulation in french: A fiberoptic study. *Journal of Phonetics*, 5(2), 149-158. DOI:10.1016/S0095-4470(19)31125-8
- [4] Pua Schleif E, Pelland CM, Ellis C, Fang X, Leierer SJ, Sutton BP, Kuehn DP, Blemker SS, Perry JL. (2020). Identifying Predictors of Levator Veli Palatini Muscle Contraction During Speech Using Dynamic Magnetic Resonance Imaging. *J Speech Lang Hear Res*, 63(6):1726-1735. DOI: 10.1044/2020_JSLHR-20-00013
- [5] Perry JL, Kuehn DP, Sutton BP, Gamage JK. (2014). Sexual dimorphism of the levator veli palatini muscle: an imaging study. *Cleft Palate Craniofac J*, 51(5):544-52. DOI: 10.1597/12-128
- [6] Jordan HN, Schenck GC, Ellis C, Rangarathnam B, Fang X, Perry JL. (2017). Examining Velopharyngeal Closure Patterns Based on Anatomic Variables. *J Craniofac Surg*, (1):270-274. DOI: 10.1097/SCS.00000000000003284
- [7] Munhall, K. G., Vatikiotis-Bateson, E., & Tohkura, Y. (1995). X-ray film database for speech research. *The Journal of the Acoustical Society of America*, 98(2), 1222-1224. DOI:10.1121/1.413621
- [8] Rasband, W.S. (1997). *ImageJ*. U. S. National Institutes of Health. Bethesda, Maryland. USA. <https://imagej.nih.gov/ij/>
- [9] R Core Team. (2020). *R: A language and environment for statistical computing*. R Foundation for statistical computing. Vienna, Austria. <https://www.R-project.org>
- [10] Kuznetsova, A., Brockhoff, P. B., & Christensen, R. H. (2017). *lmerTest* package: tests in linear mixed effects models. *Journal of statistical software*, 82(13), 1-26. DOI:10.18637/jss.v082.i13.

DEVELOPMENT OF AN INTRA-AURAL PROTECTIVE DEVICE FOR HEARING-IMPAIRED INDIVIDUALS WORKING IN NOISY ENVIRONMENTS

Solenn Ollivier^{*1}, Hugues Nélisse^{†2}, Fabien Bonnet², Rachel E. Bouserhal¹, Christian Giguère³, and Jérémie Voix^{‡1}

¹Université du Québec, École de technologie supérieure, Montréal, Québec, Canada

²Institut de recherche Robert-Sauvé en santé et en sécurité du travail, Montréal, Québec, Canada

³Université d'Ottawa, Ottawa, Ontario, Canada

1 Introduction

Occupational hearing loss (OHL) is one of the most common occupational diseases, affecting 16 to 24% of the population worldwide [1,2]. For this sensorineural type of hearing loss, permanent damage is caused to the inner-ear organs after repeated hazardous noise exposure. OHL not only has an impact on hearing and communication capabilities, but also contributes to unemployment, social isolation and psychological disorders. In Canada, approximately 40% of workers have reported being exposed to hazardous noise exposure [3]. Hearing impairment, whether it is noise-induced or age-related, causes difficulties in communication as well as in the perception and localization of sound. Due to the slow and stealthy onset of hearing loss coupled with an aging working population, more and more workers in the industry suffer from hearing impairment. In a work environment, the consequences of impaired hearing include difficulties to perform tasks and communicate efficiently, as well as safety issues. To mitigate these consequences and to keep doing their job in a safe, efficient and autonomous way, most hearing impaired workers wear hearing aids while at work. However, while these devices appear as a preferred solution, their use in a noisy environment raises important challenges. Even though remarkable progress has been made to improve fitting algorithms in the last decade, they are not specifically designed for use in a noisy workplace. In fact, audiologists usually recommend not to wear hearing aids when being exposed to loud sounds. Current products are not yet able to recognize sounds of interest, thus amplifying already high level ambient sounds, and increasing the risk of further hearing loss. Moreover, no reliable existing solution can assess the noise exposure of workers wearing hearing aids [4].

A recent study on workers needing to wear hearing aids, and their work conditions, highlighted four main guidelines : 1) the establishment of recommendations to support hearing-impaired (HI) workers, 2) research on a reliable noise exposure measurement method for HI individuals in professional settings, 3) the development of an intra-aural device with features of both a protector and a hearing aid which could directly measure the noise dose, 4) study of the benefits of active sound restoration devices through electroacoustic and psychoacoustic measurements [4]. This paper focuses on the methods and preliminary works around the implementation of hearing aid algorithms on an intra-aural device intended to be used as both a hearing protector and a hearing aid.

*. sollivier@critias.ca

†. hugues.nelisse@irsst.qc.ca

‡. jeremie.voix@etsmtl.ca

2 Creating a protective hearing aid

Following the third recommendation of Leroux *et al.* [4], a solution to support HI workers is to develop a unique protective hearing aid device that can allow for both sound attenuation and amplification to communicate properly in noisy environments. In this project, hearing aid algorithms will be implemented within a device that features two earpieces, each instrumented with a loudspeaker and two microphones, such that the final prototype offers benefits from both hearing aid and hearing protection devices. Not only will this device amplify and protect, it will also monitor the individual's noise exposure and provide research evidence on the needs of hearing-impaired workers in loud workplaces. To this aim, in-ear dosimetry will be included for real-time monitoring of the wearer's noise exposure. Combining these three features into one single intra-aural device to create the final prototype could reduce the risk of further hearing loss among HI workers and enhance the development of a unique platform for research.

The development will follow two main phases. The first phase consists of the platform and prototype development. Laboratory tests and electroacoustic measurements will provide guidance in choosing key features for hearing aid algorithms, including wide dynamic range compression (WDRC), hearing aid fitting algorithms and filters. These algorithms, alongside those for in-ear dosimetry, will be implemented in MATLAB (MathWorks, Natick, MA, USA) and tested on an acoustic test fixture. After being implemented on the hardware, further described in section 3, the algorithms will be tested to evaluate the benefits of continuous monitoring and fitting algorithms while simulating low to severe hearing loss.

The second phase will consist of subjective measurements on human subjects such as psycho-acoustic tests. A wide range of conditions typical of industrial noise environments will be tested, with speech and non-speech signals. This validation step will enable a better understanding of how to practically adapt hearing aid algorithms and parameters in various noise environments.

3 Developing hearing aid compression algorithms

The final prototype will use the TYMPAN.org open platform (under MIT license, Massachusetts, USA), an open source hearing aid development platform that includes a hardware audio board featuring a Teensy 3.6 programmed with an 8 band WDRC. It can be used with Arduino and Teensyduino

add-on, and transmit information to the two aforementioned earpieces. Aside from the WDRC algorithm used, one of its benefits is the possibility for it to provide binaural sound transmission. Before the final algorithms are implemented in TYMPAN, simulations aiming to select the right programming features and parameters will be performed on MATLAB. The architecture of the hearing aid algorithm will be inspired from the hearing aid simulator coded in the MATLAB Speech Testing Environment (MSTE), initially designed to allow measurement of speech reception thresholds (SRT) under various listening and processing conditions [5]. This hearing aid algorithm includes a signal-enhancement module with noise reduction algorithms, the NAL-RP linear hearing-loss prescription [6], an amplitude compression algorithm implementing an input-controlled automatic gain control (AGCi) system, a volume control block, an amplitude compression algorithm implementing an output-controlled (AGCo) system, and symmetric peak or center clipping. WDRC demonstrates better opportunities when it comes to speech recognition in noise for individuals with moderate to severe hearing loss [7]. Splitting the signal into bands allows to independently adapt compression features depending on the frequency range. The number of bands should be chosen by finding a compromise between vowel recognition (wider range compression needed) and consonant recognition (smaller dynamic range needed) [8]. The 8-band WDRC algorithm from TYMPAN seems to be a good fit for the hearing aid device wanted and will be tested.

4 Preliminary Results

To later run the simulations through MATLAB, the WDRC code was transferred from TYMPAN to MATLAB. Filter and compression functions were compared at the outputs of TYMPAN and MATLAB. The filterbank implemented in TYMPAN is made up of third order successive Butterworth filters. Their linearity and flat response in the pass band make them ideal for hearing aid algorithms. The consistency between the MATLAB coded filter and the TYMPAN original filter is verified by comparing the filter spectrum from TYMPAN to the one of a white noise signal passed through the MATLAB filter. As shown in figure 1, the MATLAB coded filter response, illustrated by the solid line, is the one expected with cutoff frequencies being consistent.

The compressor response was also studied and compared. While speech treatment seemed to be consistent between TYMPAN and MATLAB, noise was clearly compressed with the TYMPAN version and not with the MATLAB coded compressor. This can be due to the adaptive feedback cancellation part of the TYMPAN algorithm that was not implemented in MATLAB.

5 Conclusions

The need for a device able to combine sound amplification, sound attenuation and dosimetry has been established. To achieve this, algorithms must be developed, implemented and tested using, at each step, the most advantageous platform.

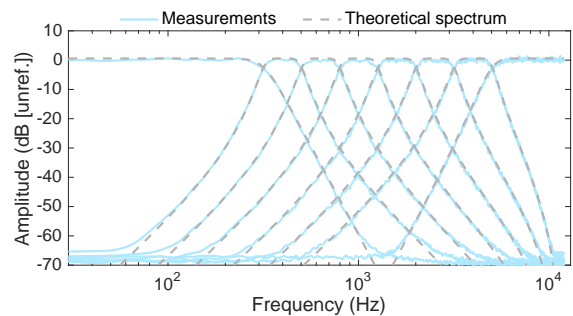


Figure 1: Frequency response of the filterbank : comparison between implemented TYMPAN filters responses (solid lines) and designed MATLAB filters (dashed lines)

Preliminary simulations involving the use of WDRC in two different coding environments seem promising. While features need to be adapted, and some work yet needs to be done for the two environments to be fully consistent, it has been shown that transfer between both platforms is possible without losing main characteristics.

Acknowledgments

First author acknowledges the financial support received from EERS Global Technologies Inc. during her internship at the NSERC-EERS Industrial Research Chair in In-Ear Technologies (CRITIAS). Authors would like to thank Mr. Nithin Raj, MITACS Globalink intern at CRITIAS, and Mrs. Danielle Benesch, master student at CRITIAS for their technical support and coordination, respectively.

References

- [1] D.I. Nelson, R.Y. Nelson, M. Concha-Barrientos, and M. Fingerhut. The global burden of occupational noise-induced hearing loss. *American journal of industrial medicine*, 48(6) :446–458, 2005.
- [2] S. Brown, L.M. Jenstad, A. Ryall, and E. Stephenson. Changes in the prevalence and characteristics of hearing loss in a noise-exposed population between 1980 and 2015. *Canadian Acoustics*, 49(1) :21–30, 2021.
- [3] K. Feder, D. Michaud, J. McNamee, E. Fitzpatrick, H. Davies, and T. Leroux. Prevalence of hazardous occupational noise exposure, hearing loss, and hearing protection usage among a representative sample of working Canadians. *Journal of occupational and environmental medicine*, 59(1) :92, 2017.
- [4] T. Leroux, C. Laroche, C. Giguère, and J. Voix. Hearing aid use in noisy workplaces. *IRSSST Studies and Research R-1015*, 2018.
- [5] N.N. Ellaham, C. Giguère, and W. Gueaieb. A new research environment for speech testing using hearing-device processing algorithms. *Canadian Acoustics*, 42(3) :92–93, 2014.
- [6] D. Byrne, A. Parkinson, and P. Newall. Hearing aid gain and frequency response requirements for the severely/profoundly hearing impaired. *Ear and hearing*, 11(1) :40–49, 1990.
- [7] L. M. Jenstad, R.C. Seewald, L.E. Cornelisse, and J. Shantz. Comparison of linear gain and wide dynamic range compression hearing aid circuits : Aided speech perception measures. *Ear and Hearing*, 20(2) :117–126, 1999.
- [8] P.C. Loizou, M. Dorman, and J. Fitzke. The effect of reduced dynamic range on speech understanding : implications for patients with cochlear implants. *Ear and hearing*, 21(1) :25–31, 2000.

COMPUTER ASSISTED SEGMENTATION OF TONGUE ULTRASOUND AND LIP VIDEOS

Pertti Palo*¹

¹Indiana University, Bloomington, Indiana

1 Introduction

In many speech analysis tasks, such as evaluating reaction times, combining direct measurement of articulation or muscular activation with audio data is preferable to using only audio data [1, 2]. However, compared to segmenting acoustic speech data, time domain analysis of tongue ultrasound data and lip videos is challenging and there is yet to develop a consensus on best tools for the task. The most widely used method is to select time points for articulatory analysis on the basis of audio segmentation. In contrast, for acoustic analysis the spectrogram provides an easy way of analysing time and frequency domain characteristics of the speech signal in one glance.

Among articulatory measurement methods tongue ultrasound is currently one of the most used. While analysing extracted tongue contours is perhaps the most popular method of analysing tongue ultrasound data, recently methods that analyse the whole ultrasound image have received attention [3–5].

One such method is an analysis tool called Pixel Difference (PD), which can be used for direct phonetic analysis of tongue ultrasound data [6, 7]. The tool is an application of the Euclidean distance metric to the whole ultrasound image. It can be used to easily visualise over all change in the data. This study extends PD for simultaneous analysis of synchronised tongue ultrasound and lip videos. Analysis results of a sample data set of synchronously recorded ultrasound and lip video from a single speaker will be discussed in the presentation.

2 Materials

The speech materials come from a delayed naming experiment, which were recorded with the high-speed ultrasound facility at Queen Margaret University. The data is described in more detail as Experiment 2 of the author’s PhD thesis [6]. In it lexical /CVC/ words were produced by speakers of Standard Scottish English. The materials analysed here come from a young adult male speaker designated P1.

In the experiment the participants were asked to remain at rest until they heard the go signal – a 1 kHz pure tone – and then produce the target word as soon and as accurately as possible. Ultrasound was captured at 120 fps and FOV was 137 degrees. And lip videos from a side view camera mounted on the ultrasound helmet at 29.97 fps and de-interlaced to 59.94 fps. Results and further details have been published in the thesis [6].

*. pertti.palo@taurlin.org

3 Method : Pixel Difference (PD)

Pixel Difference (PD) is a change metric which can be used on any pixelated data. In this study, we use PD on raw ultrasound frames (probe return data). PD is the Euclidean distance between consecutive frames where each frame is interpreted as an N-dimensional vector (N is the number of pixels in the raw ultrasound frames). In many cases (e.g. top panel of Figure 1) PD provides a clear view of tongue gestures and is particularly useful in identifying articulatory utterance onset.

4 Results

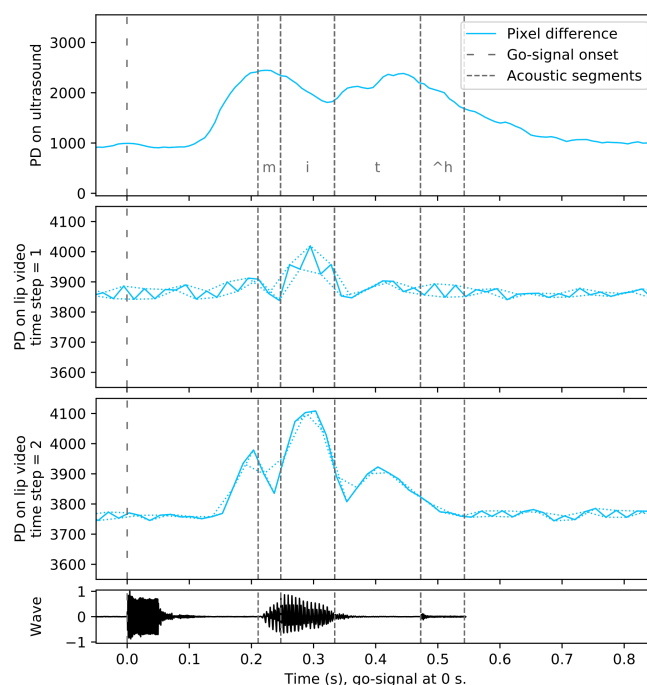


FIGURE 1 – Scottish English speaker pronouncing /meet/. PD on raw ultrasound (top panel) and on lip video data : second panel – time step = 1 ; third panel – time step = 2).

4.1 Selection of time step

One of the choices available in fine tuning PD to a given data source or set, is selection of the used time step. Given no other constraints it is preferable to compare consecutive data frames without skipping any [6]. This means using a time step of 1. In other words, that the individual pixel differences are calculated as $\Delta_i(t + .5) = pixel_i(t) - pixel_i(t + 1)$ where i spans the pixels in a frame and $PD(t + .5) = \sqrt{\sum_{i=1}^n \Delta_i^2}$. Using a longer step means we loose time locality of PD : $\delta_i(t + s/2) = pixel_i(t) - pixel_i(t + s)$, where $s > 1$. Yet qualities of the data may force us take this choice [6].

As we can see in the second panel of Figure 1, PD on lip video data has a clear sawtooth wave riding on it when we use a time step of 1. In some extreme cases any analyzable change in the curve is masked by this sawtooth effect. The ripple alternates between consecutive frames. Envelope curves have been drawn on the image with dotted lines to aid visual analysis.

To find a solution to this problem, time steps between 1 and 5 were used on a small test data set. The results provided evidence for the effect being a consequence of odd vs. even frame comparison as it was smallest on even time steps (comparing even with even and odd with odd), but largest with odd time steps. Since using a time step larger than 2 did not bring much additional clarity to the curves, this step was chosen as recommended one.

Third panel from top in Figure 1 shows the same data as the previous panel, but now analysed with time step of 2. As we can see, almost all of the sawtooth is gone and the changes in the curve are much clearer to the eye. Some sawtooth noise does still remain.

4.2 Other observations

As we can see by looking at the y-scale of the middle panels of Figure 1, PD on lip videos required zooming to make the changes visible. Fortunately, the PD signal level is constant within a recording session with a relatively stable noise floor, which in this example session was about 3750 PD units. Due to changes in image content the noise floor and signal levels change from session to session making it necessary to adjust the y-scale each time data is processed.

As is visible in the displayed example, the tongue and lip PD curves at times move in synchrony and at times they are out of phase. In particular, in this data set lip PD with very few exceptions trailed behind tongue PD at the start of an utterance. This is true even for /s/ onsets, which based on previous results should have broken the pattern (see Experiment 3 in [6], /t/ is not comparable here as participant of Experiment 3 was a Finnish speaker).

5 Discussion

The tool presented here provides a method of viewing overall change in both ultrasound and lip video data as a time varying function. As has been previously reported, having access to such functions makes movement onset detection a fast and simple task [8]. It changes the work flow from time consuming back-and-forth viewing of video frames to just inspecting a single curve.

However, for detailed analysis of within-utterance-movements it would be useful to be able to access the videos – both the ultrasound sequence and the lip video – based on the PD curves. This would make it possible to not only find movement maxima and minima, but also inspect the quality of movement at a given point. Implementing a suitable GUI that will display the video frames that correspond to selections on the PD curve is a project for the near future.

Code availability

All PD analysis code was written in Python 3.7.4, NumPy 1.17.2, Scikit-video 1.11.1 and plots drawn with Matplotlib 3.1.1. The code is available as open source code under the GPL license as part of the Speech Articulation ToolKIT (SATKIT) [7, 9].

Acknowledgments

I wish to thank Steve Cowen for assistance with the ultrasound recordings and Professor Alan Wrench for advice and help on extracting the raw ultrasound data and lip videos from AAA and subsequent post-processing of the data. This work has been in part supported by a grant from the Emil Aaltonen Foundation.

References

- [1] Alan H. Kawamoto, Qiang Liu, Keith Mura, and Adrianna Sanchez. Articulatory preparation in the delayed naming task. *Journal of Memory and Language*, 58(2) :347 – 365, 2008.
- [2] Lotje van der Linden, Stephanie Kathleen Ries, Thierry Legou, Boris Burle, Nicole Malfait, and F-Xavier Alario. A comparison of two procedures for verbal response time fractionation. *Frontiers in Psychology*, 5(1213) :1 – 11, 2014.
- [3] E. Drake, S. Schaeffler, and M. Corley. Articulatory evidence for the involvement of the speech production system in the generation of predictions during comprehension. In *Architectures and Mechanisms for Language Processing (AMLAP)*, Marseille, 2013.
- [4] T. G. Csapó, K. Xu, A. Deme, T. E. Grácz, and A. Markó. Transducer misalignment in ultrasound tongue imaging. In *Proceedings of the 12th International Seminar on Speech Production (ISSP 2020)*, pages 166 – 169, Online / New Haven, CT, 2020.
- [5] M. Saito, F. Tomaschek, C.-C. Sun, and R. H. Baayen. An ultrasound study of frequency and co-articulation. In *Proceedings of the 12th International Seminar on Speech Production (ISSP 2020)*, pages 206 – 209, Online / New Haven, CT, 2020.
- [6] P. Palo. *Measuring Pre-Speech Articulation*. PhD thesis, Queen Margaret University, Edinburgh, Edinburgh, 2019.
- [7] Palo, P. and Moisić, S. R. and Faytak, M. SATKIT : Speech Articulation ToolKIT [Python software package]. Available in a public software repository, accessed 28 Aug 2021, 2020. <https://github.com/giuthas/satkit>.
- [8] P. Palo. Can we detect initiation of tongue internal changes before overt movement onset in ultrasound? In *Proceedings of the 12th International Seminar on Speech Production (ISSP 2020)*, pages 242 – 245, Online / New Haven, CT, 2020.
- [9] M. Faytak, S. R. Moisić, and P. Palo. The speech articulation toolkit (satkit) : Ultrasound image analysis in python. In *Proceedings of the 12th International Seminar on Speech Production (ISSP 2020)*, pages 234 – 237, Online / New Haven, CT, 2020.

THE CONTEXTUAL EFFECTS OF NASAL VOWELS ON VELOPHARYNGEAL OPENING IN QUÉBÉCOIS FRENCH

Charissa Y. Purnomo^{*1}, Linda X. Wu¹, Jahurul Islam¹, Gillian de Boer¹, and Bryan Gick^{1,2}

¹Department of Linguistics, University of British Columbia, Canada

²Haskins Laboratory, New Haven, Connecticut, United States of America

1 Introduction

In oral sound production, the velum is typically held against the posterior pharyngeal wall (PPW), separating the oral and nasal cavities, while for nasal sounds there is a velopharyngeal opening (VPO), allowing sound to resonate in the nasal cavities [1].

Though nasality may be phonologically characterized as a binary feature (e.g., [+nasal] vs. [-nasal]), the phonetic realization of nasalisation is dependent upon a host of other properties both within the segment itself (e.g., vowel height, consonant voicing) and combined with surrounding segments (e.g., coarticulation) [2]. Contextual nasalisation is the coarticulatory nasalisation of a speech segment due to the nasality of the surrounding environment. The nasalisation of an oral sound preceding a nasal segment is referred to as anticipatory nasalisation while the nasalisation of an oral sound following a nasal is referred to as carryover nasalisation [3].

Coarticulation studies attempting to provide insight into the complex interactions of linguistic and physiological factors required for nasalisation have frequently compared the velum's behaviour during anticipatory and carryover nasalisation [2 - 5]. French is the language of reference in the literature due to the contrast in oral and phonemically nasal vowels. Existing literature suggests that the carryover phenomenon demonstrates a greater degree of nasalisation than its anticipatory counterpart for both nasal vowels and nasal consonants [3 - 5]. However, the generalization of such results is limited by indirect measurements of VPO (e.g. airflow, electromagnetic midsagittal articulography), and/or small numbers of speakers incorporated in the methodology.

To verify existing claims regarding the VPO during contextual nasalisation in French, the present study applies a more direct measurement of VPO—the distance between the velum and the PPW—from X-ray data across a larger number of speakers. Furthermore, our data samples come from sentence-level speech, unlike the previous studies which used isolated words, syllables, or vowels. As such, the following experiment investigated the effect of phonemically nasal vowels on the VPO of oral vowels that precede (carryover) or follow (anticipatory) them.

2 Method

2.1 Database

For this experiment, we used the Université Laval X-ray cine-fluorographic database [6] of speakers recorded in 1974. We

analysed the films of 9 speakers (4 female) of Québécois French aged 19-30 years at the time of data collection.

2.2 Measurement

In order to measure the VPO for each segment we extracted the frames from each video at a rate of 30 fps. In ImageJ [7], we drew a line for the best “path of velum” across the VPO, determined by inspecting stacks of images (See Figure 1). The posterior coordinates of the line were where the velum met the PPW and the anterior coordinates were set at the portion of the velum at rest that first started to move towards the PPW. The number of black pixels along this line was used to determine the degree of opening for each frame (more black pixels = greater opening). The number of pixels was converted to a ratio for each speaker, where 1 = maximally open and 0 = maximally closed.



Figure 1: Example of a “path of velum” line for one speaker.

For segment identification we extracted the audio from the videos, transcribed at the breath-group level, and then ran it through Montreal Forced Aligner [8] to label each segment. Manual adjustments were made as needed. Using a custom Praat [9] script, we extracted the timing and labeling information for each segment. This information, along with the timing of the degree of VPO at each frame was combined and analysed.

2.3 Statistical analysis

Using R [10] we analysed the contextual effects of nasal vowels on oral vowels. As the segments spanned multiple frames, a single VPO measure was calculated by taking the mean VPO across the whole segment. As mentioned before, we looked only at oral vowels that either preceded (anticipatory nasalisation) or followed (carryover nasalisation) phonemically nasal vowels. Instances where there was a nasal segment preceding and following the oral vowel were excluded

* charissa.purnomo@ubc.ca

(i.e. $\tilde{V}\tilde{V}\tilde{V}$), as to not double count the segments. We ran linear mixed effects models (lmerTest) and an ANOVA to conduct a likelihood ratio test and check for interaction effects. The predictor model had Nasal Context and Sex as fixed effects and intercepts for individual speakers as random effects. P-values were obtained by comparing the predictor model with models without the fixed effect in question.

3 Results

Overall, the average VPO for anticipatory nasalisation ($M = 0.28$, $SD = 0.15$) was higher than that of carryover nasalisation ($M = 0.22$, $SD = 0.10$) with an indication that the pattern is consistent across both sex groups.

Figure 2 shows the distribution of VPO in anticipatory nasalisation ($N = 108$) and carryover nasalisation ($N = 87$) in an oral vowel adjacent to a nasal vowel. The y-axis represents the mean VPO ratio. The x-axis is participant sex.

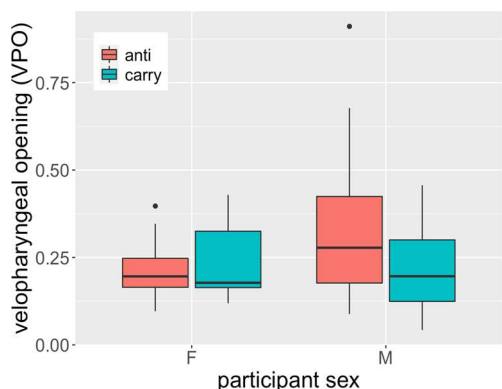


Figure 2: Boxplots of VPO ratio by gender (4F, 5M), for anticipatory and carryover nasalisation due to nasal vowels.

The linear mixed effects analysis revealed a significant interaction effect between Sex and Nasal Context ($\chi^2 = 10.96$, $df = 1$, $p < .001$). The summary of the predictor model revealed no significant main effect of Sex or Nasal Context, but there was a significant Nasal Context-Sex interaction effect ($df = 188.09$, $t\text{-value} = -3.34$, $p < .001$). For males, the VPO for anticipatory nasalisation ($M = 0.31$, $SD = 0.16$) was significantly larger than for carryover nasalisation ($M = 0.21$, $SD = 0.10$).

4 Discussion

Overall, our results suggest that in Québécois French, males have greater VPO for anticipatory nasalisation than for carryover nasalisation, contradicting past results in other French studies [3 - 5]. A possible reason for sex differences are that males are reported to have more coronal velic closures, while females are reported more circular closure [11]. Due to the angle of the videos, we are only able to measure from a sagittal perspective and may not capture a more circular closure.

Limitations

Our research is confined by the database, which was recorded nearly fifty years ago. As such, there is potential that our results may not apply to present day Québécois French. As well, the conditions of read speech in a lab, in contrast to natural running speech, may have had an impact on the results. Lastly, our study was on Québécois French alone, while past studies have also looked at Belgian French and Standard French.

Acknowledgments

The authors would like to thank Chiachih Lo, Ernest Tse, Hillary Smith and Erin Mawhinney for their assistance with data preparation and Yadong Liu and Jacqueline (Ama) Murray for assistance with editing and formatting. Work funded by the NIH grant number DC-002717 to Haskins Laboratories and NSERC Discovery grant RGPIN-2021-03751 to Bryan Gick.

References

- [1] Perry JL. Anatomy and physiology of the velopharyngeal mechanism. In *Seminars in speech and language*. 2011 May; 32(2): 083-092. © Thieme Medical Publishers.
- [2] Delvaux V, Demolin D, Harmegnies B, Soquet A. The aerodynamics of nasalization in French. *Journal of Phonetics*. 2008 Oct 1;36(4):578-606.
- [3] Rochette, CE., Grégoire L. Contribution à l'étude des coarticulations de consonnes occlusives et de voyelles en français. Centre international de recherche sur le bilinguisme/The International Research Center of Bilingualism. 1983.
- [4] Basset P, Amelot A, Vaissière J, Roubeau B. Nasal airflow in French spontaneous speech. *Journal of the international phonetic association*. 2001 Jun;31(1):87-99.
- [5] Rossato S, Badin P, Bouaouini F. Velar movements in French: an articulatory and acoustical analysis of coarticulation. In *Proceedings of the 15th International Congress of Phonetic Sciences 2003* (pp. 3141-3144). Barcelona, Spain.
- [6] Munhall, K. G., Vatikiotis-Bateson, E., & Tohkura, Y. X-ray film database for speech research. *The Journal of the Acoustical Society of America*, 1995;98(2):1222-1224.
- [7] Rasband, W.S. 2018. ImageJ, U. S. National Institutes of Health, Bethesda, Maryland, USA, <https://imagej.nih.gov/ij/>, 1997-2018.
- [8] McAuliffe M, Socolof M, Mihu, S, Wagner M, Sonderegger M. Montreal Forced Aligner: trainable text-speech alignment using Kaldi. *Proceedings of the 18th Conference of the International Speech Communication Association*. 2017.
- [9] Boersma P. Praat, a system for doing phonetics by computer. *Glott International*. 2001; 5:9/10:341-345.
- [10] R Core Team. R: A language and environment for statistical computing. R Foundation for Statistical Computing, Vienna, Austria. 2020. Retrieved from <https://www.R-project.org/>.
- [11] Jordan, HN., Schenck, GC., Ellis, C., Rangarathnam, B., Fang, X., & Perry, JL. Examining Velopharyngeal Closure Patterns Based on Anatomic Variables. *J Craniofac Surgeon*, 2017;28(1):270-274.

SPEAKER ACCOMMODATIONS TOWARDS VUI VOICES ON THE DIMENSIONS OF VOICE ONSET TIME AND PITCH RANGE

Gracellia Purnomo^{*1}, Chloë Farr², Charissa Purnomo³, Nicole Ebbutt³, Amanda Cardoso³ and Bryan Gick^{3,4}

¹School of Audiology and Speech Sciences, University of British Columbia, Canada

²Department of Linguistics, University of Victoria, Canada

³Department of Linguistics, University of British Columbia, Canada

⁴Haskins Laboratory, New Haven, United States of America

1 Introduction

There is a growing presence and integration of voice-user interfaces (VUIs) in the form of virtual assistants such as Siri, Alexa, and Google Home. VUIs are inanimate objects, however they use animate (human) voices to interact with their client.

Accommodation occurs when an interlocutor adjusts their speech in relation to another interlocutor [1], either by converging (becoming more similar) to, or by diverging (becoming more different) from, the other speaker. Speakers may accommodate on any level of the hierarchy of linguistic features, including syntactic features, lexical choices, or phonetic features of their speech [2], the last of which is the focus of the current investigation. On the phonetic level, voice onset time (VOT) [3] and pitch range [4, 5] have been identified as common features in which speakers accommodate to an interlocutor.

The present paper considers whether or not interlocutors may employ the same types of speaker accommodation towards these inanimate objects. In addition, since the human-likeness, or perceived animacy of VUIs can be different amongst operating systems, the additional question arises of whether the perceived human-likeness may further increase the likelihood of the device being treated as such. The present study examines whether speakers accommodate voice onset time (VOT) and pitch to VUI voices and the extent to which the human-likeness of the voice influences accommodation.

2 Methods

2.1 “VUI” voices

Four Amazon Polly [6] synthetic voices were rated by 26 linguists for perceived human-likeness and the voices rated most and least human-like were used in the experiment. Polly’s standard system was used as the robotic voice (hereafter “R”), and Polly’s neural system was used as the human-like voice (hereafter “H”) as a consequent of these ratings. As VOT was similar for both voices, in order to be able to see the extent of accommodation, the VOT was manipulated in Praat [7] so that the VOT of the voiceless plosive consonants of R were twice the length of the Amazon Polly output, and half the length for H. These voices were used to mimic a VUI system in that the responses would be played directly after a participant read out pre-determined prompts.

2.2 Experiment

The study took place virtually via UBC-secured Zoom. Participants were asked to read two practice prompts (pre-test) presented on their screen, from which they heard no response. This was followed by thirteen prompts for which they heard a response from the VUI voice (post-test). For example, the participant read the prompt “Where can I buy pots and pans?” which the VUI responded by saying “You can buy pots and pans from Canadian Tire.” This procedure was repeated with the same prompts for “R” and “H”. Participants then completed a survey regarding their professional and personal experiences with VUIs, and what they believed the experiment to be about. No participants had professional experience with VUI and all participants believed that they were interacting with an authentic VUI system.

2.3 Participants

Forty-two English-speaking participants were recruited through UBC’s Linguistics in the Classroom (LOC) system. Participants with poor audio or speakers who did not report English as their dominant language were omitted, leaving 25 participants. Participants were assigned to one of two counterbalanced presentations of the voices (voice order).

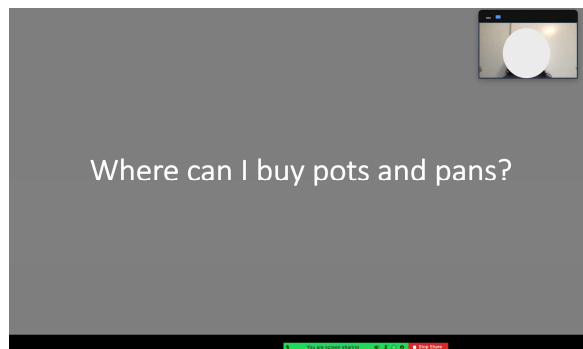


Figure 1: Screenshot of participants' view.

2.4 Measurements

Textgrids for participants' audio recordings were generated using Montreal Forced Aligner [7]. Each voiceless plosive VOT length was manually marked with high interrater reliability and then extracted using a Praat script. Pitch trajectories of acoustic syllables for each prompt sentence were extracted automatically using Prosogram [8]. We report the results for mean and median F0 in semitones and TrajPhonZ, which is essentially a Z-scored measure of how variable the pitch is.

* gracellia.purnomo@gmail.com

3 Results

Linear mixed effects models were applied to the VOT and pitch results with H or R voice and voice order group as fixed effects with an interaction, and participant and prompt as random effects.

It should be noted that speakers demonstrate a wider range of pitch variation in the pre-test speech compared with the post-test (H, R) speech. None were found to be significant. In other words, there is no difference in either VOT values (Figure 2) or pitch (mean, median, variation) (Figure 3) between pre-test and post-test responses by the speakers nor between the speakers' responses to the two voice types (H, R).

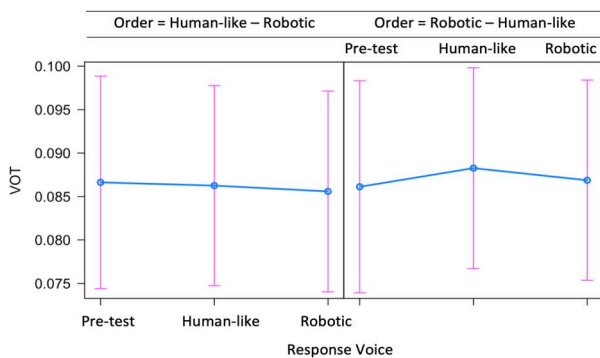


Figure 2: VOT results by voice order group and response voice.

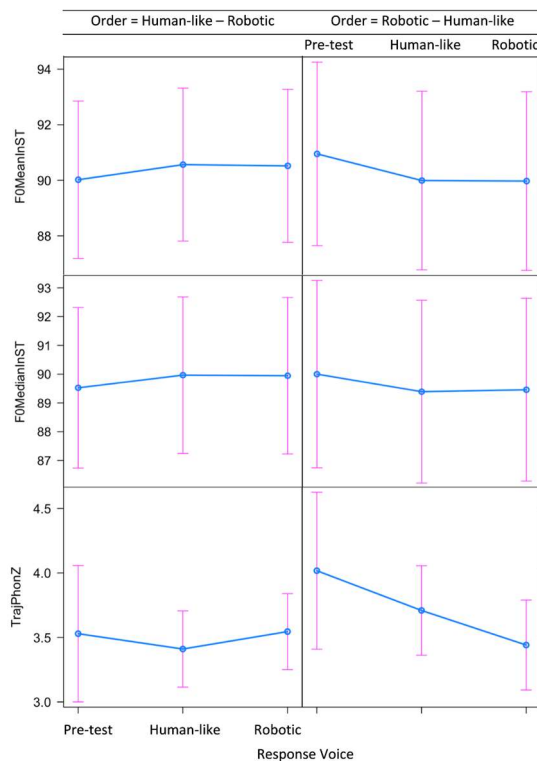


Figure 3: Pitch results by voice order group and response voice.

Furthermore, visual inspection of the individual speaker results suggest that while at a group level there were no significant differences, at an individual level, there are some speakers who are accommodating to the VUI voices.

4 Discussion

The current findings do not point to a consensus on whether and how interlocutors accommodate towards VUIs. Although some participants did show some tendency for accommodation, there was not consistency in whether speakers diverged or converged. Further investigation of who these speakers are and why they accommodate is in progress. Accommodation is in part motivated by an interlocutor's awareness of social standing. Such motivation may be less likely to exist when interacting with a VUI, and may play a part in the lack of accommodation.

Acknowledgments

The authors would like to thank Kristen Eredics for her contributions towards analysis. This work was supported by the National Institutes of Health grant number DC-002717 to Haskins Laboratories and SSHRC Insight Grant 435-2019-0426 to Bryan Gick.

References

- [1] Bell A. Language Style as Audience Design. *J Language in Society*. 1984 Jun [cited 2021 Aug 11];13(2):145-204. Available from: <https://doi.org/10.1017/S004740450001037X>
- [2] Lindblom B. Explaining phonetic variation: A sketch of the H&H theory. In: Hardcastle W, Marchal A, editors. *Speech Production and Speech Modeling*. Springer Netherlands; c1990. p. 403-439.
- [3] Asano Y, Gubian M. "Excuse meeee!": (Mis)coordination of lexical and paralinguistic prosody in L2 hyperarticulation. *J Speech Communication* [Internet]. 2018 May [cited 2021 Aug 11];99:183-200. Available from: <https://doi.org/10.1016/j.specom.2017.12.011>
- [4] Babel M, Bulatov D. The role of fundamental frequency in phonetic accommodation. *J Language and Speech*. 2011 Sep [cited 2021 Aug 11];55(2):231-248. Available from: <https://doi.org/10.1177/0023830911417695>
- [5] Oviatt S, Maceachern M, Levow GA. Predicting hyperarticulate speech during human-computer error resolution. *J Speech Communication*. 1998 May [cited 2021 Aug 11]; 24:87-110. Available from: [https://doi.org/10.1016/S0167-6393\(98\)00005-3](https://doi.org/10.1016/S0167-6393(98)00005-3)
- [6] Amazon Web Services. Amazon Polly. 2019. Retrieved from <https://aws.amazon.com/polly/>
- [7] McAuliffe M, Socolof M, Mihy, S, Wagner M, Sonderegger M. Montreal Forced Aligner: trainable text-speech alignment using Kaldi. Proceedings of the 18th Conference of the International Speech Communication Association. 2017.
- [8] Mertens P. Polytonia: a system for the automatic transcription of tonal aspects in speech corpora. *J Speech Sciences*. 2014 Jan;4(2):17-57.

THE EFFECTS OF MICROGRAVITY ON TONGUE HEIGHT

Arian Shamei^{*1} and Bryan Gick^{†1,2}

¹University of British Columbia, Canada

²Haskins Labs, New Haven, United States of America

1 Introduction

A previous investigation comparing astronaut speech during and after the Apollo 11 mission reported a significant increase across all formants during microgravity exposure, which was interpreted as evidence the tongue is lower in the mouth during articulation in microgravity conditions [1]. However, the microgravity (space) condition speech used in this analysis was routed through telephone channels while the earth condition was not. As telephone speech is known to result in an increase to formant values [2], it is unclear whether any observed effect was due to microgravity or telephone bandwidths. Furthermore, comparing speech during and after microgravity exposure is problematic because adaptation effects to microgravity can be observed in the vowel space following prolonged exposure to microgravity [3]. Using higher quality audio from the STS-129 and 135 missions and linear mixed effects models, we compare the first vowel formant (F1) of two astronauts immediately before and during exposure to microgravity during space travel.

2 Methods

The North American Space Association (NASA) provides audio-logs for all missions through the public NASA audio archive (<https://archive.org/details/nasaaudiocollection>). Audio files featuring speech from Charlie Hobaugh during the STS 129 and and Chris Ferguson during the STS 135 missions were selected. These files were chosen because they provide high quality audio interviews conducted preflight (serving as 1g condition data), and midflight (serving as microgravity condition data) by each Astronaut. All preflight condition speech was produced on Earth shortly before departure, and all midflight speech was produced aboard the International Space Station.

For each participant, approximately 90 seconds of speech were extracted from each condition for analysis. Each file was manually transcribed and subsequently assessed using semi-automated alignment and formant extraction via the Dartmouth Linguistic Automation suite (DARLA) [4], using the Montreal Forced Aligner [5] and FAVE-extract [6]. Stopwords were omitted from the analysis along with unstressed vowels and tokens where the formant bandwidth exceeded 300Hz. The quality of automatic alignment was verified manually for each file, and formant extraction values were examined for impossible values, of which none were observed. A total of 7 vowels met the selection criteria of providing at least ten tokens in each condition. Selected vowels and their counts in each condition are outlined in Table 1.

*. arian@alumni.ubc.ca

†. gick@mail.ubc.ca

Table 1: Number of vowel tokens for each condition

	AA	AE	EH	EY	IY	OW	UW
Preflight	13	15	31	18	25	17	21
Midflight	14	26	29	38	28	20	11

A variable-slope linear mixed-effect model evaluating F1 was fit to the data in R [7] using the lme4 package [8] and the optimx optimizer [9]. This model was designed to evaluate the effect of condition (1g, microgravity) while controlling for the effect of speaker and vowel. Our model included random intercepts by speaker and vowel; random slopes over condition by speaker and random slopes over condition by vowel. The corresponding lme4 formula in R is as follows :

```
F1 ~ condition +  
      (1 + condition | speaker) +  
      (1 + condition | vowel)
```

Statistical significance of the main effect was calculated using a likelihood-ratio test comparing our model to one omitting the main effect of condition.

3 Results

Results of the linear mixed effects regression are outlined in Table 2. The first column denotes condition, while the second and third columns provide the F1 (in Hz) and standard error of the mean as calculated for each condition. Note that the mean F1 between conditions are similar, although standard error of the mean in the microgravity condition is substantially higher.

Table 2: F1 per condition as calculated via LMER

	F1 (Hz)	St. Err
Preflight	487.6	8.5
Midflight	491.2	38.6

The results of our LRT-based model comparison demonstrate that condition did not have a significant effect on F1 ($\chi^2 = 0.17$, $df = 1$, $p = 0.68$). In other words, we found no evidence to support the claim that vowels are articulated lower in the mouth in microgravity conditions.

For illustrative purposes, a cross-conditional vowel plot illustrating the mean F1 and F2 of all vowel tokens for both speakers is provided in Figure 1. F1 is provided on the Y axis with values inverted, F2 is provided on the X axis. Midflight tokens are indicated in orange and preflight tokens in blue. Note that both height and backness of the vowel space does not differ noticeably between conditions.

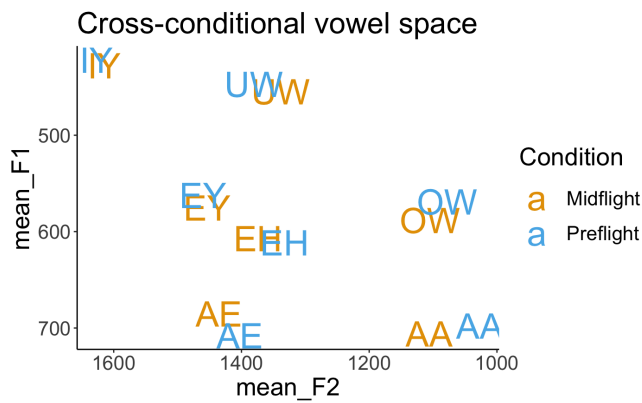


Figure 1: Cross-conditional vowel plot illustrating mean F1 and F2 for both speakers

4 Discussion and Conclusion

The results of our linear mixed effects model found no effect of microgravity on tongue height. Overall, no difference in vowel space could be observed for speech produced prior or during microgravity exposure. These results do not support previous observations of increased F1 (decreased tongue height) in microgravity conditions [1]. We note that the previous investigation used audio data from the Apollo 1969 moon landing mission. All in-flight audio in the Apollo 1969 missions was transmitted through telephone channels in Houston. Considering that previous work made use of speech routed through telephone channels in the microgravity condition, but not for the control condition, it is unsurprising that an increase to all formants was observed. A sharp increase to formants in telephone speech is a well-documented phenomenon known as the "telephone effect" [2]. As the authors made no mention of controlling for the telephone effect, this remains the likeliest explanation for the discrepancy between our findings.

In the present study, microgravity condition speech was transmitted to earth from the ISS using satellite-broadcast Ku-band radio frequencies [10]. The high quality nature of this signal avoids the characteristic frequency warping of telephone speech.

We also note that [1] used speech from post-flight interviews as the control condition data. Recent work demonstrates speech following prolonged exposure to microgravity is characterized by a generalized lowering of the vowel space [3]. This reflects adaptation to microgravity conditions where articulatory effort to counteract gravity is not required.

5 Conclusions

Our results do not support previous work describing an increase to formants in microgravity conditions. An increase to formants observed in previous work was likely the result of telephone bandwidth alterations. We conclude that future investigations of astronaut speech must take care to ensure audio bandwidth is comparable across conditions, and that data serving as the control condition is taken prior to microgravity

exposure rather than after.

Acknowledgments

This work was funded by NIH Grant DC-002717 awarded to the second author.

References

- [1] Chengzhu Yu and John HL Hansen. A study of voice production characteristics of astronaut speech during apollo 11 for speaker modeling in space. *The Journal of the Acoustical Society of America*, 141(3) :1605–1614, 2017.
- [2] Francis Nolan. The 'telephone effect' on formants : a response. *Forensic linguistics*, 9(1) :74–82, 2002.
- [3] Arian Shamei and Bryan Gick. The effects of outer space on vowel space. *Canadian Acoustics*, 47(3) :110–111, 2019.
- [4] Sravana Reddy and James N Stanford. Toward completely automated vowel extraction : Introducing darla. *Linguistics Vanguard*, 1(1) :15–28, 2015.
- [5] Michael McAuliffe, Michaela Socolof, Sarah Mihuc, Michael Wagner, and Morgan Sonderegger. Montreal forced aligner : Trainable text-speech alignment using kald. In *Interspeech*, volume 2017, pages 498–502, 2017.
- [6] Ingrid Rosenfelder, Josef Fruehwald, Keelan Evanini, Scott Seyfarth, Kyle Gorman, Hilary Prichard, and Jiahong Yuan. Fave (forced alignment and vowel extraction) suite version 1.1.3, May 2014.
- [7] R Core Team et al. R : A language and environment for statistical computing. 2013.
- [8] Douglas Bates, Deepayan Sarkar, Maintainer Douglas Bates, and L Matrix. The lme4 package. *R package version*, 2(1) :74, 2007.
- [9] John C Nash, Ravi Varadhan, et al. Unifying optimization algorithms to aid software system users : optimx for r. *Journal of Statistical Software*, 43(9) :1–14, 2011.
- [10] Sandra May. The space network : Cell towers for astronauts, Sep 2018.

3D FINITE ELEMENT MODEL OF THE HUMAN THORAX TO STUDY ITS LOW FREQUENCY RESONANCE EXCITED BY AN ACOUSTIC HARMONIC EXCITATION ONTO THE CHEST WALL

Arife Uzundurukan^{*1,2}, Philippe Micheau^{†1,2}, Sébastien Poncet^{‡1}, Pierre Grandjean^{§1,2}, and Daria Camilla Boffito^{¶3}

¹Department of Mechanical Engineering, Université de Sherbrooke, Sherbrooke, Québec, Canada

²Centre de Recherche Acoustique-Signal-Humain de l'Université de Sherbrooke, Sherbrooke, Québec, Canada

³Department of Chemical Engineering, Polytechnique Montréal, Montréal, Québec, Canada

1 Introduction

Chest physiotherapy (CPT), the standard current treatment method, is known as effective for bronchial drainage. By development of the technology, CPT shows a tendency to be independent of physiotherapists in order to provide patient accessibility of the treatment, whenever and wherever they need an airway clearance therapy (ACT) at low cost [1]. A realistic mechanical and numerical models, which is created by a real Computerized Tomography (CT), could be used to enhance our understanding of relevant sound transmission phenomena in the examination of respiratory disease and render the study possible to go further.

The acoustic studies in the literature deal with thorax geometry generally focus on the lung parenchyma and by using the difference in the propagation of shear wave provides the detection of the vicinity of parenchyma [2]. The interest in the application of Biot theory for the determination of physical material properties of the lungs has been increased because of the restriction of validity of the medium effective theory.

Ong and Ghista [1] have investigated the average chest resonance frequency for healthy male and female volunteers as 26.7 Hz and 27.8 Hz, respectively, in the frequency range of 15-50 Hz. Resonance occurs when a system is able to store and easily transfer energy and tends to vibrate at a higher amplitude. For ACT devices used in CPT, vibrations effect on the viscoelastic, shear-thinning, and thixotropic properties of bronchial mucus, liquefying it to ease expectoration. The influence of the range of frequency and the viscoelasticity [3] and the thermophysical properties [4] of mucus have been determined previously. However, any studies have been conducted so far to examine 3D finite element model (FEM) of the human thorax, which renders it possible to see the effects on the inside of airways for living bodies, by an acoustic harmonic excitation in the low frequency range.

In this study, it is aimed to investigate the thorax response in the low frequency range, 20-60 Hz, by a realistic 3D FEM of the human thorax. The acoustic harmonic excitation is investigated by 28 mm radius cylindrical shape under 5 N, which equals to 160 dB_{SPL} onto the back chest surface wall.

2 Method

The dimensions of the geometries belong to a male were determined by using CT scans via 3D Slicer 4.10.2. After the simplification, repairment, and conversion to solid geometries, the finite element model (FEM) has been created. The created FEM model in front view, in back view, under .stl meshes and under real meshes in the back view are illustrated in Fig. 1a., Fig. 1b., Fig. 1c., and Fig. 1d., respectively.

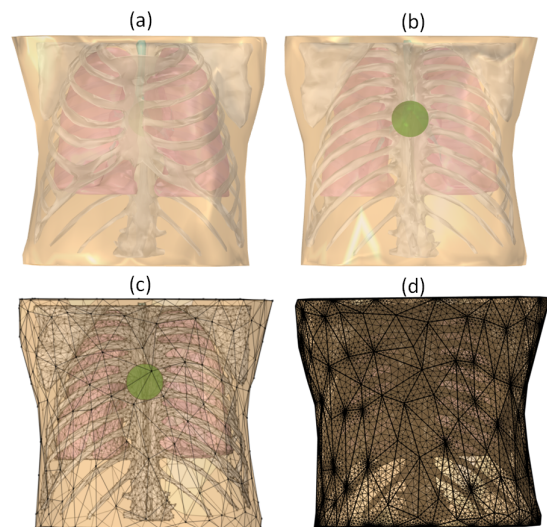


Figure 1: The modelled human thorax (a) in front view, (b) in back view, and in the back view (c) .stl meshes and (d) real meshes

The geometry shown in Fig. 1c. consists of 3×10^5 tetrahedral and 5.4×10^4 triangular meshes. The minimum and the maximum skewness quality of the geometry illustrated in Fig. 1d. are of 0.014 and 0.578, respectively. The result is taken within 2 h 32 min with the processor Intel(R) Core(TM) i7-9700 CPU @ 3.00 GHz with 16 GB RAM memory.

The physical properties of the airways was determined by $\rho_a=1000 \text{ kg/m}^3$, $E_{a1}=0.28 \text{ MPa}$, $E_{a2}=0.124 \text{ MPa}$, $\nu_a=0.49998$ [2]. For the soft tissue, which includes muscle, fat, and etc., and osseous region, which consists of rib cage, scapula, sternum, and etc., are considered as viscoelastic material. Therefore, Voight model is used. For the osseous region the material properties are taken as $\rho_o=1500 \text{ kg/m}^3$, $\lambda_{1,o}=2.6 \text{ GPa}$, $\lambda_{2,o}=0 \text{ GPa}$, $\mu_{1,o}=10 \times 10^6 \text{ kPa}$, $\mu_{2,o}=20 \text{ Pa}$ and for the soft tissue $\rho_s=1000 \text{ kg/m}^3$, $\lambda_{1,s}=2.6 \text{ GPa}$, $\lambda_{2,s}=0 \text{ GPa}$, $\mu_{1,s}=2.5 \text{ kPa}$, $\mu_{2,s}=5 \text{ Pa}$ [5]. The physical properties of the lungs has been calculated by using Biot theory by using

*arife.uzundurukan@usherbrooke.ca

†philippe.micheau@usherbrooke.ca

‡sebastien.poncet@usherbrooke.ca

§pierre.grandjean@usherbrooke.ca

¶daria-camilla.boffito@polymtl.ca

following Eqn. 1 and in Eqn. 2.

$$\omega^2(-\rho + \beta\rho_f)u_i = \mu u_{i,jj} + (K_b + \mu/3)u_{j,ij} - (\alpha - \beta)p_i + F_i \quad (1)$$

$$\beta p_{ii} + (\phi^2/R)\rho_f\omega^2 p + \rho_f j\omega a = -\rho_f\omega^2(\alpha - \beta)u_{i,i} \quad (2)$$

where u is the steady-state dynamic oscillatory displacement, p represents the dynamic pressure of the air in the lungs in the frequency domain, α , β and R are the coupling parameters between the lung parenchyma and air, F_i shows the external inputs of force, ω is the angular velocity, and a is the rate of introduction of gas volume. When external excitation is negligible, Eqn. 1 forms as Eqn. 3, illustrates the shear behaviour.

$$\mu u_{i,jj} = -(\rho - \beta\rho_f)\omega^2 u_i \quad (3)$$

where

$$c_s = \sqrt{\mu/(\rho - \beta\rho_f)} \equiv \sqrt{\mu/\rho} \quad (4)$$

$$k_s = c_s/\omega \quad (5)$$

In here, c_s and k_s represent the shear wave and shear wave number, respectively. As for the compression waves, they are calculated from the slow compression wave numbers k_{ps} and fast compression wave numbers k_{pf} by using Eqn. 1 and Eqn. 2, where c_{pf} and c_{ps} are the fast and slow compression wave speeds. The density of the lungs is derived by Eqn. 8.

$$c_{pf} = \omega/k_{pf} \quad (6)$$

$$c_{ps} = \omega/k_{ps} \quad (7)$$

$$\rho = \phi\rho_p + (1 - \phi)\rho_t \quad (8)$$

where lung tissue density is $\rho_t=1000 \text{ kg/cm}^3$, air density in the lung $\rho_p=1.21 \text{ kg/cm}^3$ and the air volume fraction of a healthy lung is $\phi=0.75$. Therefore, the lung physical properties are calculated as $\rho_l=250.9 \text{ kg/m}^3$, $c_{sl1}=26.04 \text{ m/s}$, $c_{sl2}=2.44 \text{ m/s}$, $c_{pl1}=4.45 \text{ m/s}$, $c_{pl2}=0.61 \text{ m/s}$.

3 Results

As a result of this study, 3D FEM of the human thorax is created and the acoustic harmonic excitation is investigated by 28 mm radius cylindrical shape under 160 dB_{SPL} onto the back chest surface as shown in Fig. 1b. The acceleration amplitude data is read from against the front of the chest wall surface as illustrated in Fig. 1a. under the frequency range of 20-60 Hz. As illustrated in Fig. 2, the acceleration amplitude, which reaches the peak point as 0.6332 m/s^2 at 28 Hz, is 0.4785 m/s^2 and 0.2021 m/s^2 at the lowest and highest frequencies in this frequency range.

4 Discussion

28 Hz is investigated as the resonance frequency with the inertance of $0.1266 \text{ m/s}^2 \cdot N$ in the frequency range of 20-60 Hz as shown in Fig. 2b. Even both of the resonance frequency and the inertance value depend on the chest size, gender, and body-mass index, the numerical results consistent

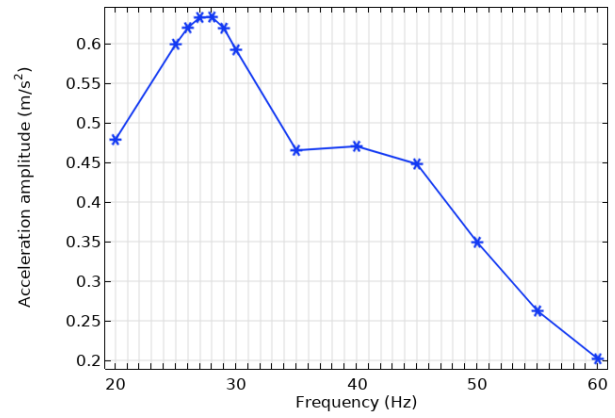


Figure 2: Acceleration amplitude in the low frequency

with the reported average CPT experimental data with 23 volunteers in the literature [1].

At 28 Hz, therefore, the thorax is able to store and easily transfer the energy and tends to vibrate at a higher amplitude. However, to determine the best CPT frequency, the viscoelastic, shear-thinning, and thixotropic properties of mucus has to be also investigated in this frequency range. Because even the maximum vibration occurs on the chest surface at 28 Hz frequency, it can differ for airways.

5 Conclusions

In the present study, the numerical results present the vibratory harmonic responses under the frequency range of 20-60 Hz onto the back surface of the thorax. The chest-resonance frequency under the excitation is obtained as close to 28 Hz. Despite the detailed complex human thorax geometry, the results are consistent with reported experimental CPT data in the literature. As a future study, a set of multidisciplinary experimental study for the viscoelastic, shear-thinning, and thixotropic properties of mucus will be conducted to go further in this acoustic study.

References

- [1] J.H. Ong and D.N. Ghista. Applied chest-wall vibration therapy for patients with obstructive lung disease. *Human Respiration: Anatomy and Physiology, Mathematical Modeling, Numerical Simulation and Applications*, 3:157, 2006.
- [2] Z. Dai, Y. Peng, B.M. Henry, H.A. Mansy, R.H. Sandler, and T.J. Royston. A comprehensive computational model of sound transmission through the porcine lung. *The Journal of the Acoustical Society of America*, 136(3):1419–1429, 2014.
- [3] D. Schieppati, R. Germon, F. Galli, M.G. Rigamonti, M. Stucchi, and D.C. Boffito. Influence of frequency and amplitude on the mucus viscoelasticity of the novel mechano-acoustic Frequenter. *Respiratory Medicine*, 153:52–59, 2019.
- [4] O. Lafforgue, N. Bouguerra, S. Poncet, I. Seyssiecq, J. Favier, and S. Elkoun. Thermo-physical properties of synthetic mucus for the study of airway clearance. *Journal of Biomedical Materials Research Part A*, 105(11):3025–3033, 2017.
- [5] H.E. Von Gierke, H.L. Oestreicher, E.K. Franke, H.O. Parrack, and W.W. von Wittern. Physics of vibrations in living tissues. *Journal of Applied Physiology*, 4(12):886–900, 1952.

PROSODIC DIFFERENCES IN MANDARIN SPEAKERS WITH ALZHEIMER'S DISEASE

Yadong Liu^{*1}, Arian Shamei^{†1}, Linda Wu^{‡1} and Bryan Gick^{♦1,2}

¹Department of Linguistics, University of British Columbia, Canada

²Haskins Laboratory, New Haven, United States of America

1 Introduction

Alzheimer's disease (AD) is a progressive neurodegenerative disorder, and the most common cause of dementia [1]. Previous research has documented changes to the speech of AD patients, including altered voice quality [2] and reduced pitch modulation in speakers of English [3]. Martínez-Sánchez et al. [4] compared the prosodic profile of Spanish-speaking AD patients and neurotypical controls and found AD speech was characterized by a flattened prosodic profile, including reduced variability of F0 and flattened prosodic trajectories within and across syllables.

To our knowledge, no work has investigated whether a flattened prosodic profile can be observed in AD patients speaking a tonal language such as Mandarin. The present study seeks to substantiate the utility of prosodic change as an acoustic biomarker for AD in Mandarin speech. Our study provides insights into how prosodic impairment caused by AD affects users of tonal languages.

2 Methods

2.1 Participants

Speech from ten AD patients (5 male, 5 female) were extracted from DementiaBank Lu corpus [5]. Patients performed picture naming tasks and the Cookie theft picture description task [6]. As no control data was provided in the Lu corpus, speech from ten gender-matched neurotypical older controls (mean age: 65.6, range: 54-74) were extracted from YouTube interviews and talks. Speech samples in both groups were selected to provide naturalistic speech in Taiwan Mandarin. Approximately 50 seconds of continuous speech was extracted for each speaker in both groups. No demographic information was provided for AD patients in the Lu corpus.

2.2 Data processing and analysis

Each audio file was trimmed to remove speech from additional interlocutors. Trimmed files were then run through Prosogram [7] to extract prosodic features. For all files, manual pitch ranges were specified based on gender (males: 70-200 Hz, females: 100-300 Hz) and automatic syllable segmentation was employed. The glissando threshold was specified to 0.16T², DG=20, dmin = 0.035) and frame period to 0.005.

We investigated eight prosodic features, including pitch range (Pitch range), average F0 value (Mean F0), standard deviation of F0 (SD F0), percentage of nuclei with pitch change greater than 4 semitones (% dynamic nuclei), percentage of nuclei with pitch rising greater than 4 semitones (% rises), percentage of nuclei with pitch falling greater than 4 semitones (% falls), intra-syllabic pitch change per second (Intrasyll traj) and inter-syllabic pitch change per second (Intersyll traj). Using the statistical software suite R [8], a one-way analysis of variance (ANOVA) was conducted to evaluate the effect of condition for each feature.

3 Results

We present results for all eight metrics that are summarized for each group in Table 1. All measurements are taken in semitones to allow comparisons between genders. Except for mean pitch, the AD group had reduced means for all metrics. ANOVA test results demonstrated a significant effect of condition for pitch range, SD pitch, % dynamic nuclei, % rises, % falls, intrasyllabic and intersyllabic trajectories observed in the control group compared to the AD group. However, no significant difference was observed for mean pitch between the AD and the control group.

Table 1: Mean and standard deviation of eight prosodic features among AD and control speakers, and ANOVA test results between two groups for each feature.

	AD	Control	ANOVA results
	Mean (SD)	Mean (SD)	
Pitch range	11.7(2.1)	14.8(1.3)	Df=1, F=15.4, $p = 0.001$
Mean pitch (ST)	87.1(4.6)	86.6(3.7)	Df=1, F=0.09, $p = 0.772$
SD pitch (ST)	2.6(0.5)	3.6(0.4)	Df=1, F=24.3, $p < 0.001$
% dynamic nuclei	7.3(4.2)	17.2(5)	Df=1, F=23.2, $p < 0.001$
% rises	0.3(0.3)	1.3(0.7)	Df=1, F=19.6, $p < 0.001$
% falls	7.1(4.1)	16(5.5)	Df=1, F=17.1, $p < 0.001$
Intrasyll traj.	11.4(4.3)	19.6(3.2)	Df=1, F=23.7, $p < 0.001$
Intersyll traj.	17(3.2)	27(4.5)	Df=1, F=32.5, $p < 0.001$

Figure 1 provides comparative prosograms illustrating prosodic trajectories in the AD (top) and the control group (bottom). Within each prosogram, the y-axis reflects pitch

* yadong.liu@ubc.ca

† arian.shamei@ubc.ca

‡ lindaw0207@gmail.com

♦ gick@mail.ubc.ca

range, and the x-axis reflects time. Intrasyllabic trajectories are denoted by black bars. Green and magenta contours represent absolute and band-passed intensity. Note that F0 trajectories in the AD group are observably flatter than those in the control group within individual syllables, reflecting reduced intrasyllabic trajectory measurements. Variation in F0 between syllables is also reduced, reflecting reduced inter-syllabic trajectories.

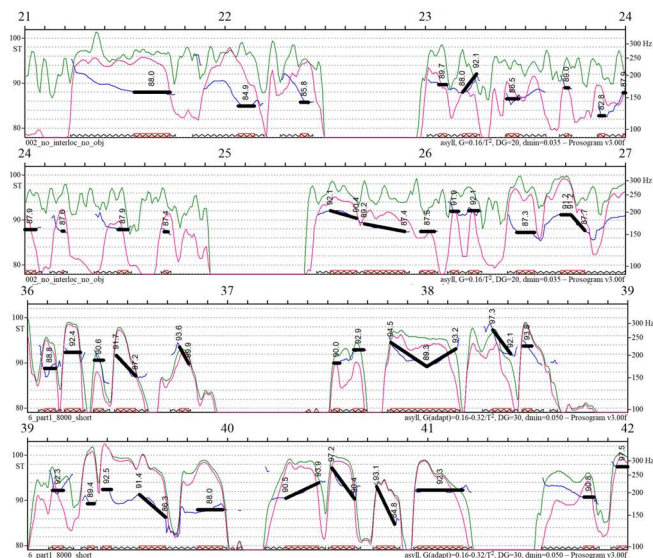


Figure 1: Comparative prosograms of an AD patient (top) and control (bottom).

4 Discussion and conclusion

The results of our prosographic analysis align with previous observations of a flattened prosodic profile for AD patients in Spanish [4] and English [3].

In the present analysis, AD patients exhibited reduced pitch range and reductions to pitch trajectories within and across syllables, comparable to those previously observed in [4]. Our data suggests that prosodic impairments observed in AD affect speakers of languages that make use of phonemic tone.

We acknowledge that differences in the nature of speech samples between AD and control groups (experimental speech task vs interview/lecture) may have contributed to differing prosodic profiles, but consistency between the present findings and previous work grant us confidence in our findings. Future work may benefit from comparing a larger number of speakers and ensuring consistency between speech tasks in the control and AD group.

Acknowledgments

The authors would like to thank Melissa Wang and Kaiwen Yu for performing data collection and transcription. Work funded by the NIH grant number DC-002717 to Haskins Laboratories and NSERC Discovery grant RGPIN-2021-03751 to Bryan Gick.

References

- [1] Waldemar G, Phung KT, Burns A, Georges J, Hansen FR, Iliffe S, et al. Access to diagnostic evaluation and treatment for dementia in Europe. *International Journal of Geriatric Psychiatry: A journal of the psychiatry of late life and allied sciences*. 2007 Jan;22(1):47-54.
- [2] Luz S, Haider F, de la Fuente S, Fromm D, MacWhinney B. Alzheimer's dementia recognition through spontaneous speech: the ADReSS Challenge. *arXiv preprint arXiv:2004.06833*. 2020 Apr 14.
- [3] Horley K, Reid A, Burnham D. Emotional prosody perception and production in dementia of the Alzheimer's type. *Journal of Speech, Language, and Hearing Research*. 2010; 53(5): 1132-1146.
- [4] Martínez-Sánchez F, JJ GM, Pérez E, Carro J, Arana JM. Expressive prosodic patterns in individuals with Alzheimer's disease. *Psicothema*. 2012 Feb 1;24(1):16-21.
- [5] MacWhinney, B., Fromm, D., Forbes, M. & Holland, A. (2011). *AphasiaBank: Methods for studying discourse*. *Aphasiology*, 25,1286-1307.
- [6] Cummings L. Describing the cookie theft picture: Sources of breakdown in Alzheimer's dementia. *Pragmatics and Society*. 2019 Jul 5;10(2):153-76.
- [7] Mertens, Piet (2004) *The Prosogram : Semi-Automatic Transcription of Prosody based on a Tonal Perception Model*. in B. Bel & I. Marlien (eds.) *Proceedings of Speech Prosody 2004*, Nara (Japan), 23-26 March. (ISBN 2-9518233-1-2)
- [8] R Core Team (2020). *R: A language and environment for statistical computing*. R Foundation for Statistical Computing, Vienna, Austria. URL <https://www.R-project.org/>.



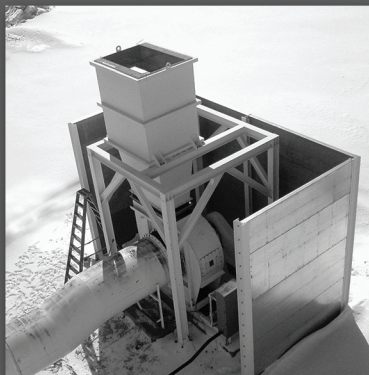
INDUSTRIAL | COMMERCIAL | ENVIRONMENTAL

Noise Control

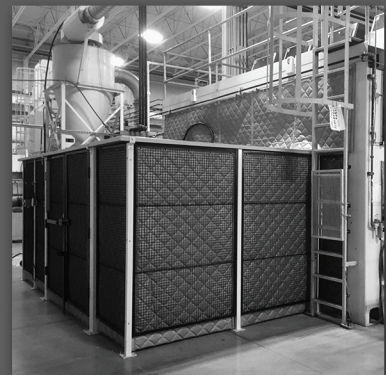
Engineered Products and Services



EQUIPMENT YARD NOISE
RIGID ABSORPTION PANELS



FAN NOISE
BARRIERS & SILENCERS



INDUSTRIAL NOISE
NOISE CONTROL CURTAINS



kineticsnoise.com
canadiansales@kineticsnoise.com
1-800-684-2766

ABSTRACTS FOR PRESENTATIONS WITHOUT PROCEEDINGS PAPER RÉSUMÉS DES COMMUNICATIONS SANS ARTICLE

Performance Of Tonal And Broadband Backup Alarms In Terms Of Worker Safety

Christian Giguère, Chantal Laroche, Hugues Nélisse, Véronique Vaillancourt

Backup alarms are installed and are often mandatory on heavy vehicles to alert workers and passersby of safety risks associated with reverse operations. The performance of backup alarms depends on many technical (e.g., alarm sound power level, placement of alarm device on vehicle), acoustic (e.g., sound distribution around vehicle) and psychoacoustic (e.g., detection and reaction thresholds, ability to localize alarm, effect of hearing loss and hearing protection) factors. A series of studies on these factors was conducted jointly by the University of Ottawa and the "Institute de Recherche Robert-Sauvé en Santé et Sécurité du travail" in Montreal. This paper focuses on comparing the relative benefits of two types of backup alarms, the conventional tonal alarm ("beep-beep") and the emerging broadband alarm ("pschtt-pschtt"). Results indicate that the broadband alarm yields better overall performance than the tonal alarm, as demonstrated by more uniform sound distribution patterns in the danger zone behind the vehicle, lower alarm reaction thresholds and easier sound localization. The broadband alarm is particularly advantageous when hearing protectors are worn. Preliminary results also indicate that the broadband alarm may be a better choice than the tonal alarm in the presence of hearing loss.

Comparison Of Two Commercial Binaural Dummy Heads

Pierre Grandjean, Olivier Robin, Alain Berry, Philippe-Aubert Gauthier

Binaural listening allows to reproduce auditory source localization cues, and thus to spatialize a sound scene using a simple audio headset. A method to obtain binaural recordings is to use a binaural dummy head, generally consisting of a head (sometimes a torso), and two ears in which microphones are placed. Such device allows to directly consider the time and space modifications induced by the presence and the geometry of a human body (involving interaural time and level differences). Dummy heads are offered by several companies for entertainment and research applications. It is difficult to estimate whether the large price differences that can be seen on the market (factors up to a 100) translate into a substantial difference in terms of measurement quality. To partially answer this question, measurements in an anechoic room were made for four configurations: (1) a G.R.A.S. KEMAR dummy head, (2) a Binaural Enthusiast B1-E dummy head; both equipped with their original microphones. Then, configurations (3) and (4) were based on microphone switching between the two dummy heads. The presentation will present the experimental setup, current results and future works.

Prosodic Differences In Emotional Speech: Comparison Between Love And Sorrow

Ikuyo Kaneko, Noriko Yamane

This study explores how English prosodic features are used when expressing two different emotions, love and sorrow. American professional narrators (AE) and Japanese college students (JP) were instructed to read aloud and record a love letter and a condolence letter. Each participant read the love letter assuming that s/he would express affection on the third anniversary of their relationship and read the condolence letter assuming that s/he would convey his/her sadness and sympathy to the family of a nurturing high school teacher. Booster expressions, defined as lexical grammatical items which increase effectiveness of emotional utterances, were selected for analysis. Consonant duration, pitch range, intensity, and speech rate were measured. AE lengthened an initial consonant, raised pitch dynamically, and enhanced intensity of booster words in both types of letters. Unlike AE, JP raised pitch slightly with no consonant lengthening across boosters, and enhanced intensity selectively among words. Both AE and JP read the love letter faster than the condolence letter. The results suggest JP should be aware of the diversity of phonetic features to deliver emotions and when to use them, how pitch range should be expanded, and how an initial consonant is lengthened in booster expressions.

Speaking Versus Smiling: The Labiodentalization Of Bilabials In Korean

Elisabeth H Kang, Yadong Liu, Annabelle Purnomo, Melissa Wang, Bryan Gick

Opposing movements occurring simultaneously in speech production present a conflict that the body must resolve. Previous research has found labiodentalization of some English bilabial stops (i.e., /p/ → [f]) in instances of conflict between smiling and production of bilabials [Chan et al. 2018, JASA, 144(3)]. However, as labiodentals exist in English, it remains unclear whether this conflict was resolved through a physiological or phonological (i.e.,

learned substitution) process. The present study investigates the articulation of bilabials in neutral and smiled contexts in Korean, a language with no labiodentals. Tokens were extracted from the natural running speech of 24 YouTube interviews and vlogs from 26 speakers. The degree of intensity of the associated facial Action Units (AU), “lip corner puller” (AU12) and “lip tightener” (AU23), in the production of bilabials was analyzed using OpenFace 2.0 [Baltrusaitis et al. 2018, IEEE]. Labiodentalization of bilabial stops was observed during smiled conditions, indicating that it is a physiological rather than learned process in Korean. In the smiling condition, AU intensity results reveal decreased intensity of “lip corner puller” during bilabial closures and “lip tightener” during labiodental closures, suggesting our body could resolve the opposing forces conflict by suppressing one movement.

Characterizing End Of Utterance Movements

Pertti Palo, Steven M. Lulich

Silent speech interfaces depend on the ability to accurately map articulatory variables to acoustic speech output, but some articulatory gestures, such as those immediately preceding or following an utterance, do not generate an acoustic signal. Characterizing pre- and post-acoustic articulatory movements is therefore important for distinguishing the beginning or end of an utterance from its continuation. Because silent speech interfaces can be developed for both children and adults, it is important to characterize the speech of both populations. For the beginning of the utterance, Author (2019) provides a characterization based on tongue ultrasound: When starting from rest in a delayed naming task, the duration of the silent movement shows a strong correlation with acoustic utterance duration indicating that the silent movement happens at the same articulatory rate. Using the same methodology (see Figure), we study tongue movements after the end of the acoustic utterance. Our data comes from both adults and elementary school-aged children. Articulatory variables include lingual gestures as recorded using 3D/4D ultrasound imaging.

Prise En Charge Du Sonore En Aménagement Et En Urbanisme : Du Guide Au Terrain

Amaury Sainjon

Le bruit environnemental est une préoccupation grandissante pour les citoyens et les décideurs (Steele D., 2018). Mais au-delà de sa gestion comme une nuisance et surtout a posteriori, se pose la question de son intégration en amont dans la conception de projets urbains (Broche J. et al., 2020). En d’autres mots, comment faire du sonore une dimension constitutive de l’aménagement et de l’urbanisme ? Le train retrouvant progressivement ses lettres de noblesse, nous concentrerons la réflexion sur les infrastructures ferroviaires. Notre recherche s’est penchée sur les solutions proposées dans les guides à destination des professionnels de l’aménagement (Guastavino C., Brochu J. et al., 2021). Nous les avons extraites et identifiées en fonction de leurs approches de prise en charge du sonore. Nous les avons alors confrontés à la lumière du terrain et via les lunettes de la forme urbaine. Pour ce faire, nous avons choisi la ville de Mont-Royal. Le cas est intéressant, car il s’agit d’une Cité-jardin conçue au début du 20^e siècle autour d’une voie ferrée. Aujourd’hui le Réseau express métropolitain (REM) vient-il mettre l’exemplarité de cet ensemble urbain en cause ? La communication va d’abord présenter les éléments extraits des guides liés à la mise en espace des ensembles urbains (organisation et forme urbaine) et aux processus d’élaboration. Ensuite, nous verrons comment le sonore a été pris en charge à Mont-Royal initialement puis dans sa transformation.

On The Sound Radiation Of Head Tissues In The Earcanal At Low Frequencies Induced By A Bone-Conducted Stimulation

Huiyang Xu, Franck Sgard, Kévin Carillo, Éric Wagnac, Jacques A. De Guise

The occlusion effect (OE) may cause discomfort on users of hearing protection devices. Various models have been proposed to study the OE as they can help understand the physical mechanisms and can be used to evaluate the individual contribution on the OE of the factors that may affect it (i.e., occlusion device, ear anatomy and stimulation). However, current lumped models and finite element models of truncated ears developed to study the OE induced by a bone conduction device usually overestimate its amplitudes at low frequencies compared to experimental data. This has usually been attributed to the incomplete seal in experiments which reduces the measured OEs. In this paper a finite element model of an entire head to predict the sound pressure field in its earcanals, open or occluded by earplugs, and accounting for the fluid-structure coupling of the head/earplug system with the surrounding air is used to investigate this discrepancy. The OE level frequently overestimated by previous models is explained by an underestimated open sound pressure level in the earcanal which results from the failure to account for the sound radiation from the head tissue vibrations into the surrounding air that subsequently enters the open earcanal.



NEED TO SIMPLIFY NOISE MEASUREMENT AND ANALYSIS? JOB DONE.

No matter which profession you are in, you need a sound level meter solution that gets your job done faster, easier and problem-free. The new B&K 2245 gives you absolute confidence and control through user-friendly mobile apps and functionality tailored for your task, including on-site analysis, photo embedding, smart data handling on your PC, and more.

To simplify your job-to-do, visit www.hbkworld.com/2245



bquiet
SOUNDPROOF WINDOWS



It's that quiet.

**Cut down on noise and acoustic
interference with Soundproof windows.**

www.bquiet.ca

1.877.475.9111

THEME 3 - ACOUSTICS AND COMPUTERS - THÈME 3 - ACOUSTIQUE ET ORDINATEURS

Is Enough Enough? <i>Henk De Haan, Virgini Senden</i>	62
Data-Driven Acoustic Source Localization In Turbulent Flows <i>Arnav Joshi, Hamid Daryan, Jean-Pierre Hickey</i>	64
Multi-Objective Optimization Of The Energy Efficiency And The Tonal Noise Of The Propeller Blades Of An Unmanned Aerial Systems Rotor. <i>Tenon Charly Kone, Sebastian Ghinet, Anant Grewal, Daniel Skalecki, Viresh Wickramasinghe</i>	66
Studying The Suitability And Adaptability Of Noise Maps As A Tool For Health Prevention In The Province Of Quebec <i>Jean-Philippe Migneron, Frédéric Hubert, Benoit Lalonde, Jean-François Hardy, Yves Brousseau, Jean-Gabriel Migneron, Marie-Hélène Vandersmissen, Thierry Badard, Joë Bouchard</i>	68
Abstracts for Presentations without Proceedings Paper - Résumés des communications sans article	71

Sound and Vibration Instrumentation

Scantek, Inc.



Sound Level Meters
Selection of sound level meters for simple noise level measurements or advanced acoustical analysis



Vibration Meters
Vibration meters for measuring overall vibration levels, simple to advanced FFT analysis and human exposure to vibration



Prediction Software
Software for prediction of environmental noise, building insulation and room acoustics using the latest standards



Building Acoustics
Systems for airborne sound transmission, impact insulation, STIPA, reverberation and other room acoustics measurements



Sound Localization
Near-field or far-field sound localization and identification using Norsonic's state of the art acoustic camera



Monitoring
Temporary or permanent remote monitoring of noise or vibration levels with notifications of exceeded limits

Scantek, Inc.

Sales, Rental, Calibration 

www.ScantekInc.com 800-224-3813

WHEN IS ENOUGH, ENOUGH?

Henk de Haan ^{*1} and Virgini Senden ^{†2}

¹dBA Noise Consultants Ltd, Okotoks, Alberta, Canada

1 Introduction

Noise from Oil & Gas facilities in Alberta is regulated by the Alberta Energy Regulator (AER) in Directive 038, *Noise Control* [1], while noise from utilities (e.g., power generation and distribution) is regulated by the Alberta Utilities Commission (AUC) in Rule 012, *Noise Control* [2]. Both documents are very similar. In British Columbia (BC) the Oil & Gas Commission regulates noise from Oil & Gas facilities in the “British Columbia Noise Control Best Practices Guideline” [3], a document inspired to a large extent by Directive 038.

If sound measurements are made near a residence to verify the noise impact or the ambient sound level (ASL), a minimum of 3 hours of valid data should be gathered in both the daytime (07:00 – 22:00) and the nighttime (22:00 – 07:00) period, according to [1 - 3]. This requirement can be hard to meet in practice. We therefore revisited several ASL surveys that met the regulatory requirements and assessed how much data would be needed to acquire a value, similar to the original answer.

2 Methods

2.1 Regulatory Requirements

The ASL is defined in [1] as “The sound level that is a composite of different airborne sounds from many sources far away from and near the point of measurement. The ASL does not include any energy-related industrial component and must be measured without it”. According to [2] wind noise is also not included and therefore, wind speeds more than 3 m/s are excluded. The definition included in [3] does not contain such a direct requirement but points out that sound measurements can be affected by wind, and therefore limits acceptable wind speeds. All three documents assess the ASL as L_{eq} , except [2] that includes a separate, customized regime for wind turbines.

According to ANSI Standard S1.13-2005 [4], measurement uncertainty depends on many factors and is hard to quantify exactly. Rarely will the uncertainty in the measured average sound level L_{eq} exceed a value of ± 3 -4 dB, and seldom will the uncertainty be less than 1 dB.

The parameter typically used in [1 - 3] is the L_{eq} in dBA. We used the same parameter throughout this article.

2.2 Approach

We selected two field programs where we conducted week-long (7 days) ASL surveys. The acquired data in one-minute intervals was processed according to the requirements

included in [1 - 3]. The amount of data gathered in individual 24-hour periods met the volume requirements discussed earlier, usually by a large margin. Maximum wind speed included was 3.4 m/s, and erroneous samples (e.g., sounds close to the microphone) were excluded.

Using the processed data only, we applied the “bootstrap” method to sample each individual day or night in various time bins. Bootstrapping is a process where the sample population is randomly re-sampled (with replacement) many times, in our case a 1,000 times. In each iteration, we sampled 180 minutes (3 hrs) from the “clean” data per day or night, as well as 120 minutes, 60 minutes, 45 minutes, 30 minutes, 15 minutes and finally 8 minutes. Each iteration yielded both the average sound pressure as well as the 95% confidence interval for each bootstrap sample size, expressed as L_{eq} . We compared the thus acquired L_{eq} to the original L_{eq} from all samples for each day or night.

2.3 Site Description

The first site (site A) was located approximately 2.5 km east of the QE2 Highway, and 100 m west of a farmhouse. Residents were present during the survey. This site can be qualified as rural. The 2nd site (Site B) was located atop of a river valley, near an unoccupied residence. The river valley can be qualified as natural, with minimal man-made disturbance (if at all). For site A we processed the night time data and for site B the day time data.

3 Results and Conclusions

A comparison between the “real” L_{eq} values based on the full data set and the bootstrap values for the various time bins, indicated a difference of between 0.1 and 0.5 dB, well within the accuracy of the Type 1 instrumentation used for data collection (± 1 dB).

Calculated bootstrap values were identical within 0.1 – 0.4 dB, regardless of sample size. For site A for example, the last night yielded a bootstrap value of 37.9 dBA (180 samples) compared to 37.7 dBA (8 samples). What differed is the 95% confidence interval; the smaller the sample size, the larger the spread in the confidence interval. Please refer to the figures and table on the next page.

A 95% confidence interval of ± 3 dB seems a good value to strive for in this type of survey: threshold values included in [1 - 3] increase in steps of 3 dB, and [4] indicates a measurement value of within that range as to be expected. Typically, less than 180 minutes of valid data suffice to achieve such an accuracy, but not always. Instead of a fixed requirement for data volume, it would be better to assess a confidence interval associated with the available data.

* henk@dbanoise.com

† virgini@dbanoise.com

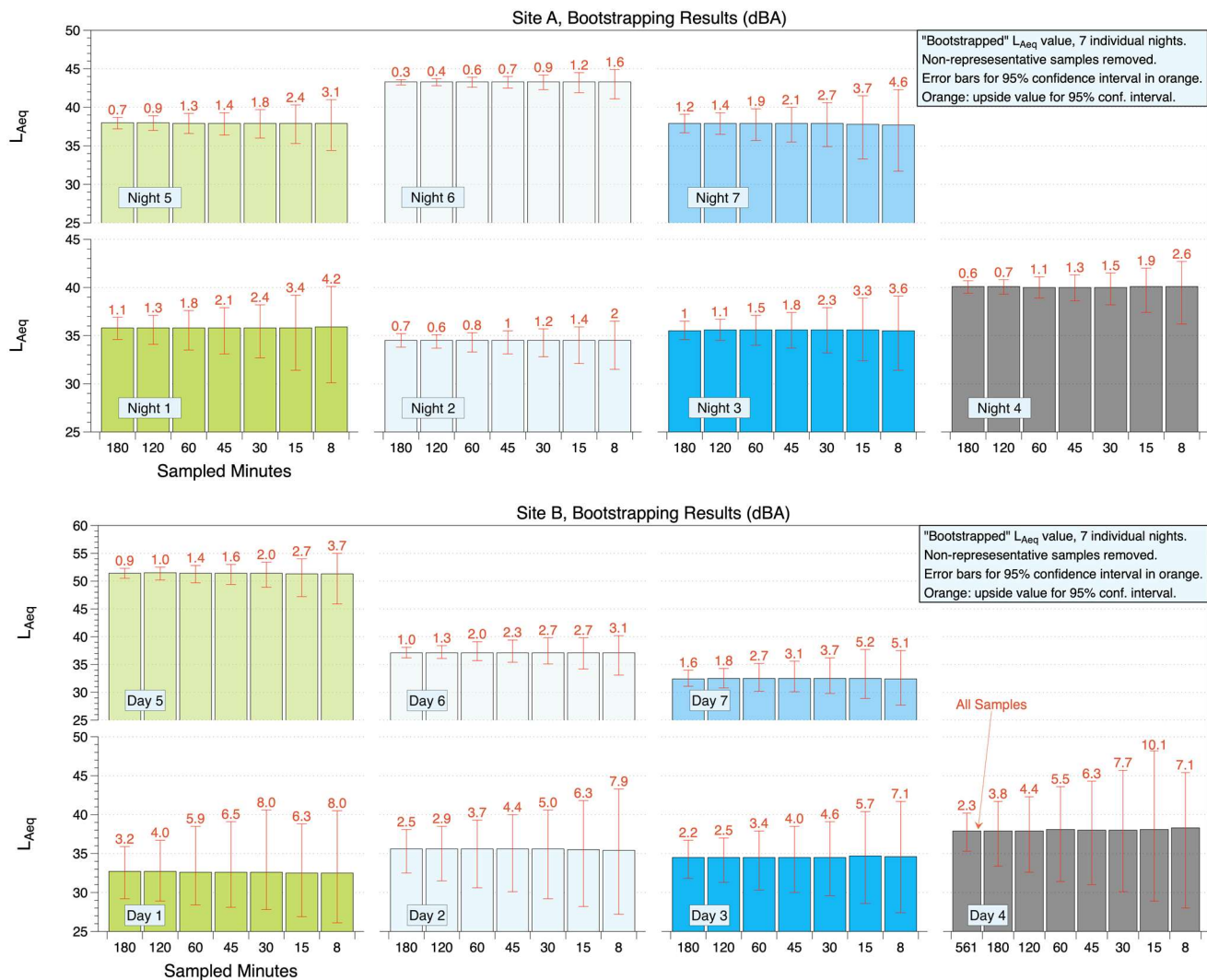


Figure 1: Bootstrapped result site A & B incl. 95% confidence intervals (dB)

Table 1: Results in dBA and required minutes of data

Description	Site A (Nighttime)			Site B (Daytime)		
	Measured L_{eq}	B. strapped L_{eq}	Req. Mins.	Measured L_{eq}	B. strapped L_{eq}	Required Mins.
Night 1 / Day 1	35.7	35.8 – 35.9	15 – 30	32.6	32.5 – 32.7	180
Night 2 / Day 2	34.4	34.5	8	35.4	35.4 – 35.6	120
Night 3 / Day 3	35.1	35.5 - 35.6	15 – 30	34.7	34.5 – 34.7	60 – 120
Night 4 / Day 4	39.8	40.0 – 40.1	8 - 15	37.9	37.9 – 38.3	All
Night 5 / Day 5	37.5	37.9 – 38.0	8 - 15	51.4	51.3 – 51.4	15
Night 6 / Day 6	43.1	43.3	8	37.0	37.1	8 -15
Night 7 / Day 7	38.1	37.7 37.9	15 - 30	32.7	32.4 – 32.5	45

References

- [1] Directive 038: Noise Control, Alberta Energy Regulator, (AER, formerly ERCB), February 16, 2007
- [2] Rule 12, Noise Control, Alberta Utilities Commission (AUC), March 1, 2021
- [3] British Columbia Noise Control Best Practices Guideline, Version: 2.2, British Columbia Oil & Gas Commission (BCOGC), July 2021

- [4] Measurement of Sound Pressure Levels in Air, ANSI S1.13-2005, American National Standard Institute (ANSI), Reaffirmed March 5, 2010.

DATA-DRIVEN APPROACH FOR ACOUSTIC SOURCE LOCALIZATION

Arnav Joshi^{*1,2}, Hamid Daryan², and Jean-Pierre Hickey²

¹Indian Institute of Technology Indore, India

²Department of Mechanical and Mechatronics Engineering, University of Waterloo, Canada

1 Introduction

Determining the strength and location of acoustic sources is crucial for studying aeroacoustic noise generation such as in vortical flows [1]. A robust technique is needed for the accurate mapping of these sources. The conventional acoustic beamforming method [2] is reliable but has limitations, suffering from spatial aliasing and poor resolution at lower source frequencies. Deep learning algorithms have emerged as powerful tools in a growing number of disciplines due to their ability to learn patterns and extract features from limited or unstructured data. Researchers have utilised deep learning to overcome the limitations of traditional methods. Xu et al [3] have used Densely connected neural networks (DNNs) for acoustic source imaging and while this paper employs largely the same methodology, it uses a Convolutional Neural Network (CNN) which is computationally less expensive, to determine the spatial and temporal characteristics of stationary and moving sound sources [4]. A training database was developed using analytically-defined monopoles which were randomly distributed over a scanning grid of fixed size. A 64-channel microphone array was simulated in a plane parallel to the plane of the scanning grid to gather information about the sources in the form of the Cross-Spectral Matrix (CSM) which was then used as an input feature to the CNN. The results showed that the CNN model was able to identify position, strength, and velocity of the sources over a range of frequencies with far better accuracy and resolution than the traditional methods.

2 Method

The proposed method is data-driven and hence a database containing enough data samples for training the CNN has to be generated first. The CNN model is then explained in detail.

2.1 Data Generation

The scanning grid is a 1.2m x 1.2m area divided into an $N \times N$ grid. The computational power and training requirement increases as the resolution of the scanning grid increases. It contains S sources distributed randomly across the N^2 grid points. The microphone array plane contains M microphones arranged in the shape of a logarithmic spiral ($M=64$ in this case) and is located 1.2m below the scanning grid. The logarithmic spiral arrangement was chosen to ensure good performance over a range of frequencies. The sound sources are modelled as monopoles and are assumed to radiate spherical pressure signals. Fast Fourier Transform has been applied on the signal to convert it from time domain to frequency domain. The pressure signal from a source s on the scanning

grid to a microphone m on the array plane [3] is given as

$$P_s(m) = \frac{e^{-j2\pi r_s/c_0}}{4\pi|r_s|} \quad (1)$$

where r_s is the distance between the particular source s and the microphone m and c_0 is the speed of sound in air which is 343 m/s. Pressure signals from every source are added at every microphone to generate the pressure vector \mathbf{P} given as

$$\mathbf{P} = \left[\sum_{s=1}^S P_s(1), \sum_{s=1}^S P_s(2), \dots, \sum_{s=1}^S P_s(M) \right] \quad (2)$$

Vector \mathbf{P} has dimensions $M \times 1$. The Cross-Spectral Matrix (CSM) is defined as

$$\mathbf{CSM} = \mathbf{P}\mathbf{P}^H \quad (3)$$

where \mathbf{P}^H is the complex conjugate of the pressure vector. The Ground Truth Matrix (GTM) contains the actual source position data. Sources are positioned randomly within the matrix and the entries that have a source are assigned the source strength values. The remaining entries (where there is no source) are assigned the value zero. The CSM is an $M \times M$ matrix and will be used as an input to the CNN. The network will be trained against the GTM which has the same dimensions as that of the scanning grid. A training sample consists of the CSM obtained from the random positioning of the sources within the GTM and, the GTM.

2.2 Convolutional Neural Network

An artificial neural network is a simulation of the biological brain composed of artificial neurons or nodes. These nodes make up layers which are interconnected to progressively extract features and learn from the data being fed to the network. The inputs to a neuron are assigned weights by the network. The activation function associated with the node calculates the output of the node based on the weighted sum of the inputs. During training, the network compares its prediction with the actual output through a loss function and modifies the weights accordingly until they reach the optimal values. Typically, an artificial neural network has an input layer, multiple hidden layers, and an output layer.

A Convolutional Neural Network (CNN) [5] is a type of neural network that finds its application extensively in image classification and segmentation. The network takes an image for its input. The convolution layer applies a series of filters to it that help the network capture the high-level features of the image. The pooling layer then reduces the dimensions of the image, preserving the dominant features and reducing the

*arnavjoshi.iiti.me@gmail.com

number of parameters and computational requirements. Once the convolution and pooling operations are done, the final image is flattened and fed to a regular neural network. The input image or feature in this case is the Cross-Spectral Matrix which encapsulates the pressure signal data of the sound sources obtained by the microphone array. The network is trained against the ground truth which too is flattened before training thus converting it into an $N^2 \times 1$ vector. The number of hidden layers can vary and while more number of hidden layers enable the model to learn better, care should be taken to avoid overfitting the data. The activation function used is Rectified Linear Unit (ReLU) which outputs the input value if it is greater than or equal to zero, and zero otherwise. The optimizer is ADAM (derived from *Adaptive Moment Estimation*) which is a gradient-based optimization algorithm for updating the weights, and the loss function is mean squared error (mse) which is given as

$$mse = \frac{\sum_{i=1}^N (y_{pred} - y_{gt})^2}{N} \quad (4)$$

where y_{pred} is the predicted vector given by the network and y_{gt} is the ground truth vector.

3 Results

Various CNN models were developed, each of them trained to detect a fixed number of uniform sources at a particular frequency. The input source strength was taken to be 1 Pa. 50000 random samples were generated for training and 10000 for validation. The models were trained for around 100 epochs. Results for a particular case- 6 sources at 8000 Hz spread randomly over a 12x12 scanning grid- are shown in this paper as a representative of the general trend.

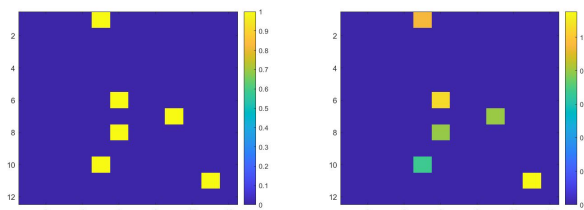


Figure 1: Ground Truth (left) and CNN prediction (right).

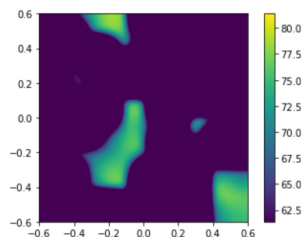


Figure 2: Beamforming Output (in decibels)

4 Discussion

Figure 1 shows that the model managed to locate all the 6 sources perfectly. The predictions were far more accurate

and of much better resolution compared to the beamforming output (Figure 2) at higher frequencies, and even more so at lower frequencies where beamforming was rendered virtually unhelpful. The model can not only detect static sources but also track moving sources. Pressure data recorded at an instant through the microphone array can be used to predict the source's position at that instant from which its velocity and acceleration can be extrapolated. Furthermore, models trained to detect random number of sources and sources with different strengths were also developed to explore the performance on more realistic scenarios.

5 Conclusions

The limitations of conventional beamforming at resolving complex source distributions, especially at lower frequencies, prompted the search for an alternative method that was more robust and accurate. A data-driven approach based on deep learning was employed. A Convolutional Neural Network trained to detect and track static and moving acoustic sources was developed. The Cross-Spectral Matrix containing the pressure data obtained by the microphone array was used as an input to the network while it was trained against the Ground Truth Matrix. Multiple CNN models were developed to span a range of source frequencies and the performance was found to be far better than acoustic beamforming. To challenge the model further, it was trained for scenarios with a greater degree of randomness like detecting sources with different strengths or detecting a number of sources within a fixed range. There is still some scope for refinement but overall, the results show much promise and it is expected that with more data and training, a robust and generalized deep learning framework for detection of acoustic sources in real-life applications can be successfully built. This preliminary work will be extended to identify locations of acoustic sources in vortical and turbulent flows.

Acknowledgments

This research was enabled in part by support provided by Sharcnet and Compute Canada (www.computeCanada.ca).

References

- [1] Hamid Daryan, Fazle Hussain, and Jean-Pierre Hickey. Aeroacoustic noise generation due to vortex reconnection. *Phys. Rev. Fluids*, 5:062702, Jun 2020.
- [2] Leandro de Santana. Fundamentals of acoustic beamforming. *Design and Operation of Aeroacoustic Wind Tunnel Tests for Group and Air Transport*, 2017.
- [3] Pengwei Xu, Elias JG Arcondoulis, and Yu Liu. Acoustic source imaging using densely connected convolutional networks. *Mechanical Systems and Signal Processing*, 151:107370, 2021.
- [4] Rémi Cousson, Quentin Leclere, Marie-Agnès Pallas, and Michel Berengier. Identification of acoustic moving sources using a time-domain method. In *bebec*, 2018.
- [5] Saad Albawi, Tareq Abed Mohammed, and Saad Al-Zawi. Understanding of a convolutional neural network. In *2017 International Conference on Engineering and Technology (ICET)*, pages 1–6. Ieee, 2017.

MULTI-OBJECTIVE OPTIMIZATION OF THE ENERGY EFFICIENCY AND THE TONAL NOISE OF THE PROPELLER BLADES OF AN UNMANNED AERIAL SYSTEMS ROTOR.

Tenon Charly Kone^{*1}, Sebastian Ghinet¹, Anant Grewal¹, Daniel Skalecki¹ and Viresh Wickramasinghe¹

¹National Research Council Canada, Flight Research Laboratory, Ottawa, Ontario, Canada

1 Introduction

Along with all the technological, operational and regulatory barriers, Unmanned Aerial System (UAS) noise radiation has been identified as a significant factor limiting the widespread adoption of UAS systems, particularly within densely populated regions. Understanding and mitigating the acoustic emissions from UAS while reducing their carbon footprint poses a significant challenge due to their unconventional vehicle layout with multiple propulsion units combined with their operation in reverberant urban environments at high thrust levels. An appropriate design of the propeller blades shape with an optimal number of blades allows, on one hand, to improve aerodynamic performance while reducing the energy dependence of the UAS, thus reducing CO2 emissions and on the other hand to have a quieter rotor. Recent advances in numerical simulation made the implementation of multidisciplinary optimization for complex shape propeller blade designs a feasible and affordable option. However, the numerical simulation linked to the optimization of complex systems such as the propeller blades is known as a task of considerable computational time and complexity. In addition, the cost associated with the required commercial software contribute to the increase in design costs. As a result, metamodel techniques using open source algorithms as a mean to explore and support the initial design concepts become standard practice to reduce the computational time required and decrease the total design cost.

This paper focusses on the reduction of the UAS rotor passage blade noise [1] which is one of the main sources of nuisance. A metamodel approach based on multi-objective optimization is proposed. Improved aerodynamic and aeroacoustics performances were demonstrated numerically for an optimized propeller blade configuration as compared to a baseline geometry configuration.

2 Materials

The reference geometry has not comprised the shrouded supports as used in the Karmal et al.'s works [2]. This geometry had $N = 3$ identical propeller blades with constant angular spacing of $360/N$ degrees mounted around a motor shaft of diameter 4.3 in and length 10.5 in with a parabolic shaped hub (Fig. 1.a). The blade was constructed using NACA 6412 type profiles. The propeller blade parameters such as the blade angle β , the chord and the thickness of each profile could be found on the page 14 of the ref. 3 The absence of the shrouded supports allowed to simplify the CFD model with only $1/N^{\text{th}}$ of the UAS rotor (Fig.1a). To

facilitate the setup, the geometry under study was placed in a cylinder of a diameter of $1.5D$, a length of $1.25D$ and sharing the same axis as the rotor. The volume of air thus defined was called the rotation volume (Fig. 1.b). The volume of rotation was also channelled in a cylindrical tunnel of diameter $4D$, length $12D$ and with the same axis. The rotation volume is located in the center of the channel (Fig 1.c).

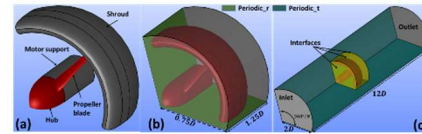


Figure 1: Baseline geometry: (a) $1/N$ th of the rotor, (b) $1/N$ th rotation volume and (c) CFD model

An incompressible solution using the OpenFoam RANS method was computed using air at 20°C and 1 atm. For the modelling of the rotation, the multi-rotational frames (MRF) approach of the OpenFoam was chosen. For all CFD calculations, a velocity of $U_\infty = 30.226 \text{ m/s}$, was applied at the tunnel inlet while zero pressure was imposed at outlet. The adhesion boundary conditions was used on the walls.

3 Optimization problem

3.1 Design parameters

There are a variety of propeller blade design parameters that can influence both the aerodynamic and aeroacoustic performances of a UAS rotor. On the basis of a preliminary study and for reasons of computation time, four of these design parameters were retained for this study. Those parameters were: the number of propeller blades N , the blade angle $\beta_{75\%}$ at 75% of the rotor radius and the blade skew. The blade skew was defined in the plane perpendicular to the rotation axis of the rotor. It was characterized by the angular position θ_s with respect to the radial of the mid-chord point of the profile considered. For this study, the blade skew profile was a polynomial of degree 2 constructed using 3 given skew angles: $\theta_{s0} = 0^\circ$ at $0.3R$, θ_{s0} at $0.65R$ and θ_{s2} at blade tip. Once the blade angle $\beta_{75\%}$ is given a correction is made on other profile blade angles. Thus, the new blade angle β becomes double the old blade angle β_{old} for each profile minus $\beta_{75\%}$ ($\beta = 2\beta_{old} - \beta_{75\%}$).

Thus, the optimization variable vector was given by:

$$X = (N, \beta_{75\%}, \theta_{s1}, \theta_{s2}). \quad (1)$$

3.2 Objective functions

The main objective of this study was to optimize the shape of a propeller blade in terms of emitted sound pressure level of the tonal noise as compared to the baseline blade while

* TenonCharly.Kone@nrc-cnrc.gc.ca

increasing the UAS rotor aerodynamic performance. It is therefore necessary to define two objective functions, one for aerodynamic performance and one to quantify the total noise.

The aerodynamic performance is proportional to the total thrust (N propeller blades, hub, motor support and shrouded) and the engine torque and is defined by:

$$\eta = \frac{TU_{\infty}}{2\pi Q\Omega/60}, \quad (2)$$

with regard to the tonal noise, it is materialized in this study by the root-mean square pressure p_{rms} of the acoustic pressure magnitude $|p|$ of the first frequency. According to the Garrick et al.[3] work, the acoustic pressure magnitude for any harmonic m is defined by the noise contribution due to the thrust of the propeller blades and that of the engine torque. The magnitude of the far-field sound pressure at a field point identified by $(x, y, 0)$ emitted by a point moving force at $(0, y_1, z_1)$, both (field point and force) in uniform motion with velocity U_{∞} along the x -direction is given by:

$$|p| = \frac{m\omega_1}{2\pi c S_0} \left| T \left(M + \frac{x}{S_0} \right) \frac{1}{\beta^2} - Q \frac{Nc}{\omega_1 R_e^2} \right| J_{mN} \left(\frac{kyR_e}{S_0} \right), \quad (3)$$

where $S_0 = \sqrt{x^2 - \beta^2 y^2}$, $\beta = \sqrt{1 - M^2}$, $M = U_{\infty}/c$, c is the sound velocity, $\omega_1 = N\Omega$ is the fundamental frequency, J_{mN} is the Bessel function of first kind, index mN , $\omega = mN\Omega = kc = m\omega_1$ is m -th harmonic frequency and $R_e = R$ or $0.8R$ is effective radius of propeller blades, with R is propeller blades radius. The propeller blades total thrust and the engine torque are placed at the effective radius R_e .

From equation (2) the sound pressure root mean square at far-field is given by:

$$p_{rms} = \frac{1}{\sqrt{2}} |p| \quad (4)$$

3.3 Definition of the optimization problem

The optimization problem aims at finding the design parameters X (Eq. 1) to maximize the aerodynamic performance (Eq. 2) while minimizing the maximum of the magnitude root mean square of the sound pressure (Eq.4) of the UAS blade rotor first frequency of passage received at $(x, 2D, 0)$. The problem to be solved is given by:

$$\begin{cases} \text{maximize } \eta(X) \text{ and} \\ \text{minimize } \left(\max_x (p_{rms}(X, x)) \right) \\ J = 0.565, \Omega = 8000 \text{ rpm}, y = 2D, N = \{3,4,5\} \\ 17^\circ \leq \beta_{75\%} \leq 30^\circ \text{ and } -30^\circ \leq \theta_{s1}, \theta_{s1} \leq 30^\circ \end{cases} \quad (5)$$

4 Method

The solution of the optimization problem (Eq. 5) was carried out in 4 stages: (i) geometry space sampling; (ii) calculate the thrust and engine torque of each sample with the CFD model and deduce the objective functions (Eqs. 2 and 4); (iii) building the Kriging metamodel; (iv) determining the optimum metamodel by the Dakota's multi-Objective Genetic Algorithm; and finally, (v) once one or more optimum is found, a CFD calculation is performed to verify the accuracy of the metamodel. If the result is satisfactory, the process stops. Otherwise the optimization returns to step

(i) by refining the discretization and / or by injecting into the sample the optimums found and repeating steps (ii) to (v). This process is iterated until one or several satisfactory optimums are found.

5 Results

A number of 123 Latin hypercube samples were needed to obtain the convergence of the Kriging metamodel. Three different solutions: 1, 2 and 3, have been found and are grouped in Table 1 and are represented in Fig. 2 as well as the baseline geometry (number 0). The predictions using the metamodel and the CFD calculation of the aerodynamic performance as well as the sound pressure level in dB are also grouped in the table. The relative error $(|f_{iCFD} - f_{imodel}|/|f_{iCFD}|)$ with $f_1 = \eta$ and $f_2 = p_{rms}$ of each of the solutions is small and is average. Compared to the baseline geometry, a gain of approximately 3% in terms of aerodynamic performance was obtained for each of the 3 solutions. Regarding the amplitude of the first blade passage frequency, a decrease of about 59 dB in its level has been obtained.

Table 1: Optimum design parameter and the obtained results.

Sol.	X			Model		CFD		
	N	$\beta_{75\%}$	θ_{s1}	θ_{s2}	$\eta(\%)$	p_{rms}	$\eta(\%)$	p_{rms}
0	3	24	0	0			66.1	92.1
1	4	25	-1.7	-11.5	68.9	31.1	69.3	30.9
2	4	24.2	18.5	-7.3	68.7	29.9	69	29.7
3	4	23.1	-17.7	11.6	68.3	28.5	68.6	28.4

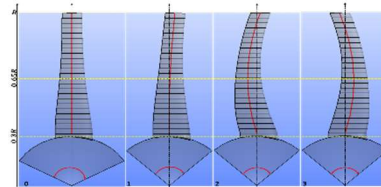


Figure 2: Propeller blade shape optimizer: (0) baseline geometry, (1) solution 1, solution 2 and (3) solution 3.

6 Conclusion

This study allowed the development of a highly multi-disciplinary optimization procedure using inexpensive open numerical tools. Three solutions quieter and better performing compared to the baseline geometry were presented. However, more design parameters and blade passage frequencies must be considered to further improve the emitted noise and efficiency of the UAS rotor.

References

- [1] R. Oleson and H. Patrick. Small aircraft propeller noise with ducted propeller. In 4th AIAA/CEAS aeroacoustics conference. p. 2284.
- [2] J. G. Kalmal, and W. G. Kenneth, "Aerodynamic Loads on an Isolated Shrouded-Propeller Configuration for Angles of Attack From -10 to 110". NASA Tech. Note D-995, Jan. 1962.
- [3] I. E. Garrick and E. Watkins. A theoretical study of the effect of forward speed on the free-space sound-pressure field around propellers, NACA, Report 1198, 1954.

STUDYING THE SUITABILITY AND ADAPTABILITY OF NOISE MAPS AS A TOOL FOR HEALTH PREVENTION IN THE PROVINCE OF QUEBEC

Jean-Philippe Migneron^{*1}, Frédéric Hubert^{†2}, Benoit Lalonde², Jean-François Hardy¹, Yves Brousseau³, Jean-Gabriel Migneron¹, Marie-Hélène Vandersmissen³, Thierry Badard² et Joël Bouchard⁴

¹ Groupe de Recherche en Ambiances Physiques, École d'Architecture, Université Laval, Québec

² Centre de recherche en intelligence et données géospatiales, FFGG, Université Laval, Québec

³ Département de géographie, Faculté de foresterie, de géographie et de géomatique, Université Laval, Québec

⁴ Bibliothèque-Direction des services-conseils, Université Laval, Québec

1 Introduction

This paper is a follow-up on the first project presented to the Canadian acoustical community in 2019 [1] about new initiatives launched by the provincial government after the publication of the Advisory on a Québec Policy to Fight Environmental Noise [2]. It aims to present a summary of the results obtained from the data classification throughout the literature review. As reported previously, the scoping review started with more than 11000 bibliographic records from which 170 scientific papers were selected.

Environmental noise mapping involves different techniques, and standards. As public authorities want to get a better understanding of what can be achieved in modern noise maps, the review looks at publications from the last 15 years to compare scientific development with general practice of noise engineering or environmental assessment. One of the main goals of the project is to share that knowledge with people that can take advantage of convenient and accurate noise maps, such as urban planners, cities, or different authorities from the provincial government.

2 Noise mapping scientific review

2.1 Selection of the bibliography

At the request of the funding partner, the project started with a scoping review on the subject of recent noise maps. The research protocol had to be adjusted according to the literature that would best covert agreed priorities of the study.

To be selected in the second level of examination, each reference had to fulfill inclusion criteria such as : the language used between English or French, the type of text, publication date really after 2003, detailed information regarding the presented noise mapping, the scale of maps (excluding small-scale analysis), good acoustics considerations, a few exclusion of particular noise sources or environment (like underwater propagation), and the availability of the paper in electronic or printed version. With two independent jurors doing this assessment on each publication, the inventory was reduced from a set of 705 abstracts obtained by keywords search in international database to a set of 170 full-length papers that would then pass to the data extraction.

2.2 Locations of reviewed studies

One of the first remarks coming from the review is that recent scientific publications on noise mapping are not common in North America, as there were only 9 papers from that part of the world. In comparison, 59 references were from Asia, and 63 from countries located in Europe. This fact raises a few questions about why noise mapping is not considered as an actual research topic in the United States or in Canada. Statistics per countries show more publications in Brazil, Turkey, China, Italy or in India alone.

Regarding the scale of interest, most examples related to citywide projects, then it is about boroughs, and areas of a few blocks like university campuses.

2.3 Preliminary findings

The scientific research on noise mapping seems to be made according to 3 different goals, which are the visual translation of noise levels in the environment for general interpretation, the design and validation of noise maps, or the calibration of noise simulations. In 16% of selected papers, two or more of those objectives were discussed.

Although 44% of the scope did not clearly list the instrumentation used for sound surveys or other related observations, there is a relatively broad inventory of methods and equipment, which includes the majority of conceivable options. About 32% percent of the papers relied on at least a precision sound level meter (class 1), while 8% used more economical technology like smartphone apps and devices. In the category summarizing other types of instrumentation, there were several cases of audio-video recordings allowing post-processing or documentation of sound events, as well as geolocation tools. In addition, at least 21 references opted for more than one class of measurement instruments.

Through the reading of chosen scientific papers, it was not always easy to determine exactly how many surveys were included in each analysis. The graph in Figure 1 provides a relative summary of the number of field measurement locations listed by authors, considering 4 categories.

In some cases, the number of measurement points may be confused with the sampling scale used to produce the noise maps, like the resolution grid in simulations. Nearly half of articles reported assessments of 100 measurements or less, while only a few references appeared to have sampling of more than 1000 measurements.

* jean-philippe.migneron.1@ulaval.ca

† frederic.hubert@scg.ulaval.ca

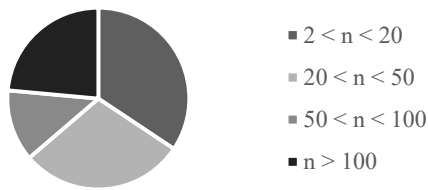


Figure 1: Number of measurement locations (n) used for noise maps reported in selected papers from the scoping review

The data extraction from those 170 publications allowed the comparison based on many parameters like:

- Height of noise level measurements above ground,
- Measurement interval,
- Time of the day taken into account,
- Noise standards or policy used,
- Noise level indicators (L_{eq} , L_{den} , L_n , etc.),
- Type of noise surveys (short, long term, recordings).

About typical categories of noise sources used in propagation models, the most common one was road traffic with 146 appearances. There was a smaller representation of railway noise, industrial noise, aircraft noise, leisure activities, and others. In 24% of the selection, the soundscape analysis included more than one type of sources.

Noise models are closely related to noise mapping, even if it is possible to draw interpolation maps only from measurements. Commercial software as Predictor-Lima, SoundPLAN, or Cadna A was cited in at least one third of cases. Besides that, 38% of all selected papers involved nationally developed tools, which can rely on the propagation standard approved.

The literature did not indicate that any particular standard takes an advantage over others. However, the implementation of CNOSSOS (Common Noise Assessment Methods in EU) could be expected to standardize practices in Europe.

2.4 Geographical comments

In geography, 2D renderings used in environmental noise are classified as thematic maps. A few criteria must be met to well design those and some rules shall be followed in order to deliver a message that is both accurate and illustrative of the reality. The representation, the choice of visual variables, the use of colors, the number of classes, and additional surrounding elements are related to the efficiency of the information reading. That was analyzed according to mapping characteristics such as:

- Spatial resolution,
- Map size (small scale to very large scale),
- Map types (choropleth, isarithmic, chorochromatic, etc.),
- Type of visual variables (color, hatch, marks, size),
- Color progression (single hue, spectral, qualitative, etc.),
- Clustering of results by ranges,
- Map's parts (title, legend, frame, orientation, scale, etc.).

According to specialized geographers, the levels of compliance with the rules of graphic semiology and the general quality of chosen documents was made according to the criteria described above. A small proportion of the studies adopts a good (15%) or very good (2%) compliance. At the

same time, only 13% of the maps were considered to be of good quality, and 1% of very good quality.

One interesting relation between geographic information sciences, geomatics, and acoustics is the description of topography. Digital ground models are getting very precise with modern technologies as LiDAR. This information can be transferred to noise modeling at some computational cost when the resolution is densified.

2.5 Next steps

The last part of the project focuses on the comparison of noise mapping design. Specialized commercial software is widely used by acoustical consultants. However, those kinds of tools can be expensive, and users must learn various details to get significant results. In Europe, open-source or low-cost software (iNoise) is more accessible or in development. For example, the NoiseModelling project [3] offers mapping results freely from an implementation of CNOSSOS standards and public data [4]. Things are not straight forward in Canada, as detailed traffic statistics are not publicly available or not shared in a global database.

3 Conclusion

In the end, 6 main categories of noise mapping methods were identified as found in Figure 2. The traditional method emerged as the most used method in more than 50% of the documents reviewed. Other methods showed some potential, such as land use regression models based on acoustic surveys.

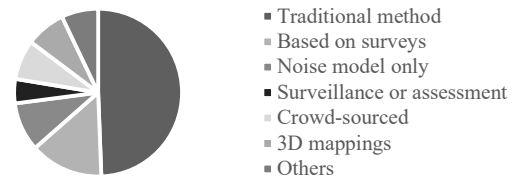


Figure 2: Classification of noise mapping methods in the review

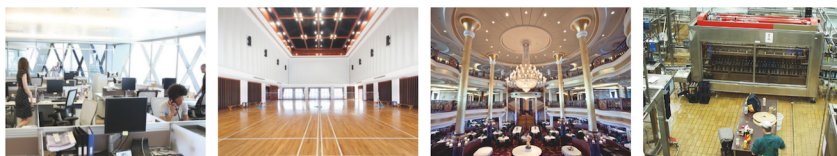
The results from this scoping review led to the design of noise maps testing between 3 case studies. Final report shall help to get an easier access to input data required for noise modeling, and also a better understanding of those methods.

Acknowledgements

This project is funded by the *Gouvernement du Québec*.

Bibliography

- [1] J-P. Migneron, J-F. Hardy, A. Potvin, J-G. Migneron, F. Hubert, Études des procédés d'évaluation, de représentation et de législation du bruit environnemental applicables au Québec, Canadian Acoustics. 2019 Oct. 16; 47(3):84-5.
- [2] R. Martin, P. Deshaies, M. Poulin, Advisory on a Québec Policy to Fight Environmental Noise: Towards Healthy Sound Environments, INSPQ, Quebec, November 2015.
- [3] <https://noise-planet.org/noisemodelling.html>
- [4] <https://www.openstreetmap.org>



CadnaR is the powerful software for the calculation and assessment of sound levels in rooms and at workplaces

❖ Intuitive Handling

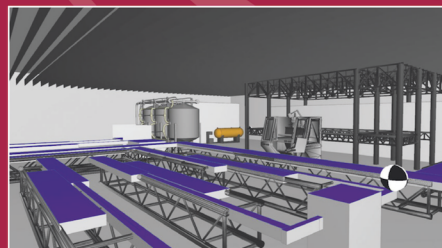
The clearly arranged software enables the user to easily build models and make precise predictions. At the same time you benefit from the sophisticated input possibilities as your analysis becomes more complex.

❖ Efficient Workflow

Change your view from 2D to 3D within a second. Multiply the modeling speed by using various shortcuts and automation techniques. Many time-saving acceleration procedures enable a fast calculation process.

❖ Modern Analysis

CadnaR uses scientific and highly efficient calculation methods. Techniques like scenario analysis, grid arithmetic or the display of results within a 3D-grid enhance your analysis and support you during the whole planning and assessment process.



Fields of Application

Office Environments

- Process your acoustic calculations and assessments according to DIN 18041, VDI 2569 and ISO 3382-3
- Receiver chains serve as digital “measurement path” and provide you with relevant insights into the acoustic quality of rooms during the planning phase
- Import of DWG-/DXF-/SKP-files (e.g. pCon.planner, AutoCAD, SketchUp)
- Visualization of noise propagation, noise levels and parameters for quality criteria like the Speech Transmission Index STI

Production Plants

- Calculation of the sound load at workplaces based on the emission parameters specified by the machine manufacturer according to the EC guideline 2006/42/EC while also taking the room geometry and the room design into account
- Tools for enveloping surfaces and free field simulations to verify the sound power of the sources inside of the enveloping surface
- Calculation of the sound power level based on technical parameters such as rotational speed or power



Distributed in the U.S. and Canada by: Scantek, Inc. Sound and Vibration Instrumentation and Engineering
6430 Dobbin Rd, Suite C | Columbia, MD 21045 | 410-290-7726 | www.scantekinc.com

ABSTRACTS FOR PRESENTATIONS WITHOUT PROCEEDINGS PAPER RÉSUMÉS DES COMMUNICATIONS SANS ARTICLE

An Efficient Simulation Methodology To Solve Friction-Induced Vibrations For A Frictional System

Farouk Maaboudallah, Nouredine Atalla

This communication deals with the modelling and the prediction of the dynamic instabilities for a rubbing system. Two hybrid approaches are introduced for dynamic instability analysis and applied to a reduced disc brake system. The methods are based on stochastic algorithms coupled with the finite element method (FEM) using the complex eigenvalue analysis (CEA) technique. By considering the input parameters as random variables, the uncertainty analysis is performed through two approaches to predict the unstable frequencies of a braking system (i) Monte-Carlo (MC) using Mersenne-Twister (MT19937) algorithm and (ii) periodic sampling technique. Since the mechanism of brake squeal involves many design parameters, stochastic finite element (SFE) approaches will be coupled with sensitivity algorithms, e.g. Variance-Based Sensitivity Analysis (VBSA) and Fourier Sensitivity Analysis Test (FAST), to analyze the contribution of each random variable on the dynamic instabilities. First, a comparison between the two stochastic algorithms is performed on standard analytical models. The objective is to validate the accuracy and to assess the numerical efficiency that FAST presents to (i) propagate the uncertainties upstream of the model and (ii) to compute the partial variances of the model output. Secondly, the coupling of the previous stochastic algorithms with FEM is carried out and tested through a reduced brake system consisting of a rotating disc with two flat pads. Results show that the hybrid approach FAST-FE is more robust and computationally more efficient compared to the widely used MC-FE for these types of problems. FAST-FE solver converges, within a reasonable computing time, either to approximate the probability density function (PDF) of the random variables or to compute the partial variances of the dynamic instabilities. Hence, it can be considered as an efficient numerical method for squeal instability analysis in order to reduce squeal noise of such a mechanical system.

Modelling Sonar Backscatter

Len Zedel, Mahdi Razaz, Axel Belgarde

In designing active sonar systems there are many applications where the exact performance of a new system can be difficult to predict. Challenging design situations that we have encountered include: the presence of physical boundaries, limitations in transducer beam shapes, and the occurrence of significant velocity shear or turbulence. In such situations, a model of acoustic backscatter is useful for evaluating or optimising system performance before committing to a particular hardware design. And, access to simulated received signals allows for preliminary testing of proposed signal processing algorithms. This paper provides a brief description of a parametric backscatter model that we have used to design Doppler sonar and split beam sonar systems. The model can accurately simulate pulse coherent signals by retaining target information between successive samples and Doppler shift information through applying a time dilation to the simulated signals. As examples of model results we show how nearfield and beam pattern effects can impact Doppler sonar systems and discuss some implications of transducer geometry choices for split-beam fisheries sonar design.

Speech Production For Hearing-Impaired Talkers In Noise With Ear Occlusion

Xinyi Zhang, Ingrid Verduyck, Rachel E. Bouserhal

The presence of noise exacerbates communication problems, especially for people with hearing difficulties. An estimated 40% of Canadian adults have at least mild hearing impairment (HI), of which a significant percentage is required to wear hearing protection devices (HPDs) in their workplace. However, this is also problematic because wearing HPDs further aggravates communication problems in a noisy environment by occluding the ear canal, affecting how people hear themselves and speak. Previous research on speech in noise for people with HI has mainly focused on their perception of speech as listeners; however, they also take on the active role of a talker in communication. It is, therefore, equally important to understand how speech production for people with HI is affected by both ear canal occlusion and the presence of noise. Thus, the objective of this study is to model speech production for people with varying degrees of hearing impairment at different levels of noise and ear occlusion. Changes in acoustic features of speech that affect intelligibility will be investigated, quantified, and modelled with respect to hearing impairment, noise, and ear occlusion. The results of this work will help adapt speech technologies to atypical conditions as a better practice of inclusive design.

Make your job easier with RION

Preferred by sound and vibration professionals around the world for more than **75** years



Dedicated sound and vibration instruments, transducers and software characterized by **ease of use, superior quality and reliability.**



Contact **RION North America** for more information

RION North America
Kensington, MD 20895

E-mail: rion@rion-na.com
<https://rion-sv.com>



LISTEN - FEEL - SOLVE

EDITORIAL BOARD - COMITÉ ÉDITORIAL

Aeroacoustics - Aéroacoustique

Dr. Anant Grewal (613) 991-5465 anant.grewal@nrc-cnrc.gc.ca
National Research Council

Architectural Acoustics - Acoustique architecturale

Jean-François Latour (514) 393-8000 jean-francois.latour@snclavalin.com
SNC-Lavalin

Bio-Acoustics - Bio-acoustique

[Available Position](#)

Consulting - Consultation

[Available Position](#)

Engineering Acoustics / Noise Control - Génie acoustique / Contrôle du bruit

Prof. Joana Rocha Joana.Rocha@carleton.ca
Carleton University

Hearing Conservation - Préservation de l'ouïe

Mr. Alberto Behar (416) 265-1816 albehar31@gmail.com
Ryerson University

Hearing Sciences - Sciences de l'audition

Olivier Valentin, M.Sc., Ph.D. 514-885-5515 m.olivier.valentin@gmail.com
GAUS - Groupe d'Acoustique de l'Université de Sherbrooke

Musical Acoustics / Electroacoustics - Acoustique musicale / Électroacoustique

Prof. Annabel J Cohen acohen@upei.ca
University of P.E.I.

Physical Acoustics / Ultrasounds - Acoustique physique / Ultrasons

Pierre Belanger Pierre.Belanger@etsmtl.ca
École de technologie supérieure

Physiological Acoustics - Physio-acoustique

Robert Harrison (416) 813-6535 rvh@sickkids.ca
Hospital for Sick Children, Toronto

Psychological Acoustics - Psycho-acoustique

Prof. Jeffery A. Jones jjones@wlu.ca
Wilfrid Laurier University

Shocks / Vibrations - Chocs / Vibrations

Pierre Marcotte marcotte.pierre@irsst.qc.ca
IRSST

Signal Processing / Numerical Methods - Traitement des signaux / Méthodes numériques

Prof. Tiago H. Falk (514) 228-7022 falk@emt.inrs.ca
Institut national de la recherche scientifique (INRS-EMT)

Speech Sciences - Sciences de la parole

Dr. Rachel Bouserhal rachel.bouserhal@etsmtl.ca
École de technologie supérieure

Underwater Acoustics - Acoustique sous-marine

[Available Position](#)



ANNOUNCEMENT

ACOUSTICS WEEK IN CANADA

MEMORIAL UNIVERSITY, ST. JOHN'S,
NEWFOUNDLAND AND LABRADOR

SEPT 27-30, 2022



Acoustics Week in Canada 2022 will be held on September 27-30 2022, in St. John's, Newfoundland and Labrador.



Vue du centre-ville de St John's

You are invited to be part of this three-day conference featuring the latest developments in Canadian acoustics and vibration. This is the first time Acoustics Week will be held in the province of Newfoundland and Labrador, and reflects Memorial University's growing profile in acoustics research.

The keynote talks and technical sessions will be framed by a welcome reception, conference banquet, Acoustical Standards Committee meeting, technical tour and an exhibition of products and services related to the field of acoustics and vibration.

Take few days before or after the conference to enjoy the area and the cultural activities! While in Downtown St. John's be sure to try some of the world-class restaurants on Duckworth and Water Street. Become an honorary Newfoundlander by kissing a cod and getting

screamed-in on George Street, while enjoying endless live music. Right next to downtown is Signal Hill National Historic Site, where Marconi received the first transatlantic radio signal. Signal Hill has great views of the city, and amazing hiking trails. For a longer hike, the East Coast Trail comprises 25 segments along the Atlantic coast of varying difficulty, most within an hour's drive of St. John's.

Venue and Accommodation

The conference will be held at the Sheraton Hotel Newfoundland in St. John's. A block of rooms in the hotel will be available at a special rate of \$179/night. Please refer to the conference website for further details and registration: <https://awc.caa-aca.ca/index.php/AWC/AWC22>

Plenary, technical sessions.

are planned throughout the conference. Each day will begin with a keynote talk of broader interest and relevance to the acoustics community. Technical sessions are planned to cover all areas of acoustics including:



Water Street, St John's

AEROACOUSTICS / ARCHITECTURAL AND BUILDING ACOUSTICS / BIO-ACOUSTICS AND BIOMEDICAL ACOUSTICS / MUSICAL ACOUSTICS / NOISE AND NOISE CONTROL / PHYSICAL ACOUSTICS / PSYCHO- AND PHYSIO-ACOUSTICS / SHOCK AND VIBRATION / SIGNAL PROCESSING / SPEECH SCIENCES AND HEARING SCIENCES / STANDARDS AND GUIDELINES IN ACOUSTICS / ULTRASONICS / UNDERWATER ACOUSTICS

Exhibition and sponsorship.

The conference offers opportunities for suppliers of products and services to engage the acoustic community through exhibition and sponsorship.

The tabletop exhibition facilitates in-person and hands-on interaction between suppliers and interested individuals. Companies and organizations that are interested in participating in the exhibition should contact the Exhibition and Sponsorship coordinator for an information package. Exhibitors are encouraged to book early for best selection.

The conference will be offering sponsorship opportunities of various conference features. In addition to the platinum, gold and silver levels, selected technical sessions, social events and coffee breaks will be available for sponsorship. Additional features and benefits of sponsorship can be obtained from the Exhibition and Sponsorship coordinator and on the conference website.

Students.

Students are strongly encouraged to participate. Students presenting papers will be eligible for one of three \$500 Best Presentation Student prizes to be awarded. Conference travel bursaries will also be available to those students whose papers are accepted for presentation.

Registration details.

Please refer to the conference web site: <https://awc.caa-aca.ca/index.php/AWC/AWC2022> 1

Contacts.

Conference Chair:

Len Zedel
(zedel@mun.ca)

Ben Zedel
(bzedel@mun.ca)



Flatrock, along the East Coast Trail



ANNONCE
SEMAINE CANADIENNE
D'ACOUSTIQUE
UNIVERSITÉ MEMORIAL, ST. JOHN'S,
TERRE-NEUVE ET LABRADOR
SEPT 27-30, 2022



La Semaine canadienne d'acoustique 2022 aura lieu du 27 au 30 septembre 2022 à St. John's, Terre-Neuve et Labrador. You



View of downtown St John's

Nous vous invitons à prendre part à cette conférence de trois jours concernant les derniers développements en acoustique et vibrations au Canada. C'est la première fois que la Semaine Canadienne d'acoustique aura lieu dans la province de Terre-Neuve et Labrador, ce qui reflète le profil croissant de recherche en acoustique de l'Université Memorial.

Les exposés principaux et les séances techniques seront encadrés par une réception de bienvenue, un banquet, une réunion du comité des normes acoustiques, une visite technique et une exposition de produits et services liés au domaine de l'acoustique et des vibrations.

Prenez quelques jours avant ou après la conférence pour profiter de la région et des activités culturelles! Au centre-ville de St. John's, assurez-vous d'essayer les restaurants de classe mondiale sur la rue Duckworth et la

rue Water. Devenez un(e) Terre-Neuvien(ne) honoraire en embrassant une morue et en vous faisant 'Screeched-in' sur la rue George, tout en profitant de la musique live sans fin. Juste à côté du centre-ville se trouve le Lieu historique national de Signal Hill, où Marconi a reçu le premier signal radio transatlantique. Signal Hill a une vue imprenable sur la ville, et des sentiers de randonnée incroyables. Pour une randonnée plus longue, le sentier de la côte Est comprend 25 segments le long de la côte atlantique de difficulté variable, la plupart à moins d'une heure de route de St. John's.

Lieu et hébergement.

La conférence aura lieu au Sheraton Hotel Newfoundland à St. John's. Un bloc de chambres dans l'hôtel sera disponible à un tarif spécial de 179\$ par nuit. Veuillez consulter le site Web de la conférence pour plus de détails et pour l'inscription: <http://awc.caa-aca.ca/AWC/AWC2022>

Des séances plénières, techniques et des ateliers.

Des séances plénières, techniques et des ateliers sont prévus tout au long de la conférence. Chaque journée débutera avec une plénière intéressante et pertinente pour la communauté de l'acoustique. Des sessions techniques sont prévues pour couvrir tous les domaines de l'acoustique, y compris :



Rue Water, St John's

AÉROACOUSTIQUE / ACOUSTIQUE DU BÂTIMENT ET ARCHITECTURALE / BIOACOUSTIQUE / ACOUSTIQUE BIOMÉDICALE / ACOUSTIQUE MUSICALE / BRUIT ET CONTRÔLE DU BRUIT / ACOUSTIQUE PHYSIQUE / PSYCHOACOUSTIQUE / CHOCS ET VIBRATIONS / LINGUISTIQUE / AUDIOLOGIE / ULTRASONS / ACOUSTIQUE SOUS-MARINE / NORMES EN ACOUSTIQUE

Exposition et parrainages.

La conférence offre aux fournisseurs de produits et de services la possibilité de faire participer la communauté acoustique par l'exposition et le parrainage.

L'exposition sur le plateau facilite l'interaction en personne des fournisseurs et des personnes intéressées. Les entreprises et organisations désirant participer à l'exposition doivent contacter le coordonnateur de l'exposition et du parrainage pour obtenir un dossier d'information. Les exposants sont encouragés à réserver tôt pour obtenir de meilleures opportunités.

Les étudiants.

Les étudiants sont fortement encouragés à participer. Les étudiants qui présenteront seront admissibles à l'un des trois prix de 500\$ pour les meilleures présentations. Des subventions de voyage seront également offertes aux étudiants dont les communications sont acceptées pour présentation.

Pour plus d'informations sur l'inscription.

Veuillez consulter le site Web de la conférence : <http://awc.caa-aca.ca/AWC/AWC2022>.

Contacts.

Président de la conférence:

Len Zedel
(zedel@mun.ca)

Ben Zedel
(bzedel@mun.ca)



Flatrock, sur le sentier de la côte Est



ACOUSTICS



NOISE



VIBRATION



HGC ENGINEERING

- > **Noise & Vibration Control in Land-use Planning**
- > **Noise & Vibration Studies: Residential and Commercial**
- > **Building Acoustics, Noise & Vibration Control**
- > **Land-use Compatibility Assessments**
- > **Third-party Review of Peer Reports**
- > **Expert Witness Testimony**

905-826-4546

answers@hgcengineering.com

www.hgcengineering.com

CANADIAN ACOUSTICS ANNOUNCEMENTS - ANNONCES TÉLÉGRAPHIQUES DE L'ACOUSTIQUE CANADIENNE

Looking for a job in Acoustics?

There are many job offers listed on the website of the Canadian Acoustical Association!

You can see them online, under <http://www.caa-aca.ca/jobs/>

August 5th 2015

Acoustics Week in Canada 2021

Because of the COVID-19 situation, the Acoustics Week in Canada (AWC) originally planned for October 2020 in Sherbrooke (QC) will be postpone to October 2021. Nevertheless, and as a "warm up", Sherbrooke's organising committee is currently looking into setting up a little 1-day online *celebration* for October 2020. You can find more information on the [AWC20](#) and [AWC21](#) websites. Please note that St-John's (NL) will host the [AWC2022](#) conference.

May 3rd 2019

COVID-19 Situation

Because of the COVID-19 situation, the Acoustics Week in Canada (AWC) originally planned for October 2020 in Sherbrooke (QC) will be postpone to October 2021. Nevertheless, and as a "warm up", Sherbrooke's organising committee is currently looking into setting up a little 1-day online *celebration* for October 2020. You can find more information on the [AWC20](#) and [AWC21](#) websites. Please note that St-John's (NL) will host the [AWC2022](#) conference.

May 13th 2020

Extended: International Year of Sound (2020 – 2021)

Highlighting the importance of sound and related sciences and technologies for all in society

The *International Year of Sound* is a project that the International Commission for Acoustics (ICA), an Affiliated Member of the ISC, has been preparing for many years. The theme of the international year is the *Importance of Sound for Society and the World* and is underscored by the UNESCO Charter of Sound and resolution 39C/49 on the [Importance of sound in today's world – Promoting best practices](#). Other partners for the international year include "La Semaine du Son" (LSdS), the International Science Council and ISC members the International Union of Pure and Applied Physics (IUPAP) and the International Union of Theoretical and Applied Mechanics (IUTAM). The main goal of any international year is to to promote international collaboration and to raise awareness on how science contributes to innovation for the benefit for all society. However, for the International Year of Sound, soon after the opening in Paris at the Grand Amphitheatre of the Sorbonne on 31 January 2020, it became clear that the impact of the COVID-19 pandemic would curtail the outreach events that had been planned throughout the year and around the globe. As expected, very few of the activities planned for 2020 were held with physical presence of the participants. Some, including major international conferences, were held online with considerable success, with the international year encouraged by new online technologies. The activities, organized by member societies and affiliates of the ISC, included scientific conferences and workshops, exhibitions, presentations explaining the importance of sound to a general public in collaboration with museums, universities, schools, research centers and cultural organizations, as well as postings in social media, podcasts and concerts. Many events, competitions and conferences have been rescheduled, and ISC members and their communities can find out more by visiting www.sound2020.org.

April 29th 2021

Acoustic Training in Canada Database: Help us to help the younger generation and seasoned professionals

CAA is building a comprehensive list of all training programs offered in acoustics in Canada and we need your help! Below is a survey to help us populate that database that will eventually be available on CAA website. Please

return all valuable input at your earliest convenience to Mr. DeGagne (wdegagne@caa-aca.ca)!

Dear CAA members, past members and friends, The purpose of this survey is to develop an online database of all the professional, undergraduate, and graduate acoustical courses and training programs offered through universities, colleges, associations, etc. This database would benefit the entire Canadian acoustic community in the following manner: 1. Track the different acoustical courses and training programs offered nationally 2. Allow CAA members to plan their acoustical training and easily select their perfect training program to meet their career aspirations 3. Allow CAA members to compare and contrast courses and training programs from different institutions 4. Allow institutions and the CAA to determine where the training gaps are and to plan for future programs demands To help us populate this database, simply return the following information at your earliest convenience to Mr. William DeGagne (wdegagne@caa-aca.ca), volunteer for CAA: 1. Place of the Course or Training program (university, colleges, etc.): 2. Name of Course or Training program: 3. Approx. date the Course or Training was followed: 4. Level (graduate, undergraduate, college course or professional training program, etc.): 5. Brief description of the Course or Training program: 6. Webpage of Course or Training program: 7. Location of Course or Training program (City, Province): 8. Course or Training program language: Thanks for you help towards the younger generation and seasoned professionals! :-)

May 31st 2021

Acoustics Week in Canada 2021 (AWC21): Call for abstracts

Acoustics Week in Canada 2021 will be held online October 05-07!

Submissions are now open for Acoustics Week in Canada 2021. The meeting will be held online, and three consecutive half-days (12:00-17:00 EST) will be punctuated by plenary lectures and 30-minute lightning talks sessions, while moving into virtual rooms. The details of a noise-related challenge among Canada will be revealed shortly. Each day will have a general theme: Day1 - Acoustics and structures, Day 2 - Acoustics and living beings, Day 3 - Acoustics and computers. The organizing committee welcomes 200-word abstracts related to any of these themes. An accepted abstract requires the submission of a 3-min video, while 2-page conference paper submission is encouraged but optional. Virtual rooms will be available for presenting other materials, like posters. The submission deadline is July 12, 2021 (<https://awc.caa-aca.ca/>).

June 12th 2021

À la recherche d'un emploi en acoustique ?

De nombreuses offre d'emploi sont affichées sur le site de l'Association canadienne d'acoustique !

Vous pouvez les consulter en ligne à l'adresse <http://www.caa-aca.ca/jobs/>

August 5th 2015

Semaine canadienne de l'acoustique 2021

En raison de la situation COVID-19, la Semaine canadienne de l'acoustique (AWC) initialement prévue en octobre 2020 à Sherbrooke (QC) sera reportée à octobre 2021. Néanmoins, et comme "échauffement", le comité organisateur de Sherbrooke étudie actuellement la possibilité de mettre en place une petite célébration d'une journée en ligne pour octobre 2020. Vous pouvez trouver plus d'informations sur le site des conférences AWC20 et AWC21. Veuillez noter que St-John's (NL) sera l'hôte de la conférence AWC2022.

May 3rd 2019

Situation COVID-19

En raison de la situation COVID-19, la Semaine canadienne de l'acoustique (AWC) initialement prévue en octobre 2020 à Sherbrooke (QC) sera reportée à octobre 2021. Néanmoins, et comme "échauffement", le comité organisateur de Sherbrooke étudie actuellement la possibilité de mettre en place une petite célébration d'une journée en ligne pour octobre 2020. Vous pouvez trouver plus d'informations sur le site des conférences AWC20 et AWC21. Veuillez noter que St-John's (NL) sera l'hôte de la conférence AWC2022.

May 13th 2020

Extension : Année internationale du son (2020 - 2021)

Mettre en évidence l'importance du son et des sciences et technologies connexes pour tous dans la société

L'Année internationale du son est un projet que la Commission internationale d'acoustique (ICA), membre affilié de la ISC, prépare depuis de nombreuses années. Le thème de l'année internationale est l'importance du son pour la société et le monde et est souligné par la Charte du son de l'UNESCO et la résolution 39C/49 sur l'importance du son dans le monde d'aujourd'hui - promouvoir les meilleures pratiques". Parmi les autres partenaires de l'année internationale figurent la Semaine du Son (LSdS), le Conseil international de la science et les membres de l'ISC, l'Union internationale de physique pure et appliquée (UIPPA) et l'Union internationale de mécanique théorique et appliquée (IUTAM). L'objectif principal de toute année internationale est de promouvoir la collaboration internationale et de faire prendre conscience de la manière dont la science contribue à l'innovation au profit de toute la société. Cependant, pour l'Année internationale du son, peu après l'ouverture à Paris au Grand Amphithéâtre de la Sorbonne le 31 janvier 2020, il est apparu clairement que l'impact de la pandémie de COVID-19 réduirait les événements de sensibilisation qui avaient été prévus tout au long de l'année et dans le monde entier. Comme prévu, très peu des activités prévues pour 2020 se sont déroulées avec la présence physique des participants. Certaines, notamment les grandes conférences internationales, se sont tenues en ligne avec un succès considérable, l'année internationale étant encouragée par les nouvelles technologies en ligne. Les activités, organisées par les sociétés membres et les affiliés de l'ISC, comprenaient des conférences et des ateliers scientifiques, des expositions, des présentations expliquant l'importance du son au grand public en collaboration avec des musées, des universités, des écoles, des centres de recherche et des organisations culturelles, ainsi que des publications sur les médias sociaux, des podcasts et des concerts. De nombreux événements, concours et conférences ont été reprogrammés, et les membres de l'ISC et leurs communautés peuvent en savoir plus en consultant le site www.sound2020.org.

April 29th 2021

Répertoire des formations en acoustique au Canada : aidez-nous à aider la jeune génération et nos professionnels d'expérience

L'ACA est en train de dresser une liste complète de tous les programmes de formation offerts en acoustique au Canada et nous avons besoin de votre aide ! Vous trouverez ci-dessous un sondage qui nous aidera à alimenter cette base de données qui sera éventuellement disponible sur le site Web de la CAA. Veuillez retourner vos précieux commentaires à M. DeGagne (wdegagne@caa-aca.ca) dans les plus brefs délais !

Chers membres, anciens membres et amis de l'ACA, Le but de cette enquête est de développer une base de données en ligne de tous les cours et programmes de formation en acoustique professionnels, de premier et de deuxième cycle, offerts par les universités, les collèges, les associations, etc. Cette base de données profiterait à l'ensemble de la communauté acoustique canadienne de la manière suivante : 1. Suivre les différents cours et programmes de formation en acoustique offerts à l'échelle nationale. 2. Permettre aux membres de l'ACA de planifier leur formation en acoustique et de choisir facilement le programme de formation idéal pour répondre à leurs aspirations professionnelles. 3. Permettre aux membres de l'ACA de comparer et d'opposer les cours et les programmes de formation de différentes institutions. 4. Permettre aux institutions et à l'ACA de déterminer où se trouvent les lacunes en matière de formation et de planifier les demandes de programmes futurs. Pour nous aider à alimenter cette base de données, il vous suffit de retourner les informations suivantes dans les meilleurs délais à M. William DeGagne (wdegagne@caa-aca.ca), bénévole pour l'ACA : 1. Lieu du cours ou du programme de formation (université, collèges, etc.) : 2. Nom du cours ou du programme de formation : 3. Date approximative à laquelle le cours ou la formation a été suivi. 4 : 4. Niveau (études supérieures, premier cycle, cours collégial ou programme de formation professionnelle, etc :) 5. Brève description du cours ou du programme de formation : 6. Page web du cours ou du programme de formation : 7. Lieu du cours ou du programme de formation (ville, province) : 8. Langue du cours ou du programme de formation : Merci pour votre aide à l'intention de la jeune génération et de nos professionnels d'expérience ! :-)

May 31st 2021

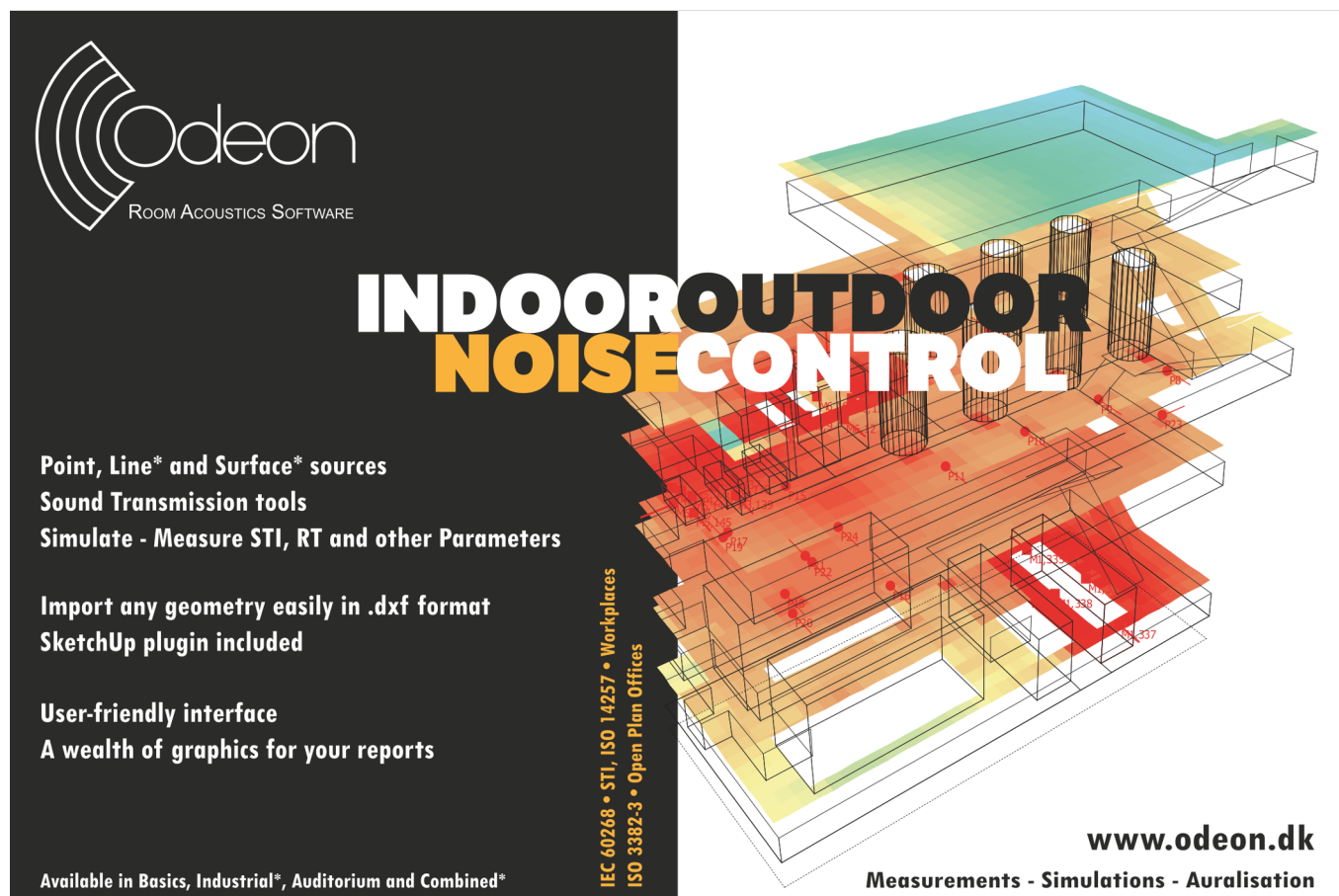
Semaine Canadienne de l'Acoustique 2021 (AWC21) : Appel aux résumés

La Semaine canadienne de l'acoustique aura lieu en ligne du 5 au 7 octobre 2021 !

-=-=- Les soumissions sont maintenant ouvertes pour la Semaine Canadienne d'Acoustique 2021. La conférence se tiendra en ligne sur trois demi-journées consécutives (12h00-17h00 HNE), et sera rythmée par des conférences plénières, des sessions éclair de 30 minutes tout en se déplaçant dans des salles virtuelles. Les détails concernant un

défi relié au bruit au Canada seront bientôt dévoilés. Chaque journée aura un thème général : Jour 1 - Acoustique et structures, Jour 2 - Acoustique et êtres vivants, Jour 3 - Acoustique et ordinateurs. Le comité organisateur accueille les résumés de 200 mots liés à l'un de ces thèmes. L'acceptation d'un résumé implique la soumission d'une vidéo de 3 minutes. La soumission d'un article de conférence de deux pages est suggérée mais facultative. Des salles virtuelles seront disponibles pour présenter d'autres supports, comme des posters. La date limite de soumission est le 12 juillet 2021

June 12th 2021



Odeon
ROOM ACOUSTICS SOFTWARE

INDOOR OUTDOOR NOISE CONTROL

Point, Line* and Surface* sources
Sound Transmission tools
Simulate - Measure STI, RT and other Parameters

Import any geometry easily in .dxf format
SketchUp plugin included

User-friendly interface
A wealth of graphics for your reports

IEC 60268 • STI, ISO 14257 • Workplaces
ISO 3382-3 • Open Plan Offices

www.odeon.dk
Measurements - Simulations - Auralisation

Why publish in Canadian Acoustics?



ISSN 0711-6659
canadian acoustics
acoustique canadienne
Journal de l'Association Canadienne d'Acoustique
SEPTEMBRE 2021
Volume ... - Numéro ...

Because, it is...

- A respected scientific journal with a 40-year history uniquely dedicated to acoustics in Canada
- A quarterly publication in both electronic and hard-copy format, reaching a large community of experts worldwide
- An Open Access journal, with content freely available to all, 12 months from time of publication
- A better solution for fast and professional review providing authors with an efficient, fair, and constructive peer review process.

Pourquoi publier dans Acoustique canadienne ?



ISSN 0711-6659
canadian acoustics
acoustique canadienne
The Canadian Acoustical Association - Journal de l'Association Canadienne d'Acoustique
SEPTEMBRE 2021
Volume 49 - Numéro 3

Parce que, c'est...

- Une revue respectée, forte de 40 années de publications uniquement dédiée à l'acoustique au Canada
- Une publication trimestrielle en format papier et électronique, rejoignant une large communauté d'experts à travers le monde
- Une publication "accès libre" dont le contenu est disponible à tous, 12 mois après publication
- Une alternative intéressante pour une évaluation par les pairs, fournissant aux auteurs des commentaires pertinents, objectifs et constructifs

Application for Membership

CAA membership is open to all individuals who have an interest in acoustics. Annual dues total \$120.00 for individual members and \$50.00 for student members. This includes a subscription to *Canadian Acoustics*, the journal of the Association, which is published 4 times/year, and voting privileges at the Annual General Meeting.

Subscriptions to *Canadian Acoustics* or Sustaining Subscriptions

Subscriptions to *Canadian Acoustics* are available to companies and institutions at a cost of \$120.00 per year. Many organizations choose to become benefactors of the CAA by contributing as Sustaining Subscribers, paying \$475.00 per year (no voting privileges at AGM). The list of Sustaining Subscribers is published in each issue of *Canadian Acoustics* and on the CAA website.

Please note that online payments will be accepted at <http://jcaa.caa-aca.ca>

Address for subscription / membership correspondence:

Name / Organization _____
Address _____
City/Province _____ Postal Code _____ Country _____
Phone _____ Fax _____ E-mail _____

Address for mailing Canadian Acoustics, if different from above:

Name / Organization _____
Address _____
City/Province _____ Postal Code _____ Country _____

Areas of Interest: (Please mark 3 maximum)

- | | | |
|--|---|---|
| 1. Architectural Acoustics | 5. Psychological / Physiological Acoustic | 9. Underwater Acoustics |
| 2. Engineering Acoustics / Noise Control | 6. Shock and Vibration | 10. Signal Processing / Numerical Methods |
| 3. Physical Acoustics / Ultrasound | 7. Hearing Sciences | 11. Other |
| 4. Musical Acoustics / Electro-acoustics | 8. Speech Sciences | |

For student membership, please also provide:

(University) (Faculty Member) (Signature of Faculty Member) (Date)

I have enclosed the indicated payment for:
 CAA Membership \$ 120.00
 CAA Student Membership \$ 50.00

Corporate Subscriptions (4 issues/yr)
 \$120 including mailing in Canada
 \$128 including mailing to USA,
 \$135 including International mailing

Sustaining Subscription \$475.00
(4 issues/yr)

Please note that the preferred method of payment is by credit card, online at <http://jcaa.caa-aca.ca>

For individuals or organizations wishing to pay by check, please register online at <http://jcaa.caa-aca.ca> and then mail your check to:

**Executive Secretary, Canadian Acoustical:
Dr. Roberto Racca
c/o JASCO Applied Sciences
2305-4464 Markham Street
Victoria, BC V8Z 7X8 Canada**

Formulaire d'adhésion

L'adhésion à l'ACA est ouverte à tous ceux qui s'intéressent à l'acoustique. La cotisation annuelle est de 120.00\$ pour les membres individuels, et de 50.00\$ pour les étudiants. Tous les membres reçoivent *L'Acoustique Canadienne*, la revue de l'association.

Abonnement pour la revue *Acoustique Canadienne* et abonnement de soutien

Les abonnements pour la revue *Acoustique Canadienne* sont disponibles pour les compagnies et autres établissements au coût annuel de 120.00\$. Des compagnies et établissements préfèrent souvent la cotisation de membre bienfaiteur, de 475.00\$ par année, pour assister financièrement l'ACA. La liste des membres bienfaiteurs est publiée dans chaque issue de la revue *Acoustique Canadienne*.

Notez que tous les paiements électroniques sont acceptés en ligne <http://jcaa.caa-aca.ca>

Pour correspondance administrative et financière:

Nom / Organisation _____
Adresse _____
Ville/Province _____ Code postal _____ Pays _____
Téléphone _____ Téléc. _____ Courriel _____

Adresse postale pour la revue *Acoustique Canadienne*

Nom / Organisation _____
Adresse _____
Ville/Province _____ Code postal _____ Pays _____

Cocher vos champs d'intérêt: (maximum 3)

- | | | |
|---|-------------------------------|--|
| 1. Acoustique architecturale | 5. Physio / Psycho-acoustique | 9. Acoustique sous-marine |
| 2. Génie acoustique / Contrôle du bruit | 6. Chocs et vibrations | 10. Traitement des signaux / Méthodes numériques |
| 3. Acoustique physique / Ultrasons | 7. Audition | 11. Autre |
| 4. Acoustique musicale / Électro-acoustique | 8. Parole | |

Prière de remplir pour les étudiants et étudiantes:

(Université) (Nom d'un membre du corps professoral) (Signature du membre du corps professoral)
(Date)

Cocher la case appropriée:

- Membre individuel 120.00 \$
 Membre étudiant(e) 50.00 \$

Abonnement institutionnel

- 120 \$ à l'intérieur du Canada
 128 \$ vers les États-Unis
 135 \$ tout autre envoi international
 Abonnement de soutien 475.00 \$
(comprend l'abonnement à
L'Acoustique Canadienne)

Merci de noter que le moyen de paiement privilégié est le paiement par carte crédit en ligne à <http://jcaa.caa-aca.ca>

Pour les individus ou les organisations qui préféreraient payer par chèque, l'inscription se fait en ligne à <http://jcaa.caa-aca.ca> puis le chèque peut être envoyé à :

Secrétaire exécutif, Association canadienne d'acoustique :

Dr. Roberto Racca
c/o JASCO Applied Sciences
2305-4464 Markham Street
Victoria, BC V8Z 7X8 Canada

BOARD OF DIRECTORS - CONSEIL D'ADMINISTRATION

OFFICERS - OFFICIERS

PRESIDENT PRÉSIDENT	EXECUTIVE SECRETARY SECRÉTAIRE	TREASURER TRÉSORIER	EDITOR-IN-CHIEF RÉDACTEUR EN CHEF
Jérémie Voix ÉTS, Université du Québec president@caa-aca.ca	Roberto Racca JASCO Applied Sciences secretary@caa-aca.ca	Dalila Giusti Jade Acoustics Inc. treasurer@caa-aca.ca	Umberto Berardi Ryerson University editor@caa-aca.ca

DIRECTORS - ADMINISTRATEURS

Alberto Behar Ryerson University albehar31@gmail.com	Michael Kieffe Dalhousie University mkieffe@dal.ca	Joana Rocha Carleton University Joana.Rocha@carleton.ca
Bill Gastmeier HGC Engineering bill@gastmeier.ca	Andy Metelka SVS Canada Inc. ametelka@cogeco.ca	Mehrzad Salkhordeh dB Noise Reduction Inc. mehrzaad@dbnoisereduction.com
Bryan Gick University of British Columbia gick@mail.ubc.ca	Hugues Nelisse Institut de Recherche Robert-Sauvé en Santé et Sécurité du Travail (IRSST) nelisse.hugues@irsst.qc.ca	

UPCOMING CONFERENCE CHAIR DIRECTEUR DE CONFÉRENCE (FUTURE)	PAST PRESIDENT PRÉSIDENT SORTANT	WEBMASTER WEBMESTRE
Olivier Robin Université de Sherbrooke conference@caa-aca.ca	Frank A. Russo Ryerson University past-president@caa-aca.ca	Philip Tsui RWDI web@caa-aca.ca
PAST CONFERENCE CHAIR DIRECTEUR DE CONFÉRENCE (PASSÉE)	AWARDS COORDINATOR COORDINATEUR DES PRIX	SOCIAL MEDIA EDITOR RÉDACTEUR MÉDIA SOCIAUX
Benjamin V. Tucker University of Alberta bvtucker@ualberta.ca	Joana Rocha Carleton University awards-coordinator@caa-aca.ca	Romain Dumoulin Soft dB r.dumoulin@softdb.com

SUSTAINING SUBSCRIBERS - ABONNÉS DE SOUTIEN

The Canadian Acoustical Association gratefully acknowledges the financial assistance of the Sustaining Subscribers listed below. Their annual donations (of \$475 or more) enable the journal to be distributed to all at a reasonable cost.

L'Association Canadienne d'Acoustique tient à témoigner sa reconnaissance à l'égard de ses Abonnés de Soutien en publiant ci-dessous leur nom et leur adresse. En amortissant les coûts de publication et de distribution, les dons annuels (de 475\$ et plus) rendent le journal accessible à tous les membres.

Acoustec Inc.

Jean-Philippe Migneron - 418-496-6600
info@acoustec.qc.ca
acoustec.qc.ca

Acoustex Specialty Products

Mr. Brian Obratoski - 2893895564
Brian@acoustex.ca
www.acoustex.net

AcoustiGuard-Wilrep Ltd.

Mr. William T. Wilkinson - 888-625-8944
wtw@wilrep.com
acoustiguard.com

AECOM

Alan Oldfield - 9057127058
alan.oldfield@aecom.com
aecom.com

Aercoustics Engineering Ltd.

Nicholas Sylvestre-Williams - (416) 249-3361
NicholasS@aercoustics.com
aercoustics.com

Dalimar Instruments Inc

Monsieur Daniel Larose - 450-424-0033
daniel@dalimar.ca
www.dalimar.ca

dB Noise Reduction

Mehrzad Salkhordeh - 519-651-3330 x 220
mehrzaad@dbnoisereduction.com
dbnoisereduction.com

FFA Consultants in Acoustics and Noise Control

Clifford Faszer - 403.508.4996
info@ffaacoustics.com
ffaacoustics.com

HGC Engineering Ltd.

Bill Gastmeier -
bill@gastmeier.ca
hgcengineering.com

Hottinger Bruel & Kjaer inc.

Andrew Khoury - 514-695-8225
andrew.khoury@hbkworld.com
bksv.com

Integral DX Engineering Ltd.

Gregory Clunis - 613-761-1565
greg@integraldxengineering.ca
integraldxengineering.ca

JAD Contracting Ltd

Jake Ezerzer - 1-855-523-2668 toll free
info@jadcontracting.ca
jadcontracting.ca

Jade Acoustics Inc.

Ms. Dalila Giusti - 905-660-2444
dalila@jadeacoustics.com
jadeacoustics.com

JASCO Applied Sciences (Canada) Ltd.

Roberto Racca - +1.250.483.3300 ext.2001
roberto.racca@jasco.com
www.jasco.com

Pliteq Inc.

Wil Byrick - 416-449-0049
wbyrick@pliteq.com
pliteq.com

Pyrok Inc.

Howard Podolsky - 914-777-7770
mrpyrok@aol.com
pyrok.com

RWDI

Mr. Peter VanDelden - 519-823-1311
peter.vandelden@rwdi.com
rwdi.com

Scantek Inc.

President, Scantek, Inc. - 1-410-290-7726
steve.scantek@gmail.com
scantekinc.com

Soft dB Inc.

Dr. Roderick Mackenzie - 5148056734
r.mackenzie@softdb.com
softdb.com

Xprt Integration

Mr. Rob W Sunderland - 604-985-9778
rob@xprt.ca